THE METALLOGENY OF Cu-Ni AND Zn-Cu-Pb DEPOSITS OF THE FREDERICKSON LAKE AREA, CENTRAL LABRADOR TROUGH

James Gebert
Department of Geological Sciences
McGill University, Montreal

A thesis submitted to the Faculty of Graduate Studies and Research in partial fulfillment of the requirements for the degree of Master of Science.

ISBN 0-315-46021-0

Abstract

In the Frederickson Lake area (Central Labrador Trough) Zn-Cu-Pb massive sulphide lenses and associated sulphide-facies iron formation occur within black argillites (Menihek Formation) adjacent to glomeroporphyritic sills (Montagnais Group) that are mineralized with Cu-Ni sulphides. Previous studies proposed a magmatic origin for both gabbro-hosted Cu-Ni and sediment-hosted Zn-Cu-Pb deposits.

The sediment-hosted deposits have an average d S34 value of +9.2 per mil, and an average S/Se ratio of 30,000. Cu-Ni sulphide lenses which occur within glomeroporphyritic gabbro sills adjacent to sulphide-enriched sediments have an average d S34 value of +3.7 per mil, have low magma/sulphide ratios (R=57 for Ni, R=53 for Cu) and a low average S/Se ratio (5,000).

The Cu-Ni deposits are interpreted to have formed by sulphide liquid immiscibility from glomeroporphyritic gabbro magmas. The contact metamorphism of stoped sulphide-facies iron formation xenoliths by glomeroporphyritic sills may have vapourized and released sulphur, causing sulphide liquid immiscibility. The Zn-Cu-Pb deposits are interpreted to have formed syngenetically by the circulation of hydrothermal fluids driven by the heat of the gabbros. These deposits are probably members of a poorly described class of sediment-hosted Zn-Cu deposits (E.g. deposits of the Swedish Caledonides and the American Ducktown region).

Résumé

Dans la région du Lac Frederickson (partie centrale, Fosse du Labrador) des sulfures de Zn-Cu-Pb et des lits de formation de fer aux faciès sulfuré sont trouvés dans les argilites noires (Formation de Menihek) adjacent aux gabbros gloméroporphyriques minéralisées en sulfures de Cu-Ni. Des travaux antérieurs suggèrent une origine magmatique pour les sulfures de Cu-Ni qui se trouvent dans les gabbros gloméroporphyriques et les sulfures de Zn-Cu-Pb qui se trouvent au sédiments.

Les gisements de Zn-Cu-Pb dans les sédiments ont une valeur moyen de d S34 de +9.2 per mil et un rapport moyen S/Se de 30,000. Les sulfures Cu-Ni aux gabbros gloméroporphyriques qui se trouvent pre des sédiments riche en soufre, ont une valeur moyenne de d S34 de +3.7 per mil, ont des rapport magma/sulfures bas (R=57 pour Ni, R=53 pour Cu), et ont des rapports bas de S/Se (5,000).

Les gisements de Cu-Ni sont interprétés de comme ayant été produits par la segregation d'un liquide sulfureux d'un magma de gabbro gloméroporphyrique. L'incorporation de xénolites de la formation de fer au faciés sulfuré et la conversion métamorphique subséquente de la pyrite en pyrrhotite auraient liberés le soufre dans le magma. Ces excès de soufre pourraient avoir provoqué l'immiscibilité du liquide sulfureux, et expliquerait les valeurs positives de d S34. Les gisements Zn-Cu-Pb sont interprétés comme représentant des gisements sédimentaires formés par la circulation de solutions hydrothermales mise en circulation en reponse a des fluxs thermiques cause par l'intrusion des gabbros. Ces gisements sont probablement membres d'un classe de gisements sédimentaires de Zn-Cu qui ne sont pas bien connues (e.g. les gisements de Caledoindes Suèdoise et Les Applaches Americain)

Acknowledgements

This study was funded and supported by le Ministère de l'Energie et des Ressources du Quebec (MERQ) and is presented with their authorization. The author wishes to acknowledge the generous support and advice given by Marc Bélanger and Tom Clark of the MERQ. Preparation and editing of this thesis was greatly assisted by thesis co-directors Dr. J. Fox and Dr. T.J. Barrett and by R. Wares. Thanks are also extended to Tom Avison for providing the drill logs from the Frederickson Lake Showing. The manuscript was improved by comments and criticisms offered by Drs. D. Francis, C. Gariepy, W. MacLean and A.E. Williams-Jones. Field assistance was provided by Y. Langlois and C. Couture.

TABLE OF CONTENTS

List of Tables

List of Figures

List of Appendices

Appendix

List of Maps

Map

CHAPTER 1. INTRODUCTION

1.1 Scope and Purpose

Although first exploited for its iron ore deposits, the Labrador Trough also contains sub-economic base metal sulphide deposits, a number of which have attracted exploration work since the early 1940s (Fig. 1, Table 1). An initial regional study divided these sulphide showings into six classes (Table 2; Fournier, 1983). The present study concerns two of these classes, glomeroporphyritic gabbro-hosted Cu-Ni deposits and sediment-hosted Zn-Cu-Pb deposits. In the Frederickson Lake area, there appears to be a spatial relationship between glomeroporphyritic gabbros of the Montagnais Group and Zn-Cu-Pb mineralization within black argillites of the Menihek Formation. This apparent spatial relationship has led to the speculation that all sulphide mineralization within the region is genetically related to the glomeroporphyritic gabbro sills (e.g. Griffis, 1943; Fournier, 1983). While the glomeroporphyritic gabbro-hosted Cu-Ni deposits are undoubtedly a magmatic product of the gabbros, a genetic relationship between sediment-hosted Zn-Cu-Pb deposits and glomeroporphyritic gabbros is less clear. Models which attempt to relate the Zn-Cu-Pb mineralization to the gabbros (e.g. Fournier, 1983) are somewhat controversial because they rely upon the magmatic segregation of zinc and lead, two elements that are normally only found in trace amounts in deposits formed by sulphide liquid immiscibility from mafic melts (e.g. Shimazaki and MacLean, 1976). The glomeroporphyritic gabbro-hosted Cu-Ni deposits are

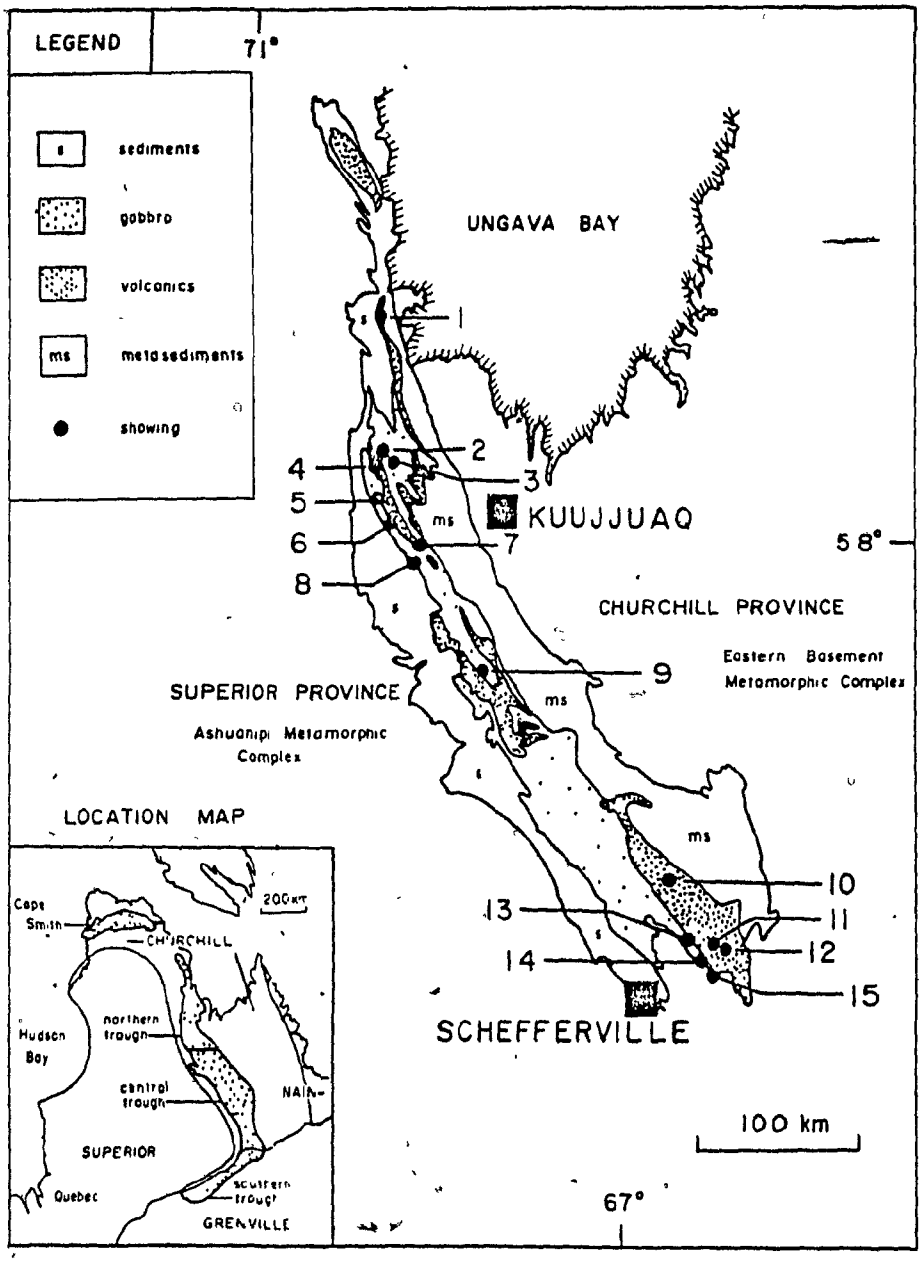

Fig. 1 Selected sulphide showings of the Quebec portion of the Labrador Trough. The numbers refer to showings listed in Table 1. The Frederickson Lake study area is indicated by number 14. Adapted from map 2001 of le Minstère de l'Energie et des Ressources, Québec (MERQ). Location map showing structural provinces adapted from Dimroth (1978).

Table 1

Grades and tonnages of selected sulphide deposits of the Labrador Trough in Quebec. Numbers refer to Figure 1.

Map #	Deposit	Deposit Type	Cu%	Ni%	Zn%	Reserves (tonnes)
1	Hopes Advance-1	Gab Cu-Ni	0.59	0.22		2 000 999
2	Soucy C	Gab Cu-Ni	0.72	0.22		129 700
	Soucy A	Sed Zn-Cu	1.49		1.80	5 444 000
3	St Pierre	Sed Zn-Cu	1.34		1.87	
4	Prudhomme-1	Sed Zn-Cu	2.04		2.66	4 303 700
5	Partington	Sed Po-Py				
6	Erickson-1	Gab Cu-Ni	1.12	0.32		519 700
7	Connolly	Gab Cu-Ni				
8	Koke	Sed Zn-Cu	0.70		6.86	1 060 400
9	Aulneau Lake	Per Cu-Ni	2.02	0.45		1 088 000
10	Chance Lake	Per Cu-Ni	0.66	0.89		649 400
11	Blue Lake	Per Cu-Ni	0.85	0.50		506 400
12	Retty Lake	Per Cu-Ni	1.50	0.67		1 360 500
13	Walsh Lake	Gab Cu-Ni				
14	Frederickson S.	Gab Cu-Ni				
	Frederickson N.	Sed Zn-Cu	0.77		4.38	279 400
15	Jimmick Lake	Sed Zn-Cu	0.26		5.20	108 800

Per = peridotite-hosted
Gab = glomeroporphyritic gabbro-hosted
Sed = sediment-hosted

Sources: Avramtchev and LeBel-Drolet (1979)
Lavergne (1985)

Table 2

Classification of the sulphide mineralization types of the Labrador Trough (after Fournier, 1983)

Type	
1	peridotite hosted Cu-Ni deposits
2	glomeroporphyritic gabbro-hosted Cu-Ni deposits
3	sediment-hosted Zn-Cu deposits
4	iron sulphides within black argillites
5	copper in late-to post-tectonic quartz-carbonate veins
6	chalcopyrite in pillowed basalt chill margins

distinctive, as the Cu-Ni sulphides are associated with concentrations of plagioclase rather than with olivine and pyroxene-bearing cumulates (e.g. Duluth Complex). This study examines the metallogeny of the Frederickson Lake region by focusing on the following three problems:

1. Were the sediment-hosted Zn-Cu-Pb deposits formed through synsedimentary or synvolcanic processes, or are they related to glomeroporphyritic gabbros as suggested by Fournier (1983)?
2. Is there a relationship between the occurrence of Cu-Ni sulphides and the glomeroporphyritic texture of these gabbros?
3. Does the spatial overlap of glomeroporphyritic gabbro-hosted Cu-Ni deposits and sulphide-rich sediments imply their formation by the incorporation of sedimentary sulphur?

1.2 Location

The Frederickson Lake study area is located 50 km northeast of Schefferville, Quebec, and covers some 80 square kilometres (latitude 54°48' to 55°07', longitude 66°17' to 66°07') (Fig. 2). Topographically, the area consists of a series of parallel ridges and valleys, which trend northwest along the regional strike of the Labrador Trough (Fig. 3). Erosionally resistant gabbro sills comprise the ridges (Fig.4) whereas argillite underlies the valley floors (Fig. 5). Good exposure is limited to the tops of gabbro ridges; ridge slopes and valley floors are covered by glacial sediments.

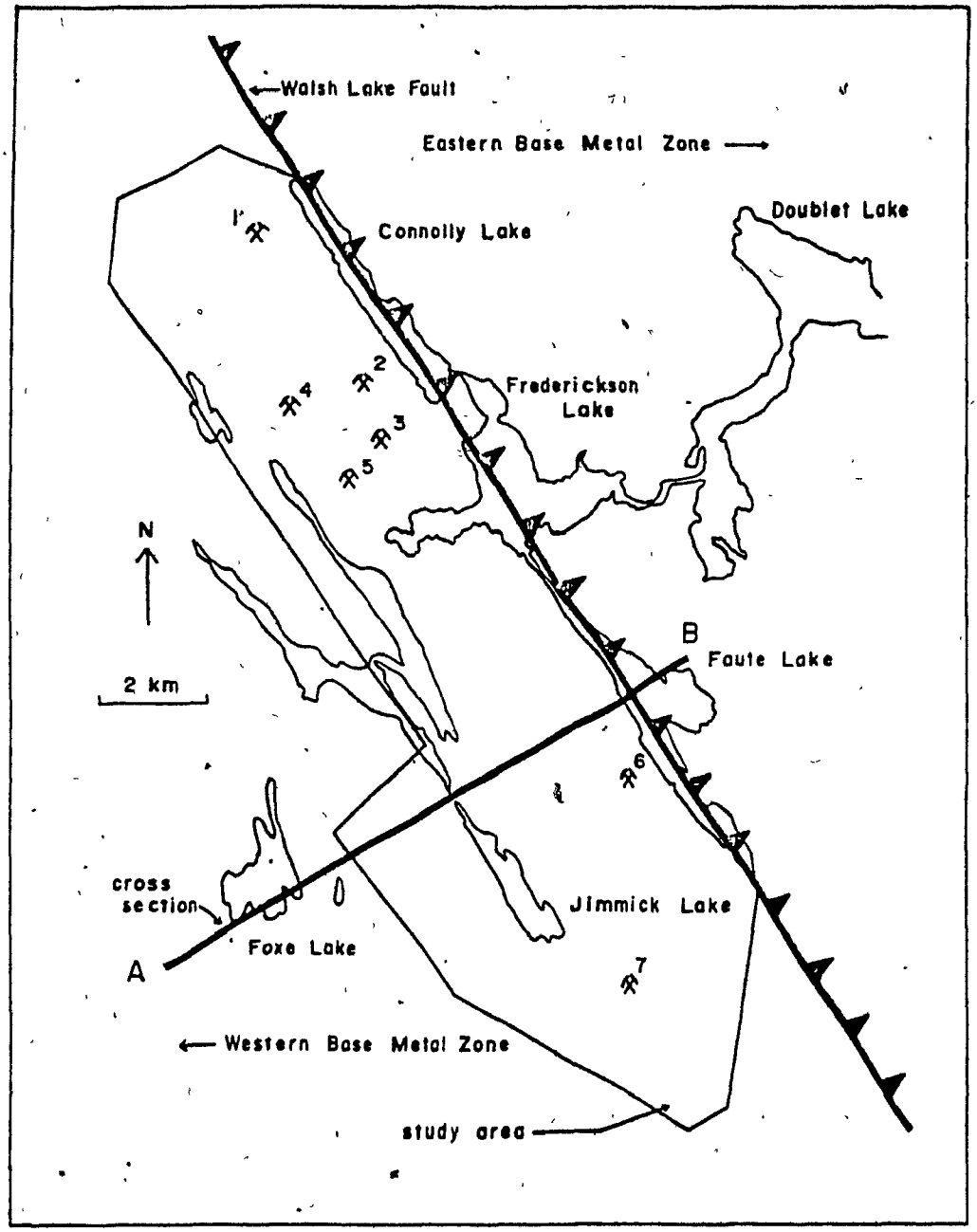

Fig. 2 Map of the Frederickson Lake study area illustrating the locations of the Cu-Ni and Zn-Cu-Pb showings discussed in the text. The cross section line refers to Figure 22.

1. Connolly (Cu-Ni)
2. Gossan 1 (Cu-Ni)
3. Gossan Lake (Cu-Ni)
4. Frederickson Lake North (Zn-Cu-Pb)
5. Frederickson Lake South (Cu-Ni)
6. Faute Lake (Po-Py)
7. Jimmick Lake (Zn-Cu)

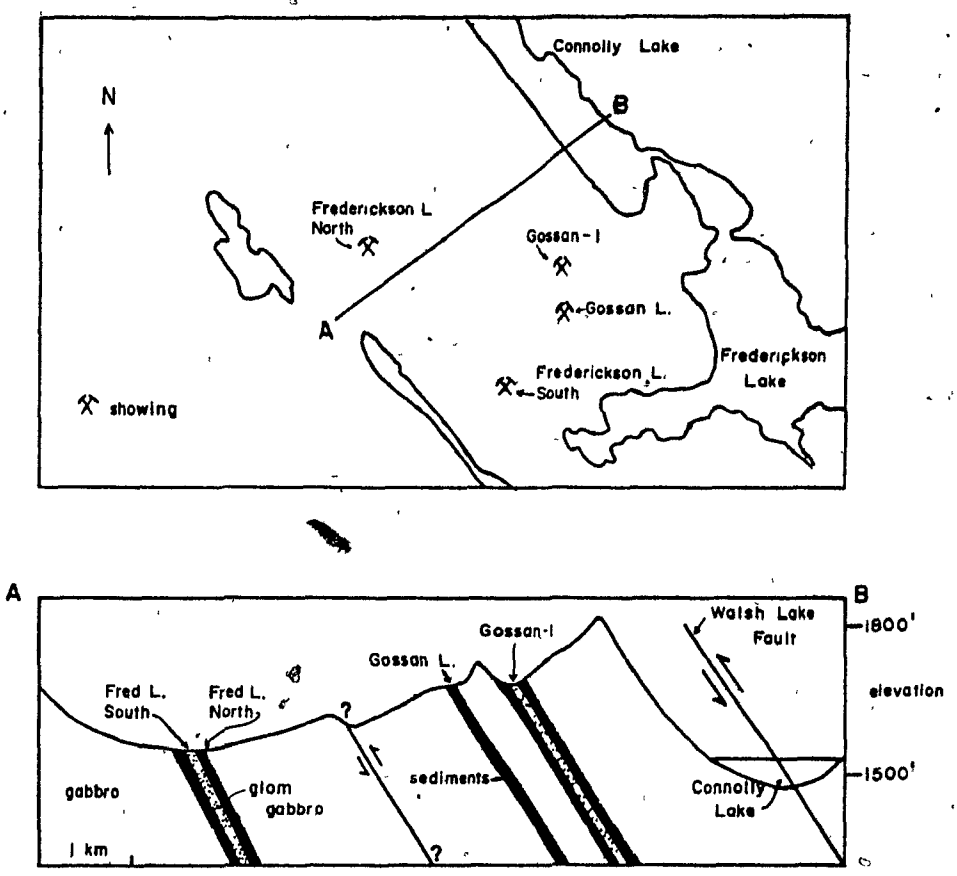

Fig. 3 Schematic cross section across the northern half of the study area. Sulphide showings have been projected on to the line of section. The ridges and valleys are composed of gabbro and sedimentary rocks respectively.

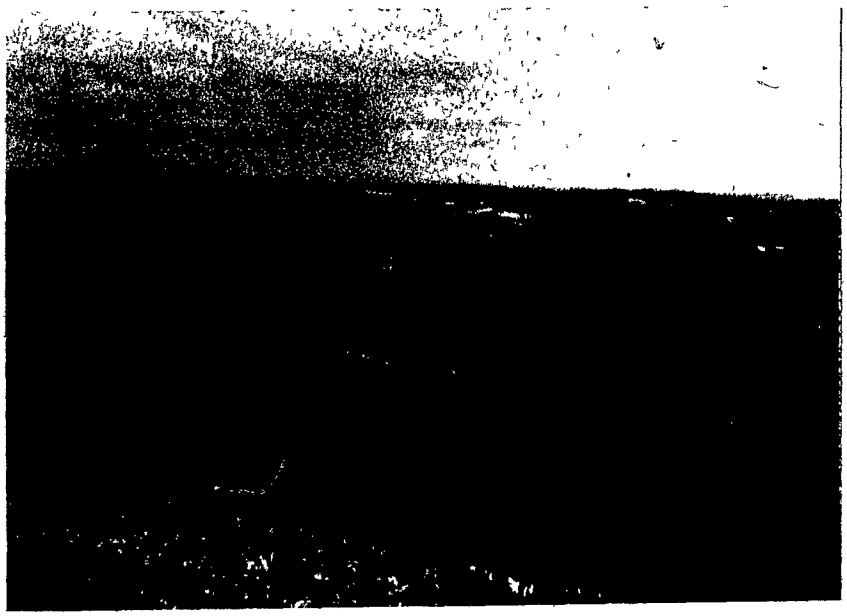

Fig. 4 Aerial photograph taken towards the northwest. The Walsh Lake Fault is marked by the lake at right of photo. The prominant linear ridge is composed of ordinary gabbro; valley to the left is floored by sedimentary rocks of the Menihek Formation.

Fig. 5 View looking northwest near the Frederickson Lake South showing. The swamp overlies sediments of the Menihek Formation. The photo is illustrative of the extreme paucity of sediment outcrop in the study area.

1.3 Investigative Methods

The author studied the map area outlined in Figure 2 during the summer of 1985. Geological information on the sulphide occurrences was difficult to obtain because of the paucity of outcrop and the destruction of primary stratigraphic relationships by the intrusion of massive gabbro sills (Fig. 3). Thus, for the sediment-hosted deposits the original deposit geometry, metal zonation, and alteration patterns could not be established. Drill core for the Frederickson Lake showings had not been kept by the original exploration companies, although drill logs are available.

As a result, emphasis in this study was placed on examining the regional mafic intrusives to determine if these played a role in the mineralization now present within the sediments. Sampling traverses were carried out across the strike of gabbro and glomeroporphyritic gabbro sills, and gabbro-sediment contacts were examined. The objective was to detect any systematic change in the distribution of elements both along and across the strike of the gabbro sills. Regional sampling of different igneous and volcanic units was also carried out in order to evaluate the magmatic evolution of this section of the Labrador Trough.

Most of the samples which were chemically analyzed were also cut for thin or polished sections. Chemical analyses (Appendix 1) were performed at Le Centre de Recherches Minérales (CRM) in Québec City by XRF or ICP. Analytical techniques, precision and uncertainties are outlined in Appendix 2. Ten samples were re-analyzed by neutron

activation at l' Université de Montréal to check data reproducibility, and to provide more accurate rare earth element data. Analyses performed by the CRM were generally accurate except for trace elements which were close to their lower limit of detection. Sulphur isotopic analyses were performed upon pyrrhotites separated from samples by hand picking. The pyrrhotite separates were analyzed at l' Université du Québec à Montréal, and at the University of Ottawa. Sulphur isotopic values are given relative to the Canon Diablo meteorite standard and have an analytical uncertainty of +/- 0.2 per mil. In addition, bulk rock sulphur was extracted from a gabbro sample by the Kiba agent (Sasaki et al. 1979), and was analyzed at the University of Ottawa. This sample had an uncertainty of +/- 0.5 per mil.

An important element of this study was the comparison of the showings within the Frederickson Lake map area to similar showings within the Northern Labrador Trough. Reference is therefore made to the work carried out by the author in conjunction with R. Wares of McGill University during the summer of 1986 in the area west of Kuujjuaq (showings 2, 3, 4, and 8 on Fig. 1).

1.4 Previous Work and Metallogenic Interpretations

Important regional studies can be found in the works of Sauvé and Bergeron (1965), Baragar (1967), Frarey (1967), Dimroth (1970, 1972, 1978), Dimroth et al., (1972, 1978), Harrison et al., (1972), Dimroth and Dressler (1978), Wardle and Bailey (1981) and LeGallais and Lavoie (1982). The

first recorded geological investigations of the Labrador Trough were undertaken in the 1890s by A. P. Low of the Geological Survey of Canada (Low, 1898). At that time the presence of iron formation was noted, although the first commercial discoveries were not made until the late 1920s. Regional base metal exploration of the Central Labrador Trough in the 1940s by the Hollinger North Shore Exploration Company (HNS) led to the division of the Trough into two separate base metal zones bounding the Walsh Lake Fault (Griffis, 1945; Fig. 3). The area of the present study belongs to the western zone, which contains glomeroporphyritic gabbro-hosted Cu-Ni deposits (Fournier's metallogenic type 2) and sediment-hosted Zn-Cu-Pb and Po-Py deposits (metallogenic types 3 and 4). East of the fault, in the eastern base metal zone, Cu-Ni sulphides are associated with ultramafic sills (metallogenic type 1).

Drilling in the Frederickson Lake region by HNS in 1943-44 revealed several deposits of relatively high grade but low tonnage. Re-examination of these showings in 1949 and in 1956 failed to find extensions to the mineralized zones (Hogg, 1957). Interest has recently been renewed in the eastern base metal sulphide zone as a result of the discovery of platinum group element (PGE) mineralization within the ultramafic-hosted Cu-Ni deposits at Retty Lake (Clark, 1987).

Since their discovery, gabbro-hosted Cu-Ni deposits of the Frederickson Lake area have been considered as magmatic products from a gabbroic source (e.g. Baragar, 1967; Fournier, 1983). However, the Zn-Cu-Pb showings, which occur within

sedimentary rocks or along gabbro-sedimentary contacts, have been attributed to both magmatic and synsedimentary processes. Initial reports emphasized the localization of these sulphide deposits to the contacts between gabbros and sediments (Griffis, 1943). As a result, early workers believed that these deposits were the result of the replacement of sedimentary rocks by fluids that were expelled from intruding glomeroporphyritic gabbro sills (Griffis, 1943; 1945). Later studies discounted a direct relationship between glomeroporphyritic gabbros and Zn-Cu-Pb mineralization, but inferred that such deposits were formed by replacement at structurally favourable sites (Auger, 1950; Kirkland, 1950). Frarey (1967) observed that iron sulphide mineralization within sedimentary rocks (sulphide-facies iron formation) was more common in areas of extensive gabbroic intrusions than in areas where gabbro sills were absent. For this reason, he attributed all of the sulphide mineralization within the region to the emplacement of basic igneous rocks. Fournier (1983) concluded that there was a relationship between a phenocryst-poor facies of glomeroporphyritic gabbro and Zn-Cu-Pb mineralization localized at gabbro-sediment contacts. He proposed that fractional crystallization within gabbroic magma chambers could give rise to both Cu-Ni-rich and Zn-Cu-Pb-rich immiscible sulphide liquids. The tapping of these liquids by higher crustal chambers would allow these two separate types of liquids to rise to higher levels in the crust, and ultimately to form Cu-Ni and Zn-Cu-Pb deposits.

Fournier postulated that a phenocryst-poor glomeroporphyritic magma would be able to transport a larger volume of sulphide-rich liquid because of its lower suspended load of phenocrysts, and suggested that the latter liquid would tend to be trapped in structural sites such as gabbro-sediment contacts.

A syngenetic origin has also been suggested for the sediment-hosted deposits. Kavanagh (1953) proposed that iron sulphide mineralization within sedimentary rocks was syngenetic because of its widespread distribution and the continuous lateral extent of individual sulphide-rich beds. However, he attributed the Zn-Cu-Pb sulphide mineralization to hydrothermal solutions originating from a gabbroic magma. Hogg (1957) supported Kavanagh's model but further proposed that remobilization was responsible for concentrating Zn-Cu-Pb sulphides in structural sites. In contrast, Baragar (1967) pointed out that the apparent spatial relationship between gabbro sills and iron-sulphide mineralization within sedimentary units did not necessarily imply a genetic relationship, and proposed that the iron-sulphide mineralization could have been produced by seafloor volcanism prior the intrusion of the sills.

CHAPTER 2 GEOLOGICAL SETTING: CENTRAL LABRADOR TROUGH

The Labrador Trough (Churchill Province) is the erosional remnant of an Aphebian volcano-sedimentary belt which was previously referred to as the Labrador geosyncline (Harrison, et al., 1972). The Trough extends 960 km in a NNW-SSE direction from the western shores of Ungava Bay in northern Quebec to the Grenville Front. It attains a maximum width of 130 km between the Ashuanipi Metamorphic Complex of the Superior Craton to the west, and the Eastern Basement Metamorphic Complex of the Churchill Province to the east (Fig. 1). Geographically, the Trough has been divided into three segments: the Northern Trough north of 57°N, the Central Trough between 57°N and the Grenville Front, and the Southern Trough south of the Grenville Front (Dimroth, 1978; Fig. 1). The age of the Trough is bracketed by K-Ar dates at ~2150 Ma for the granitoid Superior basement, and 1750 Ma corresponding to the Hudsonian Orogeny (Fryer, 1972).

2.1 Tectonic Setting

The precise tectonic setting of the Labrador Trough remains a matter of speculation because the geologic history of the complexely deformed rocks of the eastern hinterland has yet to be established. Early tectonic models (Dimroth, 1972; 1981; Dimroth and Dressler, 1978) proposed that the Labrador Trough formed in a rifted, ensialic basin floored by continental crust. Current models (Wardle and Bailey, 1981; LaVoie and LeGallais, 1982) propose that the Labrador Trough represents the erosional remnant of a rifted passive

continental margin.

2.2 Structure and Metamorphism

The Labrador Trough was affected by the Hudsonian Orogeny, during which deformation was directed westward (Dimroth and Dressler, 1978). Three separate periods of regional folding have been recognized in the Northern Trough (Goulet et al., 1987), and at least two periods are present within the Central Trough. The Central Trough can be divided into several tectonic domains, within each of which structural style appears to have been controlled by the competency of bedrock lithologies (Frarey, 1967). In the West-Central Trough, igneous intrusions are lacking and the rocks are tightly folded and overturned to the southwest, forming imbricate thrust sheets. Towards the east, thick gabbroic sills appear to have increased the lithogic competency so that the rocks have been folded into large, open structures which are upright (or slightly inclined to the northeast) and plunge towards the southwest (op. cit). The Labrador Trough itself plunges towards the south so that deeper stratigraphic levels are recorded in the Northern Trough. Basin growth faults, which were active in controlling sedimentation during rifting of the Trough, are believed to have been re-activated as thrust faults during deformation (Dimroth, 1972). Coincident with increasing amounts of deformation towards the east is an accompanying rise in metamorphic grade, from sub-greenschist facies in the west to amphibolite facies in the east (Dimroth and Dressler, 1978).

The Frederickson Lake area occurs within the sub-greenschist facies zone, although greenschist facies assemblages are locally present, having been produced by late deuteric alteration of the Montagnais gabbros (Baragar, 1967). For the purposes of this thesis the prefix "meta" has generally been excluded from rock names.

2.3 Stratigraphy

The rocks of the Central Labrador Trough belong to the Kaniapiskau Supergroup (Frarey and Duffell, 1964), which is divided into the Knob Lake, Doublet and Laporte Groups. The Knob Lake Group is restricted to the western half of the Trough and is composed of five subgroups (Table 3; Dimroth, 1978). The lowermost Seward Subgroup consists mainly of fluviatile and shallow marine clastic sediments and minor alkaline volcanics, and appears to record early rifting of the Trough. The Pistolet and Swampy Bay Subgroups together represent deposition in local, restricted sub-basins of the North-Central Trough, but are absent in the Frederickson Lake region (Fig. 6). A major marine transgression is recorded in the Attikamagen Subgroup, with shelf carbonates and shallow marine shales overlain by deeper water turbidites. These first four subgroups constitute the first sedimentary cycle of the Trough (Cycle I). In the overlying Ferriman Subgroup, a second marine transgression (Cycle II) is recorded, with sedimentation proceeding again from shelf carbonates and shales to deeper water turbidites (Wardle and Bailey, 1981).

Table 3

Stratigraphy of the Labrador Trough at 55° North. Formations of direct relevance to this study are shown in bold type. (after Dimroth, 1978)

SUPERGROUP	GROUP	SUB-GROUP	FORMATION
	Montagnais		Retty Peridotite **Wakuach Gabbro**
KANIAPISKAU			
	Doublet		**Willbob** **Thompson Lake** **Murdoch**
	Knob Lake	Ferriman	**Menihek** Sokoman Ruth Wishart
		Attikamagen	Dolly Denault Le Fer Bacchus
		Swampy Bay	absent at 55° N
		Pistolet	absent at 55° N
		Seward	Dunphy Chakonipau

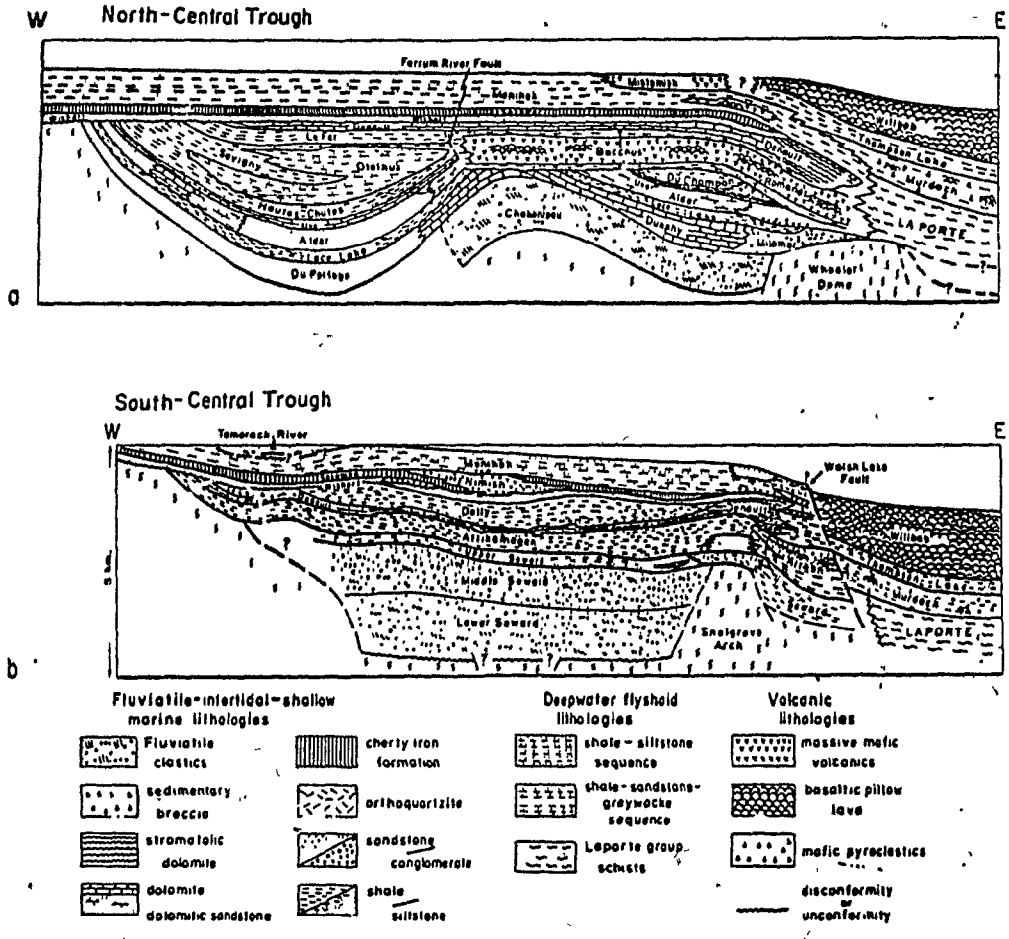

Fig. 6. Summary and stratigraphic development of the a: North-Central and b: South-Central Labrador Trough. The Frederickson Lake area is located in the South-Central Trough immediately west of the Walsh Lake Fault (From Wardle and Bailey, 1981).

The Doublet Group (or Doublet/Hellancourt) is confined to the eastern half of the of Trough and is composed dominantly of mafic volcanic rocks. This Group appears to have formed during a phase of rapid crustal rifting and incipient ocean basin development (Wardle and Bailey, 1981).

The Laporte Group (Harrison, 1952) outcrops in the extreme eastern margins of the Labrador Trough. Within the Central Trough, this Group consists of metamorphosed amphibolitic and semi-pelitic gneisses which are separated from the Doublet Group by a thrust fault. Initially the Laporte Group was not recognized as belonging to the Labrador Trough but it is now generally included in the Trough stratigraphy.

The Montagnais Group consists of intrusive rocks (the Wakuach Gabbro and the Retty Peridotite) which invade the Kaniapiskau Supergroup. The Montagnais Group is present only in the eastern half of the Knob Lake Group, whereas ultramafic sills occur dominantly in the Doublet Group. The Montagnais intrusives have been shown to be co-magmatic with the extrusive volcanic rocks of the Doublet group (Baragar, 1967; Fournier, 1983).

CHAPTER 3 LOCAL GEOLOGY

The Frederickson Lake study area encloses approximately 80 square kilometers of sediments of the Menihek Formation, and abundant gabbro sills of the Montagnais Group (Fig. 2; Map 1). These rocks constitute the subject of the present study, and will be described in detail. The geology of the Doublet Group adjoining the study area east of the Walsh Lake Fault will only be summarized.

3.1 Menihek Formation

The Menihek Formation is the uppermost unit within the Knob Lake Group (Frarey and Duffell, 1964). In the Western Trough, this formation unconformably overlies the Sokoman Formation and is composed of grey, rhythmically banded siltstone and shale. Towards the east, the Menihek Formation is in conformable contact with the Sokoman Formation and is composed of black shale, siltstone and greywacke (Wardle and Bailey, 1981). Extreme eastern exposures of these fine-grained sediments are marked by intercalated basaltic flows (Baragar, 1967). In the South-Central Trough, the Doublet Group has been thrust upon the Menihek Formation, with the contact marked by the Walsh Lake Fault (Fig. 5). Towards the northwest this fault dies out, and the Menihek Formation interfingers with the Murdoch Formation (Baragar, 1967). Regional mapping in the Central Trough indicates that the former formation thickens from 1000 m in the west to 1500 m in the east (Wardle and Bailey, 1981). The Menihek Formation is commonly correlated with the Upper Baby Formation of the

Northern Trough and an unnamed sequence of schists and gneisses in the Southern Trough. Fournier (1983) correlated the Menihek Formation with the Doublet Group across the Walsh Lake Fault.

In the study area, the Menihek Formation is poorly exposed, occurring as thin bands of sediment enclosed between thick gabbro sills. These sedimentary bands appear to be laterally continuous, although rarely lenses of sediment are enclosed by gabbro. Most gabbro sills in the region dip towards the east. As a result, sedimentary bands are preferentially preserved on the eastern sides of valleys where they have been protected from erosion by a hanging wall of gabbro. Cherty or silicified sediments, which are more resistent to erosion, outcrop as low rounded mounds on valley floors.

Massive, dense, black argillite is the dominant lithology exposed within the map area. Locally, slightly graphitic or siliceous varieties are present. In thin section, the argillites consist of a semi-opaque mass of clay-sized minerals and disseminated fine-grained iron sulphides 0.01 mm in length. With increasing iron sulphide content, these grade into sulphide-facies iron formation (Fig. 7). Finely interlaminated mudstone-siltstone and sulphide-rich layers are present on scales ranging from tenths of millimetres to centimetres (Fig. 8). Where grading is present within the siltstone-mudstone layers, sulphides are usually confined to the finest-grained fraction. The fine-scale interlamination of sulphide and mudstone bands suggests

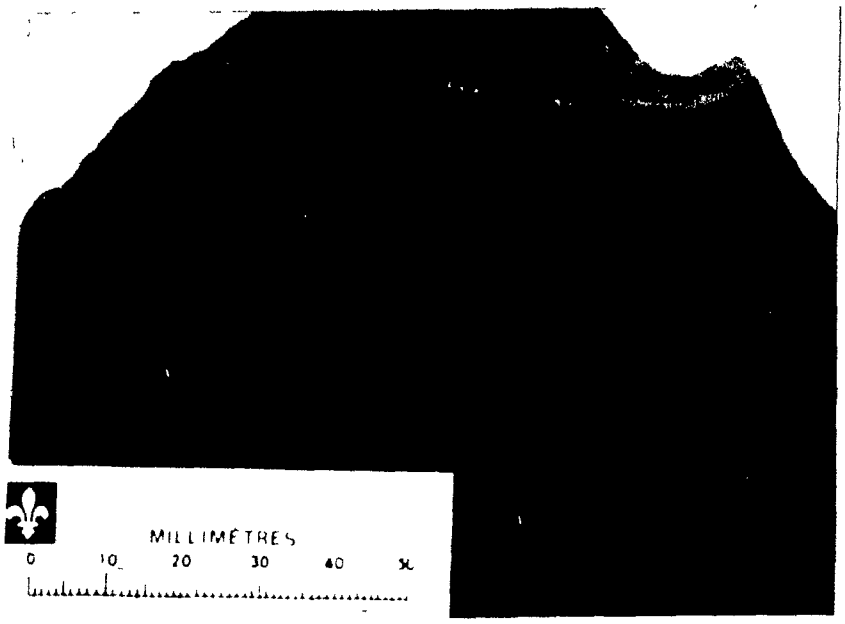

Fig. 7 Hand specimen of sulphide-facies iron formation illustrating the fine interlamination of iron sulphides (light layers) and clay-sized silicate minerals (dark layers).

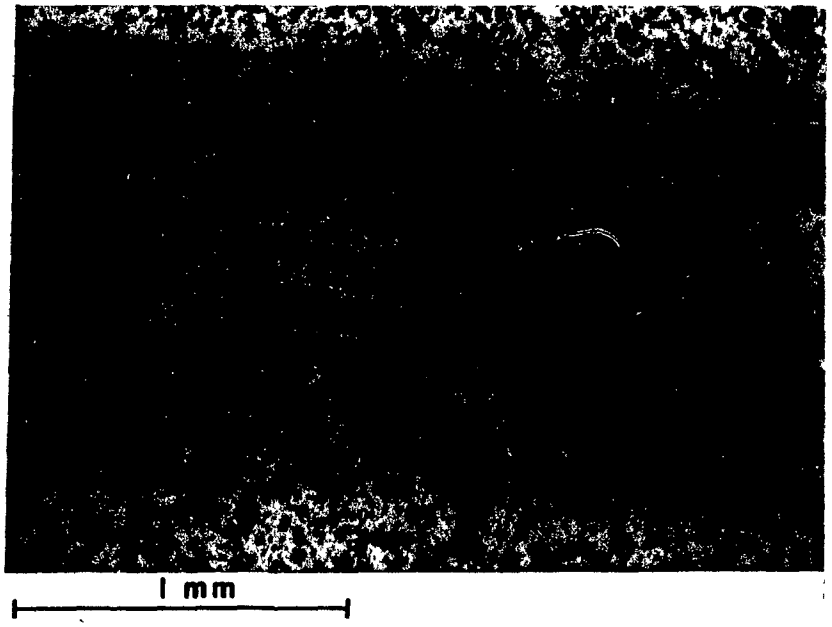

Fig. 8 Microphotograph of sulphide-facies iron formation. The banding is caused by the lamination of pyrrhotite (light mineral) and clay-sized silicate minerals (dark minerals). Note the slight intergrowth of sulphides and silicates.

that the sulphides are an original syngenetic component of these sediments.

Rhythmically laminated sandstone-siltstone outcrop at a variety of locations in the study area (Fig. 9). The sandstone layers (Fig. 10) are composed of quartz and minor feldspar, both with commonly sutured grain boundaries, and a finer-grained quartz-feldspar-sericite matrix. The siltstone layers resemble the matrix of the sandstones but contain secondary chlorite and stilpnomelane. The presence of tuff layers interbedded with the siltstones suggests that some of the material in the siltstones may also have been in part volcanogenic.

Light-weathering quartzites occur as beds up to 20 cm thick, usually interbedded with sandstone-siltstone. Framework grains of rounded to subrounded quartz (2 mm) comprise 95% of this lithology; the matrix consists of smaller quartz grains and sericite. Some quartzites near gabbro sill contacts show slight re-crystallization of grain boundaries and possible retrograde replacement of contact metamorphic minerals.

A breccia consisting of cherty argillite fragments within a pyrrhotite matrix occurs at the Frederickson Lake North showing. Similar pyrrhotitic breccias have been reported at this and other sediment-hosted deposits by Fournier (1983). A conglomerate composed of possible volcanic fragments was also reported in the drill core from this showing, and several metres of conglomerate occur 4 km north of the map area along the shoreline of Blais Lake (Griffis, 1945). The Blais Lake conglomerate occurs along strike from

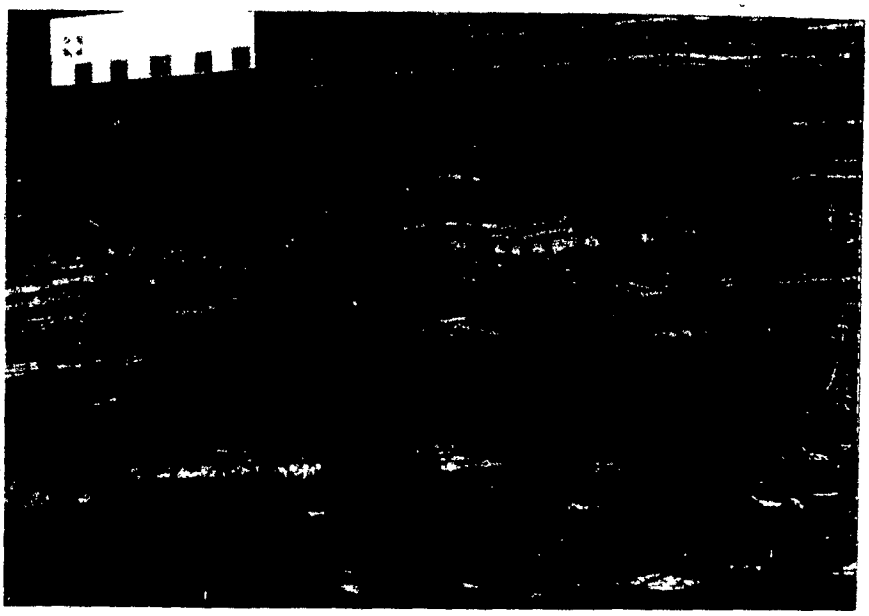

Fig. 9 Interlaminated siltstone (dark layers) and fine-grained sandstone (light layers). Squares on scale bar are one centimetre in length.

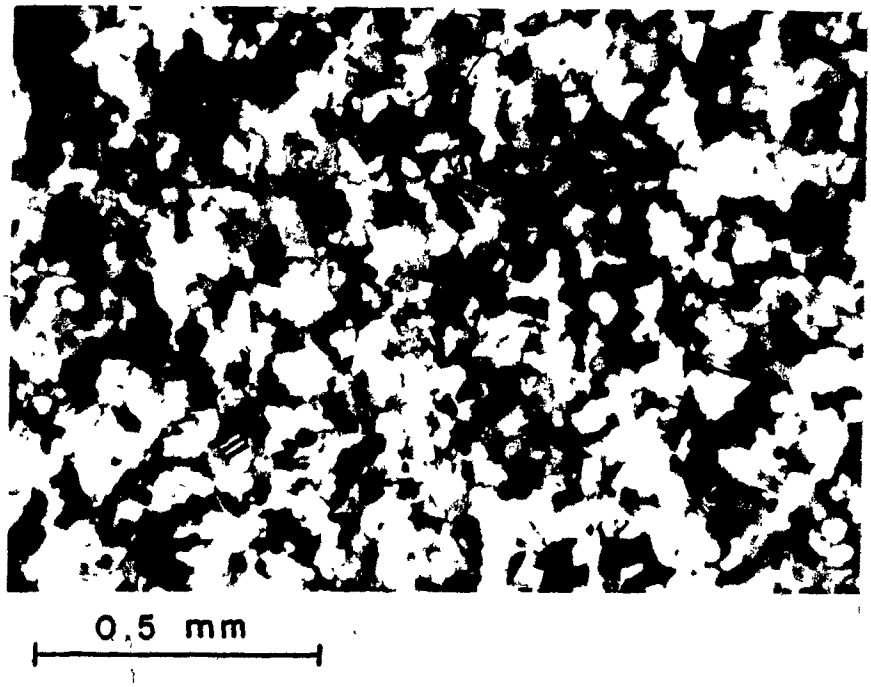

Fig. 10 Microphotograph of fine-grained sandstone. Note the slight suturing of the quartz grain boundaries and twinned plagioclase grains.

the Frederickson Lake breccia although it could not be determined this unit is laterally continuous.

Fine-grained, massive lavas occur at intervals within the upper stratigraphic levels of the Menihek Formation. These lavas, which resemble fine-grained gabbros, can be recognized by their 2 cm-thick weathering rind, which is generally composed of an oxidized orange-red outer layer and an inner grey layer. By contrast, the fine-grained gabbros possess a 2 mm-thick, weathering rind. Although only massive flows were noted in the Frederickson Lake area, poorly preserved pillow selvages are reported in the vicinity of Walsh Lake (Baragar, 1967).

Near the Connolly Lake showing, several 10 cm-thick beds of buff-weathering, dark green tuff are interbedded with fine-grained sandstones and siltstones. The tuffs have a flattened appearance which may reflect flattening of fiamme-like clasts 3 mm long. Chemical analysis indicates that this tuff is of intermediate composition (Table 4).

3.2 Murdoch Formation

The Murdoch Formation occurs in both the Northern and Central Trough and has an estimated thickness of 2000 m (Baragar, 1967). At Frederickson Lake, it unconformably overlies the Menihek Formation along the Walsh Lake Fault. For the most part the Murdoch Formation is composed chlorite-rich schists of possible tuffaceous origin, and rare thin sedimentary horizons and volcanic flows. The schists are composed of chlorite, albite, actinolite, epidote and

Table 4

Composition of sedimentary rocks of the Menihek Formation

	1 argillite	2 sandstone-siltstone	3 tuff
SiO2	41.6	67.3	59.9
Al2O2	6.7	14.7	12.0
Fe2O3	37.6	8.3	15.6
MgO	3.06	2.00	3.32
CaO	0.63	0.15	0.07
Na2O	1.26	1.16	0.30
K2O	0.83	3.69	2.68
TiO2	0.59	0.38	0.38
MnO	0.12	0.05	0.32
P2O5	0.11	0.05	0.03
LOI	7.57	2.87	4.45
TOTALS:	100.07	100.65	99.05

1 average of three samples
2 average of two samples
3 one sample

magnetite. The volcanic flows are compositionally similar but appear to contain less albite. This formation is of greenschist facies metamorphic grade and exhibits complete recrystallization. This contrasts with the lower grade of metamorphism that characterizes the Menihek Formation on the west side of the Walsh Lake fault. Fournier (1983) correlated the Murdoch Formation with the minor mafic pyroclastic tuffs described from the Menihek Formation (Baragar, 1967).

3.3 Thompson Lake Formation

The Thompson Lake Formation consists of 700 m of sediments overlying the Murdoch Formation. The contact is not exposed east of the Frederickson Lake area, although regional mapping to the northwest indicates conformable contacts (Baragar, 1967). East of Frederickson Lake, where the entire Thompson Lake Formation is exposed, it exhibits a fining-upwards cycle composed of basal greywacke, intermediate rhythmically layered siltstone-sandstone and an upper unit of black shale (Fournier, 1983). Fournier (1983) suggested that this formation is a deeper water equivalent of the sedimentary component of the Menihek Formation.

3.4 Willbob Formation

East of Frederickson Lake the Willbob Formation overlies the Thompson Lake Formation. The bulk of this formation, which is 1,500 m thick, consists of massive and pillowed volcanics, and minor interflow siltstone and shales. Fournier (1983) correlated this formation with volcanic rocks that occur in

the upper stratigraphic levels of the Menihek Formation. On a regional scale this formation is commonly correlated with the Hellancourt volcanics of the Northern Labrador Trough. The informal name Doublet-Hellancourt is often applied to the dominantly volcanic rocks that occur above the cycle II sediments. Baragar (1967) reported that three horizons of glomeroporphyritic basalt occur within the Willbob Formation, although tectonic repetition by faulting and folding could be responsible for the multiple occurrences.

3.5 Montagnais Group

Gabbroic sills of the Wakuach Gabbro invade both the Knob Lake and Doublet Group. Sills present within the Doublet Group have been referred to as metagabbro (Baragar, 1967; Fournier, 1983). They are identical to the sills in the Knob Lake Group except for their higher metamorphic grade. Amphibolite bodies within the Laporte Group to the east may also represent metamorphic equivalents of the Wakuach Gabbro. Fournier (1983) reported that ultramafic sills were much less common in the Northern Trough than in the Central Trough, although this feature could reflect different levels of erosion in these two areas. Within the Frederickson Lake region, several varieties of mafic sills belonging to the Montagnais Group are present. Folding of the gabbro-sediment sequence south of Jimmick lake indicate that the sills were injected prior to regional deformation.

3.5.1 Ordinary Gabbro Sills (Fig. 11)

The term "ordinary gabbro" was proposed by Baragar (1960) to describe all non-glomeroporphyritic sills and is retained in this thesis. Ordinary gabbro sills comprise at least 85% of the map area. Individual sills can be traced for up to 6 km, and for up to 30 km in other areas of the Trough (Baragar, 1967). Most sills maintain a constant thickness along strike, although several sills appear to pinch out. Typical sills are 400 to 600 meters thick and display a vertical zonation commonly attributed to in situ magmatic differentiation (e.g. Baragar, 1967). Thinner ordinary gabbro sills are vertically unzoned.

The lowermost portions of the differentiated gabbro sills (Fig. 11) are usually composed of two rock types, a finer-grained chilled margin and an overlying porphyritic zone. In the chilled margin, pyroxene pseudomorphs composed of chlorite and actinolite occur within a matrix of plagioclase microlites. Away from the chilled margin, embayed but unaltered anhedral augite grains 3 mm in length occur within a matrix of fine-grained plagioclase laths. Sporadic orthopyroxene grains up to 10 mm in length are completely pseudomorphed by bastite. Saussuritized plagioclase phenocrysts up to 2 cm in diameter are also irregularly distributed within the porphyritic zone, but never comprise more than 2% of the rocks. At some localities, lower chilled margins are marked by the incomplete alteration of clinopyroxene. This has created a rock with irregular light (unaltered clinopyroxene) and dark (actinolite and chlorite)

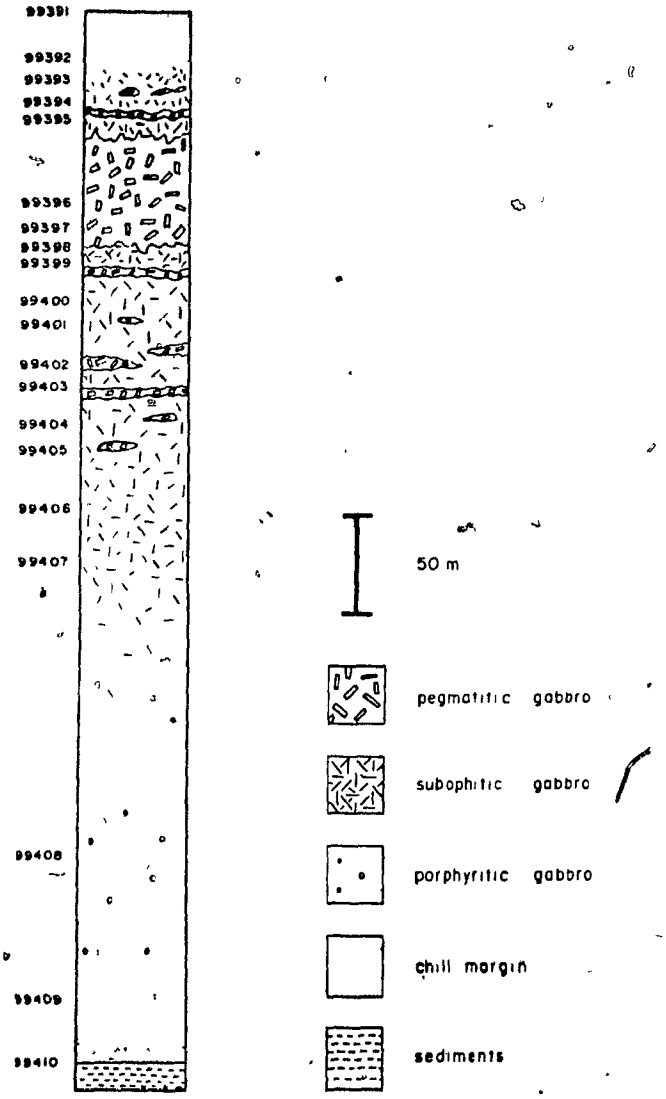

Fig. 11 Generalized stratigraphic section of an ordinary gabbro sill west of Connolly Lake. The numbers refer to chemical analyses listed in Appendix 1.

patches. This texture can be confused with primary textures of the glomeroporphyritic gabbros.

The bulk of a typical ordinary gabbro sill is fine-to medium-grained, with a sub-ophitic to ophitic texture. There is a gradual increase in grain size from the base of the sill to the transition with the overlying pegmatitic zone. The lower regions of the typical sill are characterized by irregularly shaped augite crystals within a matrix of fine-grained plagioclase laths. Pseudomorphs of serpentine and chlorite after orthopyroxene are also present. At higher levels, augite crystals become more euhedral and sometimes exhibit altered exsolution lamellae of orthopyroxene. As the pegmatitic zone is approached, there is an increase in the degree of transformation of matrix minerals to epidote, chlorite and actinolite.

The contact between the central and upper zones of a typical ordinary gabbro sill is transitional and is marked by the first appearance of pods and veins of gabbroic pegmatite. The transition to massive pegmatite takes place over an interval of approximately 60 m. The pegmatitic zone is characterized by large, tabular augite crystals up to 3 cm in length, an increased quartz content, and the appearance of quartz-potassic feldspar intergrowths (granophyre). Plagioclase grains in this zone are generally intensely saussuritized, although unaltered plagioclase grains (An 50) can also occur. Margins of augite crystals are replaced by actinolite and chlorite. In some gabbro sills, the clinopyroxenes in the pegmatitic zone have been completely

replaced by actinolite and minor stilpnomelane.

3.5.2 Glomeroporphyritic Gabbro Sills

Glomeroporphyritic gabbro is the most distinctive rock unit in the field (Figs. 12, 13), and is known by a variety of names including leopard rock, blotchy gabbro, anorthositic gabbro, feldspathic gabbro and spotty diorite. The presence of glomeroporphyritic gabbros in the sediments of the Upper Knob Lake Group, together with the occurrence of pillow lavas with glomerophenocrysts of plagioclase at the base of the Doublet Group, suggests that these gabbros occupy a specific stratigraphic interval within the Labrador Trough (Sauvé and Bergeron, 1965).

Within the Frederickson Lake region, two facies of this gabbro can be distinguished on the basis of plagioclase glomerophenocryst content (Fig. 14). Gabbro sills with greater than 65% glomerophenocrysts are designated anorthositic, while gabbro sills with 10-65% glomerophenocrysts are referred to as glomeroporphyritic. In the study area, glomeroporphyritic and anorthositic facies were never observed in the same sill.

In other areas of the Trough, ordinary gabbro sills invade the core zones of glomeroporphyritic gabbro sills to form composite intrusions, and a complete gradation between the anorthositic facies and non-porphyritic facies may be observed (Fig. 14; Baragar, 1967). Within the Frederickson Lake area, rare cross-cutting relations demonstrate that glomeroporphyritic gabbros are slightly younger than the

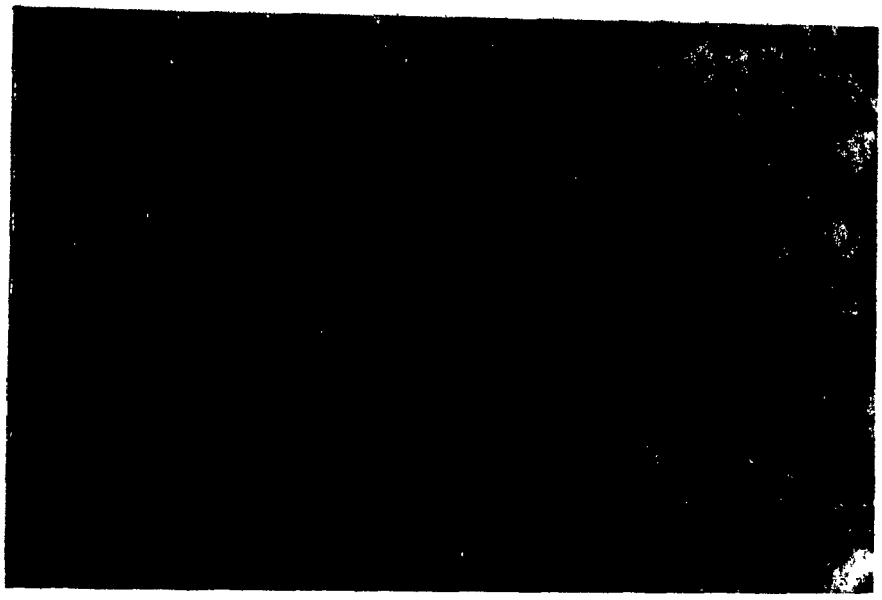

Fig. 12 Outcrop photo of an unbanded glomeroporphyritic gabbro. The white patches are glomerophenocrysts of plagioclase. The scale is given by the pencil (15 cm).

Fig. 13 Outcrop photo of banded glomeroporphyritic gabbro, showing plagioclase glomerophenocrysts concentrated into light-coloured bands. Geological hammer for scale.

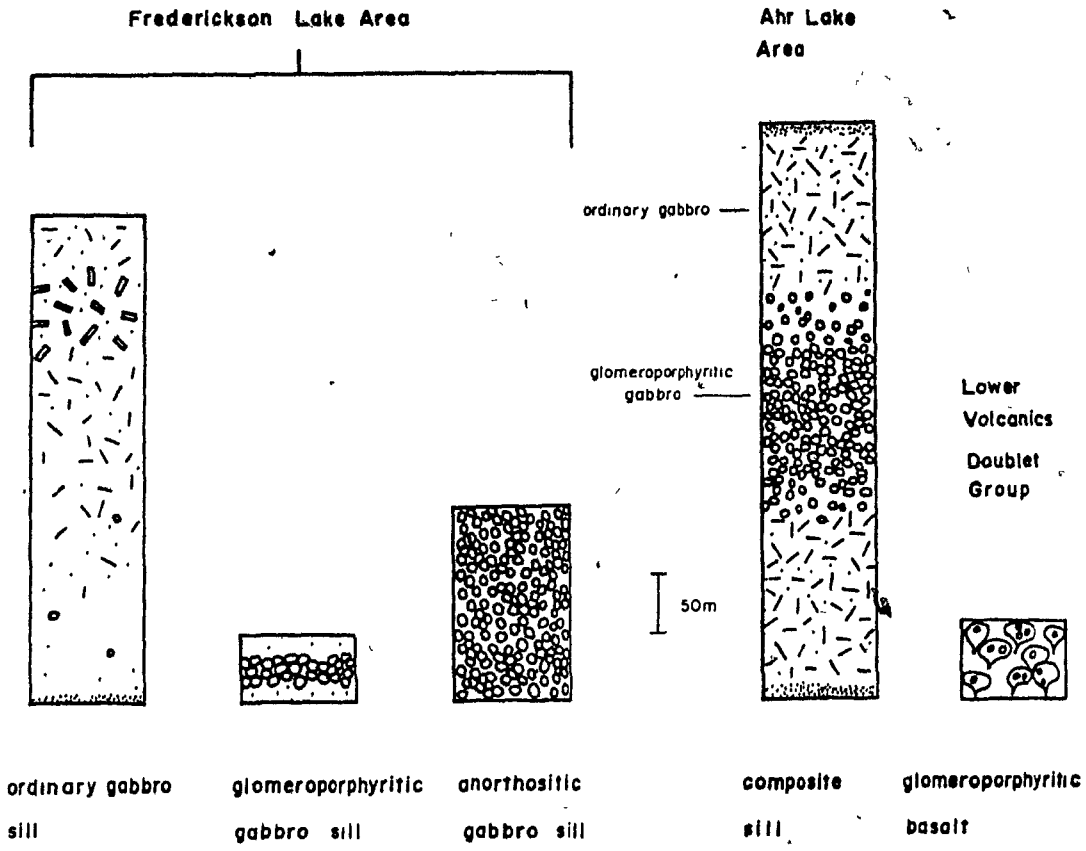

Fig. 14 Schematic diagram illustrating the differences between ordinary, glomeroporphritic and anorthositic gabbros in the Frederickson Lake study area. Note that the ordinary and anorthositic gabbros appear to represent end members containing respectively, the least and the most plagioclase glomerophenocrysts. Also illustrated are stratigraphically equivalent composite gabbro sills of the Ahr Lake area of the North-Central Trough (From Baragar, 1967) and glomeroporphyritic basalts of the Doublet Group.

ordinary gabbro sills (Fig. 15). Outside the map area, glomeroporphyritic sills may also be older than the ordinary gabbros sills (Baragar, 1967; Wares, pers. comm., 1987). On the basis of extensive work on the magmatic rocks of the Labrador Trough, Baragar (1960, 1967) concluded that all intrusive and extrusive rocks were of the same generation.

Glomeroporphyritic sills have a maximum observed thickness of 50 m (Fig. 16) in the Frederickson Lake area. Typically, plagioclase phenocrysts are concentrated near the centre of the sill. In the vicinity of the Frederickson Lake South showing, plagioclase glomerophenocrysts are concentrated in two major bands within the sill. Glomeroporphyritic sill margins are sparsely porphyritic and, by themselves, could be mistaken for non-porphyritic gabbros.

Banding within glomeroporphyritic sills occurs on both a centimetre and metre scale (Fig. 13) and is believed to have been produced by magmatic flow within the sill (Baragar, 1967). These gabbros are composed of saussuritized plagioclase glomerophenocrysts in a groundmass of less saussuritized plagioclase, clinopyroxene, orthopyroxene and olivine psuedomorphs. In hand specimen, the glomerophenocryst cores appear dark as a result of saussuritization, while the rims are pale grey. Glomerophenocrysts are up to 10 cm in diameter and are composed of clusters of plagioclase phenocrysts up to 1 cm in diameter (Fig. 17). Core zones are almost completely transformed to secondary clinozoisite and albite. Glomerophenocryst rim zones (Fig. 18) are composed of fused plagioclase phenocrysts, each of which has

Fig. 15 Glomeroporphyritic gabbro dyke crosscutting an ordinary gabbro sill, Frederickson Lake South showing. Location is given in Figure 30. The pencil is 15 cm in length.

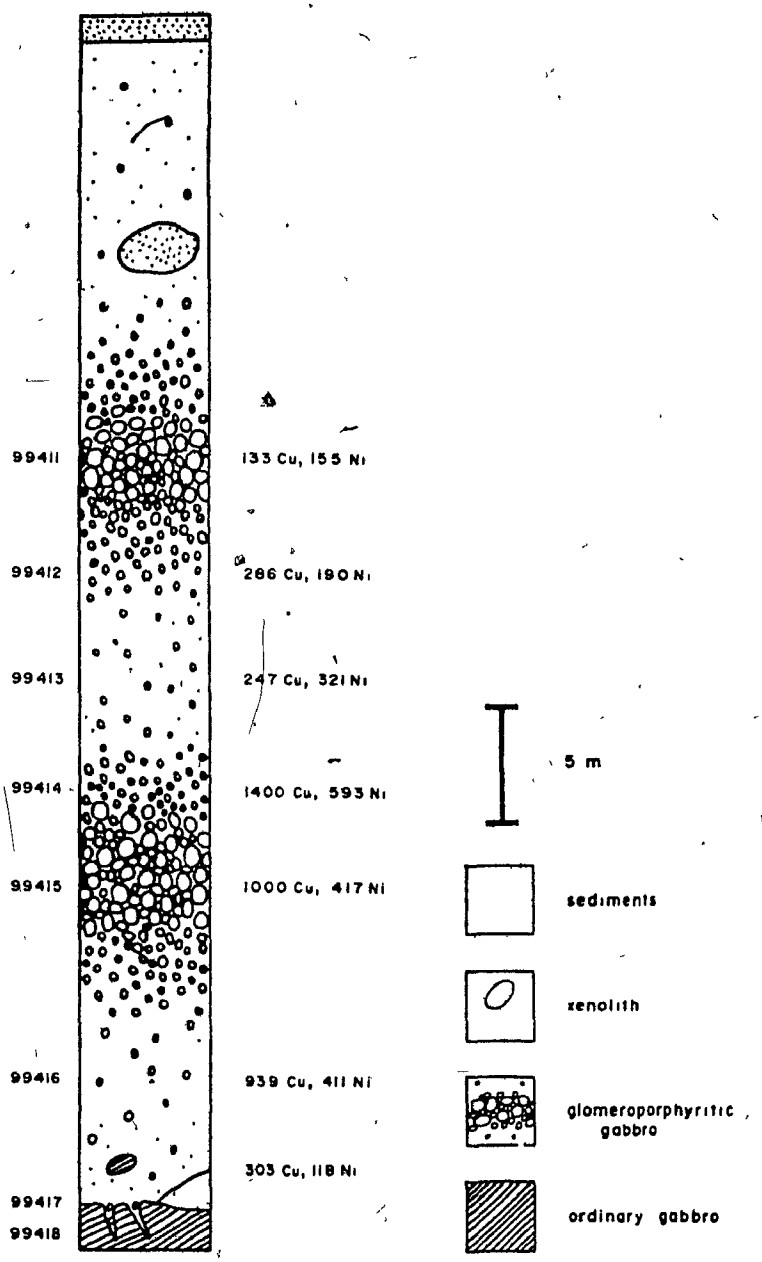

Fig. 16 Generalized stratigraphic section of a glomeroporphyritic gabbro sill at the Frederickson Lake South showing. The numbers at the left refer to chemical analyses (Appendix 1), while numbers to the right are Ni and Cu concentrations in ppm. Note that the highest base metal values occur towards the centre of the sill.

a central saussuritized core. In addition, plagioclase phenocrysts of the rim zone usually exhibit growth zoning (Fig. 19).

Glomerophenocryst clustering and agglomeration occur to varying degrees (Fig. 20). Clusters range from two phenocrysts to several tens of phenocrysts. In several sills the long axis of the clusters is parallel to flow banding (Fig. 21). This texture suggests that flow within the sills was responsible for uniting originally separate plagioclase phenocrysts and that the late plagioclase growth evidenced by the growth rims was responsible for holding the clusters together.

Anorthositic gabbros contain more plagioclase glomerophenocrysts than glomeroporphyritic gabbros. In the study area, all Cu-Ni sulphide mineralization was restricted to the glomeroporphyritic facies; the anorthositic gabbros were barren.

3.6 Local Structure

Within the study area, the gabbro-sediment sequence strikes northwest and dips 45 to 90 degrees northeast. This sequence is terminated at a low angle by the Walsh Lake Fault (Fig. 4; Map 1). South of Jimmick lake, the gabbro-sediment sequence is tightly folded into an antiformal syncline, the western limb of which is overturned (Fig. 22). A similar synclinal structure is visible on aerial photographs immediately west of the Jimmick Lake antiformal syncline. The lack of an antiformal structure between these two synforms suggests that they are separated by a NW-striking fault. A

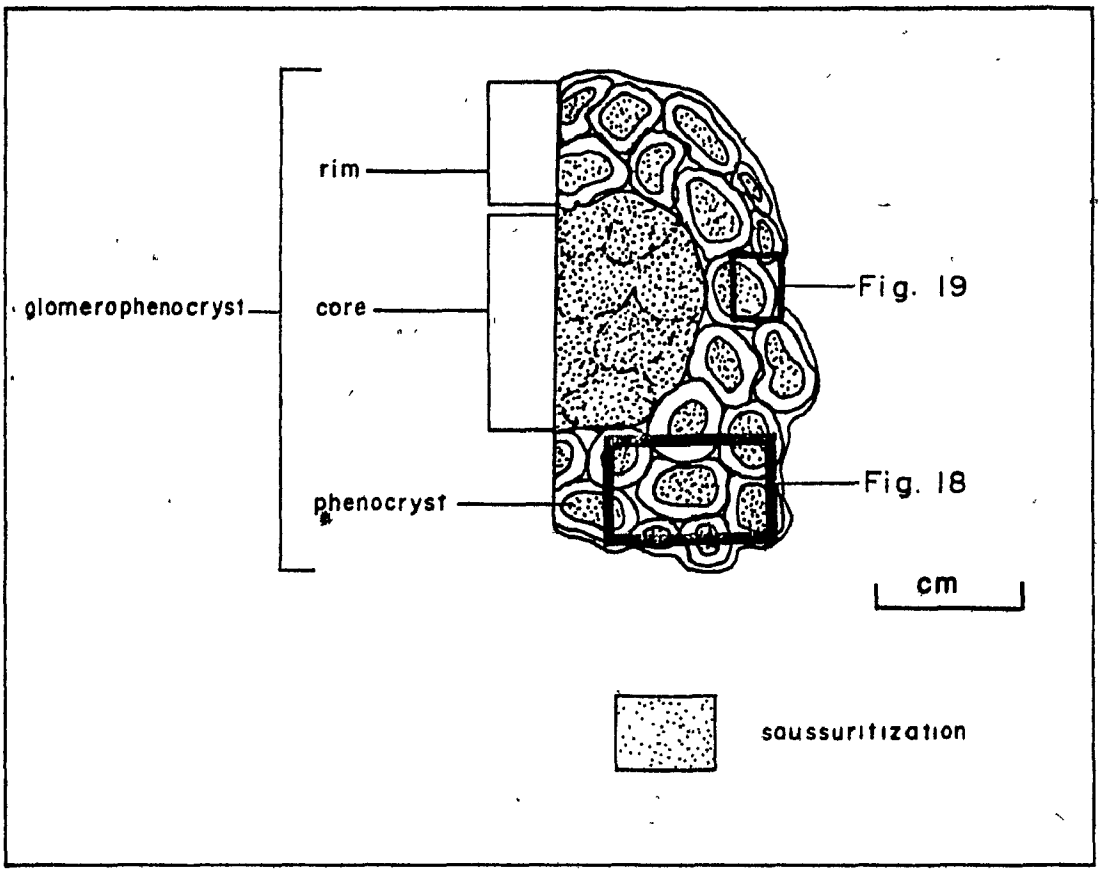

Fig. 17 Generalized diagram of a plagioclase glomerophenocryst. Saussurization, represented by black dots, is confined to the core of the glomerophenocryst and to the cores of the smaller phenocrysts which comprise the rim zone.

Fig. 18 Rim zone of a plagioclase glomerophenocryst. Each rim zone phenocryst has a centralized zone which is saussuritized. See Figure 17 for the location of the photograph.

Fig. 19 Growth rims on a plagioclase phenocryst in the rim zone of a glomerophenocryst. The core of the phenocryst is saussuritized. See Figure 17 for the location of the photograph.

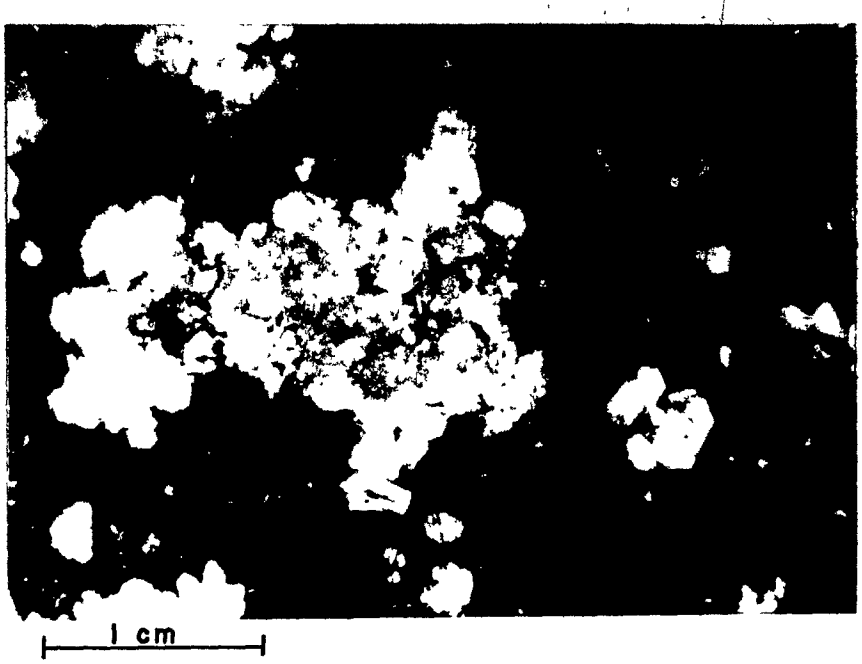

Fig. 20 Hand specimen photograph of a glomeroporphyritic gabbro showing both small and large plagioclase glomerophenocrysts.

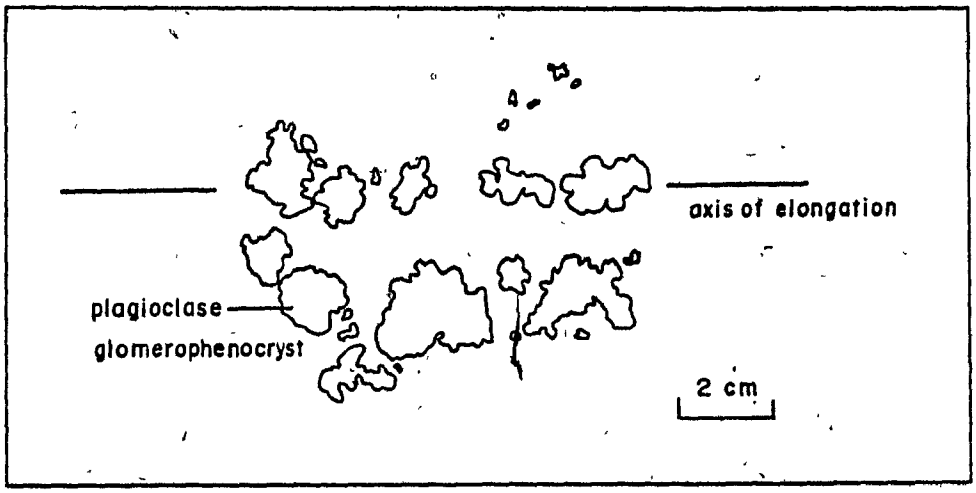

Fig. 21 Tracing of a glomeroporphyritic hand sample. Note the elongation of plagioclase clusters parallel to the banding of the plagioclase clusters.

NW-striking fault is also interpreted to occur between the Jimmick Lake antiformal syncline, and strata to the east, as both gabbro-sediment sequences have similar facing directions. Baragar (1967) described the Frederickson Lake region as a NE facing homocline, but the recognition of these faulted synforms suggests that the map area lies on the limbs of large regional isoclinal folds that have been detached by faulting.

Further evidence for tectonically induced stratigraphic repetition in the Frederickson Lake region comes from the regional mapping. Glomeroporphyritic gabbros are interpreted to occur at the upper levels of the Menihek Formation. The occurrence of abundant glomeroporphyritic gabbro sills within the Menihek Formation between Attikamagen Lake 10 km west of the map area, and the Walsh Lake fault suggests repetition of strata in this region by a combination of isoclinal folds and NW-striking faults. A more detailed elucidation of the structure in the study region is hampered by the paucity of sedimentary rock outcrops, and the lack of penetrative structures in the massive gabbros.

In addition to the large folds which have affected the gabbro-sediment sequence, minor tight folds with NW-trending hinges are locally developed in the sediments (Fig. 23). The fold axes in the sediments parallel those of the regional fold described above. Differences in observed fold wavelengths are probably caused by the competency contrasts of thick gabbro sills and thin sedimentary units (cf. Hobbs et al., 1967).

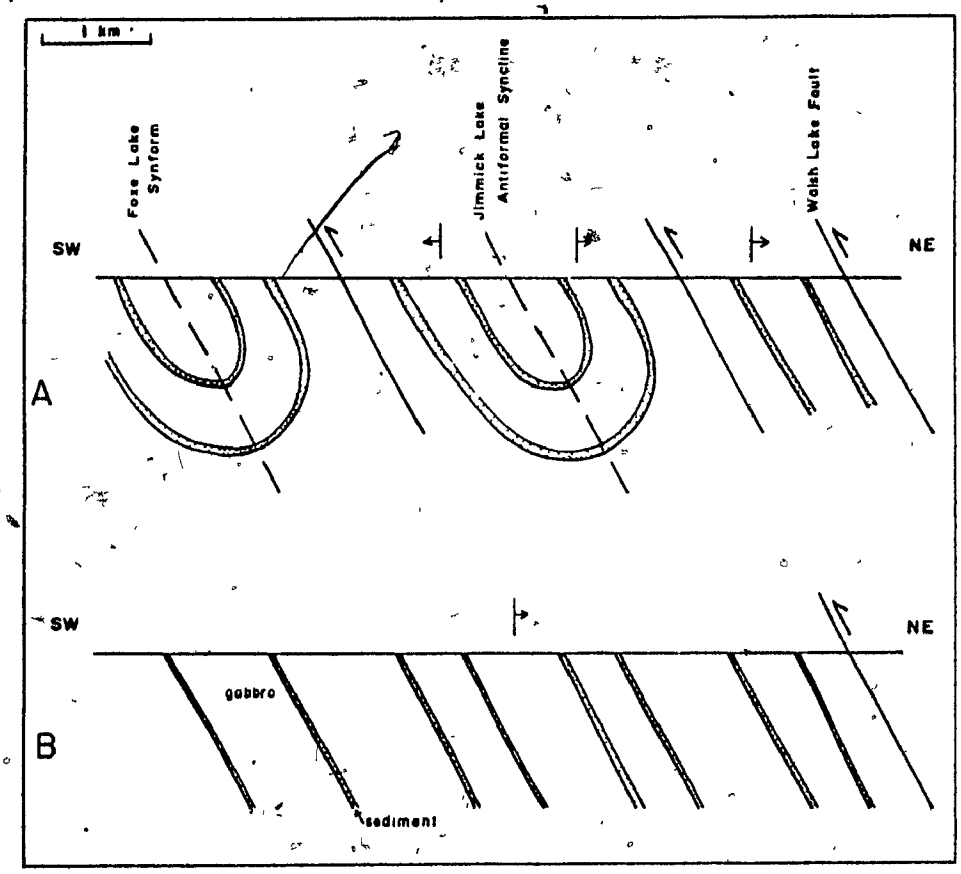

Fig. 22. Schematic cross section across the southern part of the study area. In (A) the gabbro-sediment sequence is interpreted to be folded into synclinal structures separated by northwest-trending faults. Older interpretations (B) inferred that the gabbro-sediment sequence formed a northeast-facing homocline (Baragar, 1967, Fournier, 1983). Refer to Figure 2 for the location of the cross section. (Refer to Map 1.)

3.7 Local Metamorphism

The effects of regional and contact metamorphism are subtly expressed within the Frederickson Lake area. Mafic rocks belong to the sub-greenschist facies (Dimroth and Dressler, 1978) and are characterized by the presence of pumpellyite, chlorite, actinolite, and epidote. Clinopyroxenes are generally preserved, although they are often turbid and are replaced on the rim zones by chlorite and amphibole. Orthopyroxenes and possible olivine pseudomorphs are completely transformed to chlorite, amphibole and serpentine. Plagioclase is often saussuritized; Baragar (1967) has proposed a late magmatic origin for some of the saussuritization.

Siltstones and the matrices of sandstones exhibit the development of sericite, stilpnomelane and chlorite. Quartz grains within the sandstones are recrystallized in some samples. Plagioclase framework grains are unaltered, confirming the low grade of metamorphism.

Argillaceous sediments along the margins of gabbro sills are commonly compact, well indurated, and exhibit a slight conchoidal fracture, but in general lack the development of phaneritic hornfels textures caused by contact metamorphism. The limited contact metamorphic effects in argillites of the Labrador Trough have been attributed to the intrusion of the gabbroic sills into wet sediments (Dimroth and Dressler, 1978) and also to the high level of emplacement of the sills (Wardle and Bailey, 1981). In contrast, arenaceous sediments within several meters of gabbroic sills commonly display diffuse

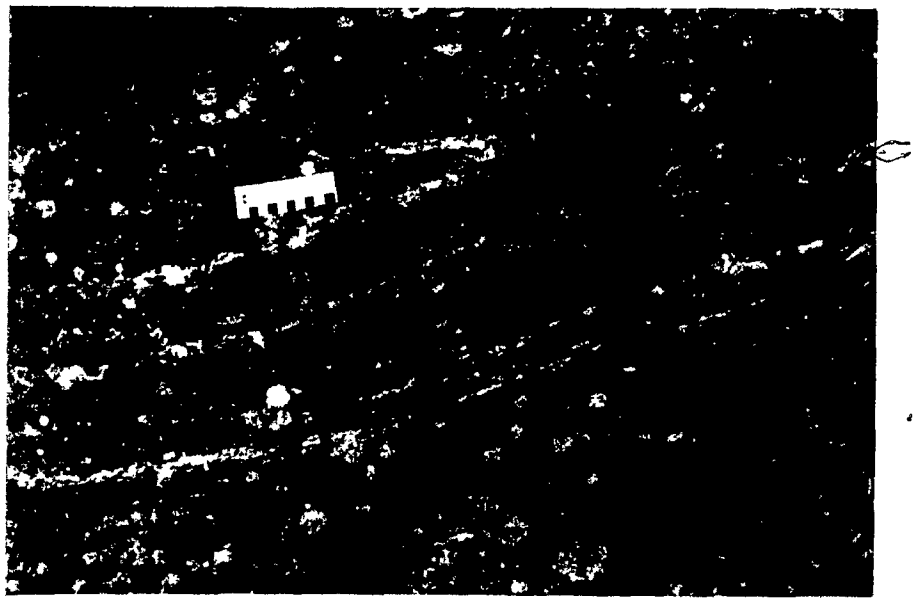

Fig. 23 Outcrop photograph of a local, tight fold in the sediments of the Menihek Formation at the Gossan Lake showing. The more competent gabbro sills on either side of the sedimentary band at this locality are not folded. The squares on the scale bar are one centimetre in length.

patches of light-coloured minerals up to 2 mm in diameter, in a darker matrix. The light-coloured patches consist of quartz within a darker, finer-grained (0.01 mm) matrix rich in chlorite. Sauvé and Bergeron (1965) describe similar "adenoles" from the contact zones of quartz-rich sediments of the Northern Labrador Trough and attribute them to the retrograde replacement of some pre-existing contact metamorphic phase.

CHAPTER 4 GEOCHEMISTRY OF GABBROIC AND VOLCANIC ROCKS

4.1 Frederickson Lake Igneous Rock Suite

Samples analyzed in the present study include ordinary gabbro sills and chilled margins (20 and 7 samples respectively), glomeroporphyritic gabbro sills and chilled margins (8 and 1 respectively), basalts of the Menihek Formation (8), volcanics of the Murdoch Formation (7) and basalts of the Willbob Formation (3). In addition, three analyses of ultramafic sills from Fournier (1983) are discussed. The tholeiitic nature of the Frederickson Lake igneous suite is illustrated in the AFM diagram (Fig. 24) and on a Jensen plot (Fig. 25). The mafic rocks of the Montagnais Group form a distinct cluster of points on Al-Si, Mg-Fe and Ca-Mg plots (Fig. 26). This cluster excludes the ultramafic rocks of the Murdoch Formation (sample set 6) and ultramafic rocks of the Montagnais Group (sample set 7). These latter rocks fall, respectively, within the komatiitic basalt and komatiite fields in a Jensen (1976) cation plot (Fig. 25). It is important to note the geochemical similarity of the basalts of the Menihek Formation with the chilled margins of the ordinary gabbros (Figs. 24-26).

Tectonic discriminant diagrams for basaltic rocks have been developed by Pearce and Cann (1973), Winchester and Floyd (1976), and Pearce and Norry (1979). These diagrams, although developed to classify Paleozoic rocks, are also commonly applied to Precambrian rocks. Basalts of the Menihek Formation and the ordinary gabbro chill margins, rock types most indicative of original liquid compositions, cluster

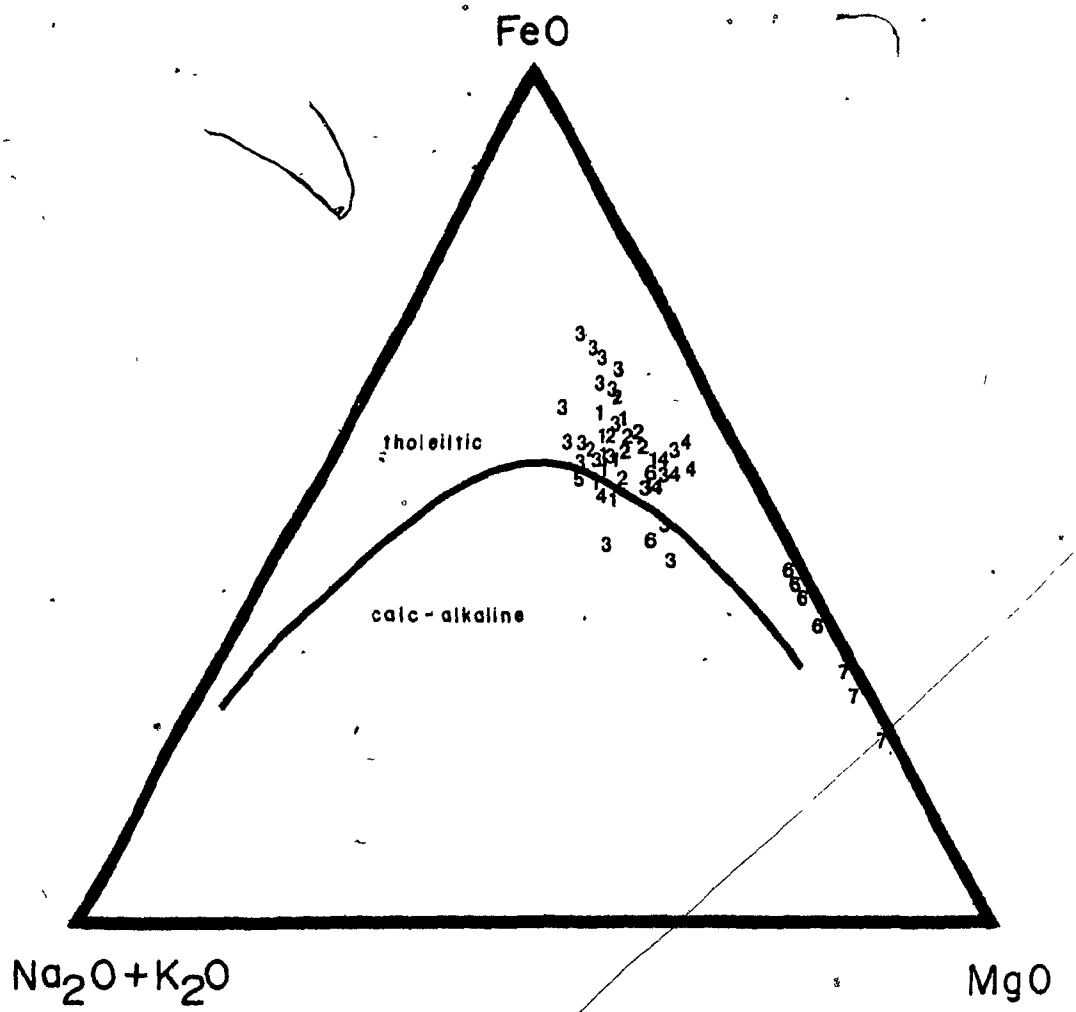

Fig. 24 AFM diagram (Irvine and Baragar, 1971) showing the complete analytical data set. The samples plot mainly in the tholeiitic field.

1=chilled margins of ordinary gabbros
2=basalts of the Menihek Formation
3=ordinary gabbros
4=glomeroporphyritic gabbros
5=chilled margins of glomeroporphyritic gabbros
6=volcanic rocks of the Murdoch Formation
7=ultramafic rocks of the Montagnais group

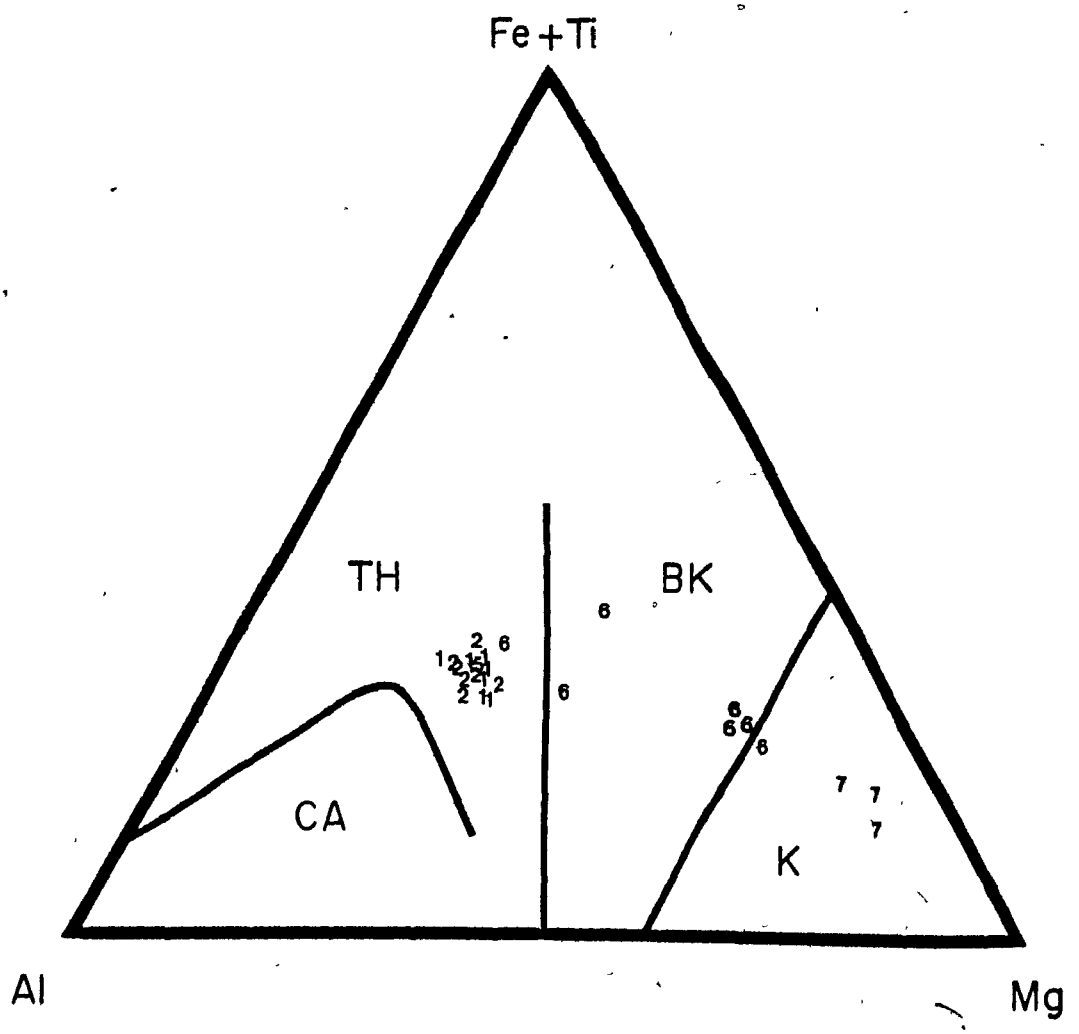

Fig. 25 Jensen (1976) cation plot. Only rocks thought to represent original liquids are plotted. Symbols as in Figure 24. CA=calc-alkaline, TH=tholeiitic, BK=komatiitic basalt, K=komatiite.

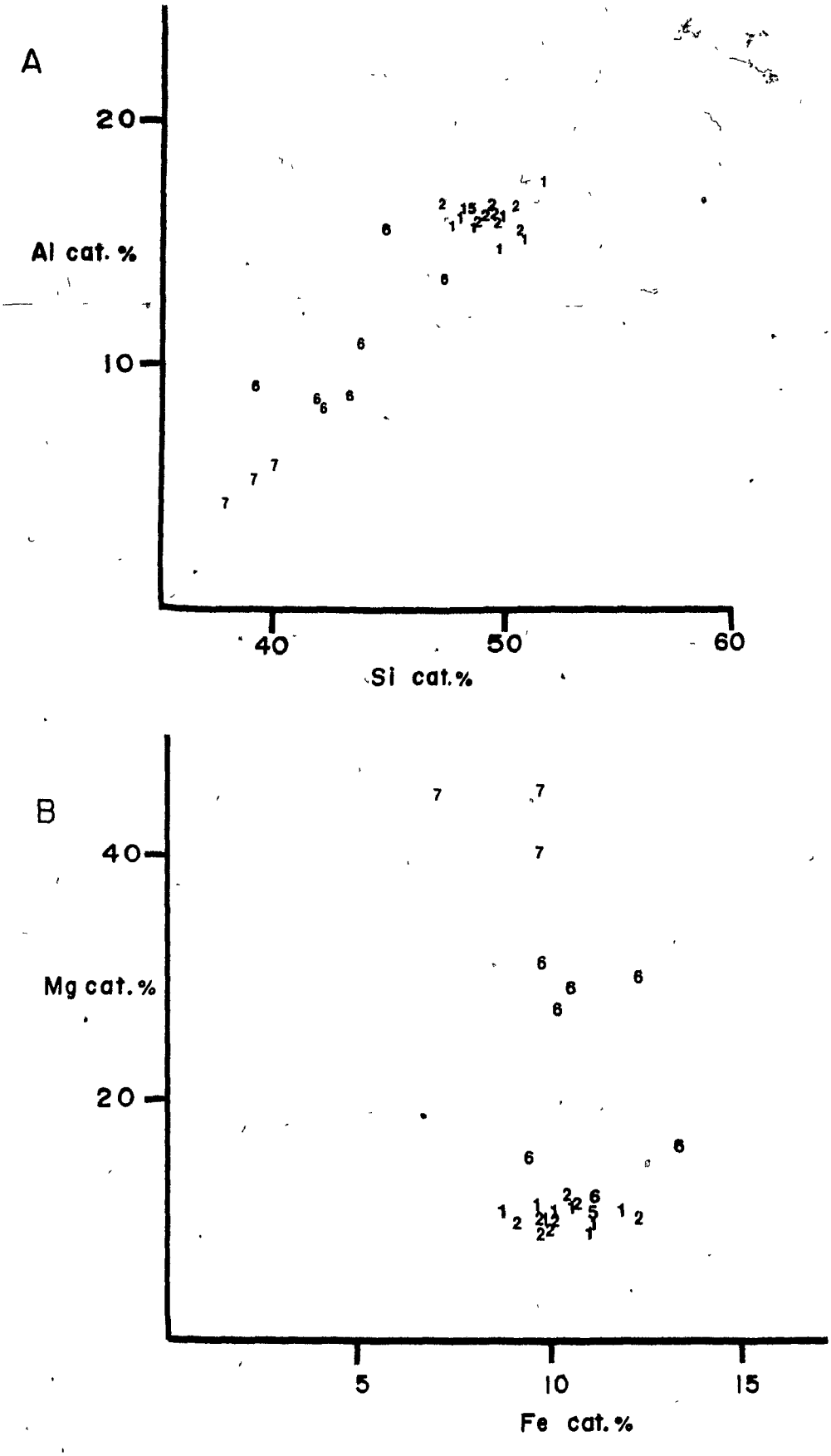

Fig. 26 a,b, Major element cationic variation diagrams. Note the compositional overlap between chill margins of the ordinary gabbros (1) and the basalts of the Menihek Formation (2). Other symbols as in Figure 24.

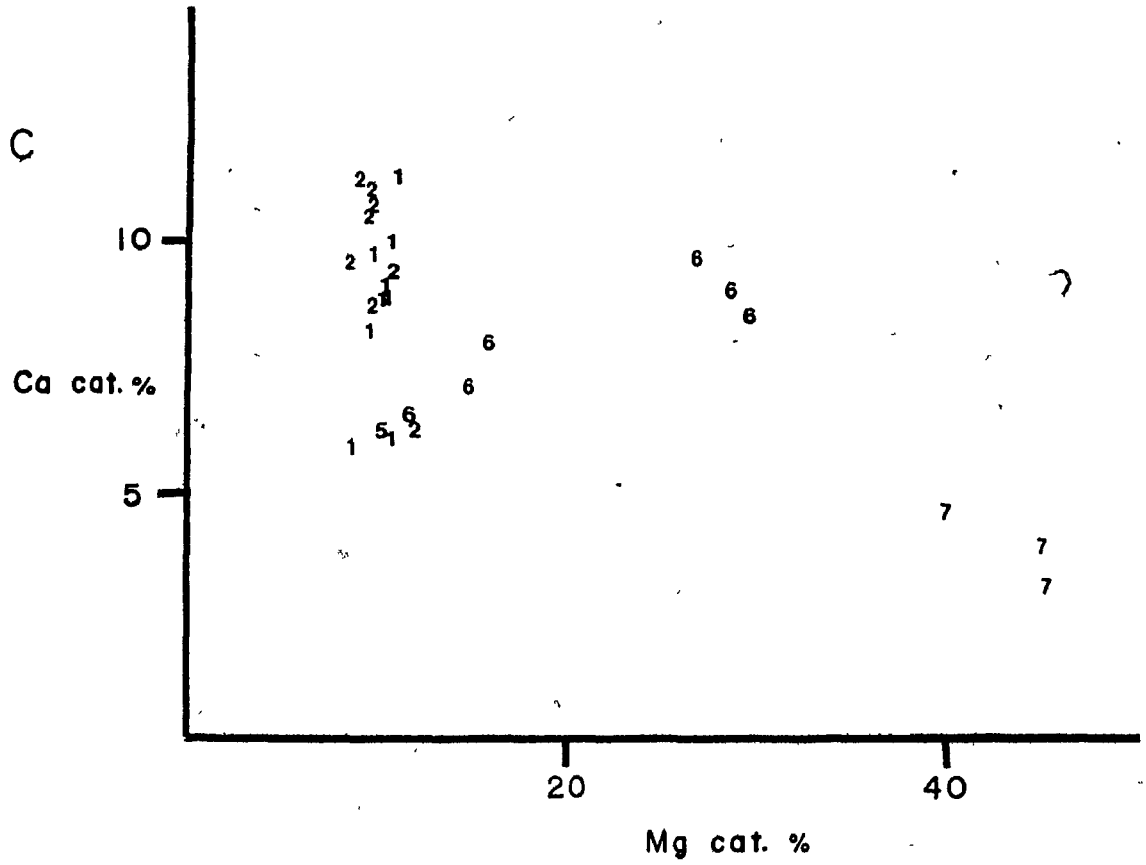

Fig. 26 c · Major element cationic variation diagram. Note the compositional overlap between chill margins of the ordinary gabbros (1) and the basalts of the Menihek Formation (2). Other symbols as in Figure 24.

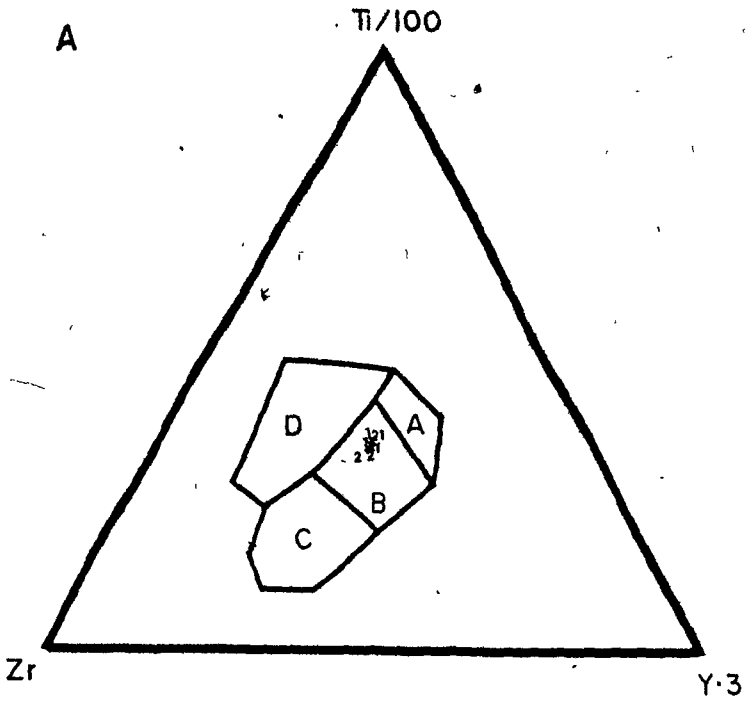

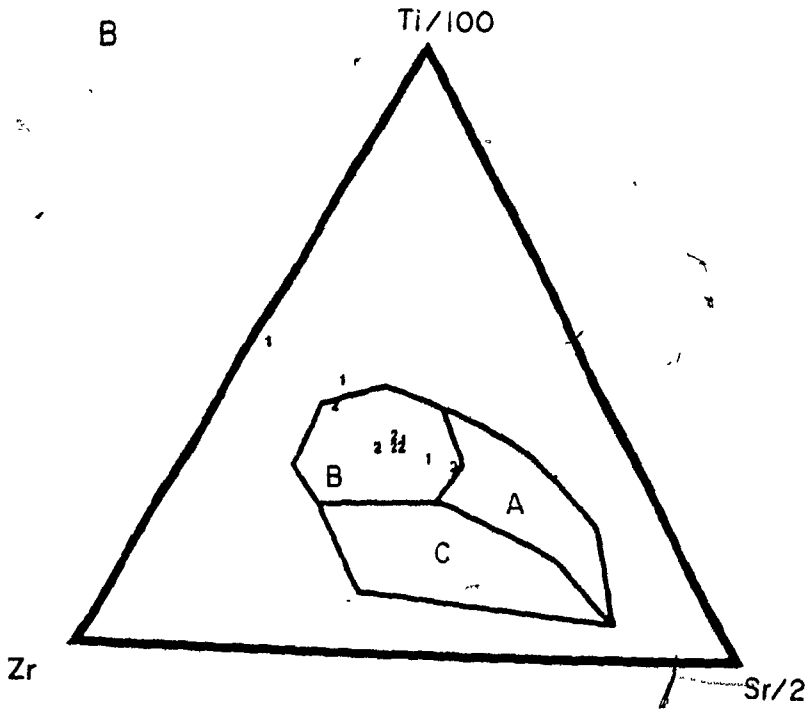

Fig. 27 a,b Tectonic discriminate diagrams (Pearce and Cann, 1973). Note the restriction of gabbro chilled margins (1) and Menihek basalts (2) to the ocean floor basalt field (B).

A=low K tholeiite
B=ocean floor basalt
C=calc-alkaline basalt
D=within-plate basalt

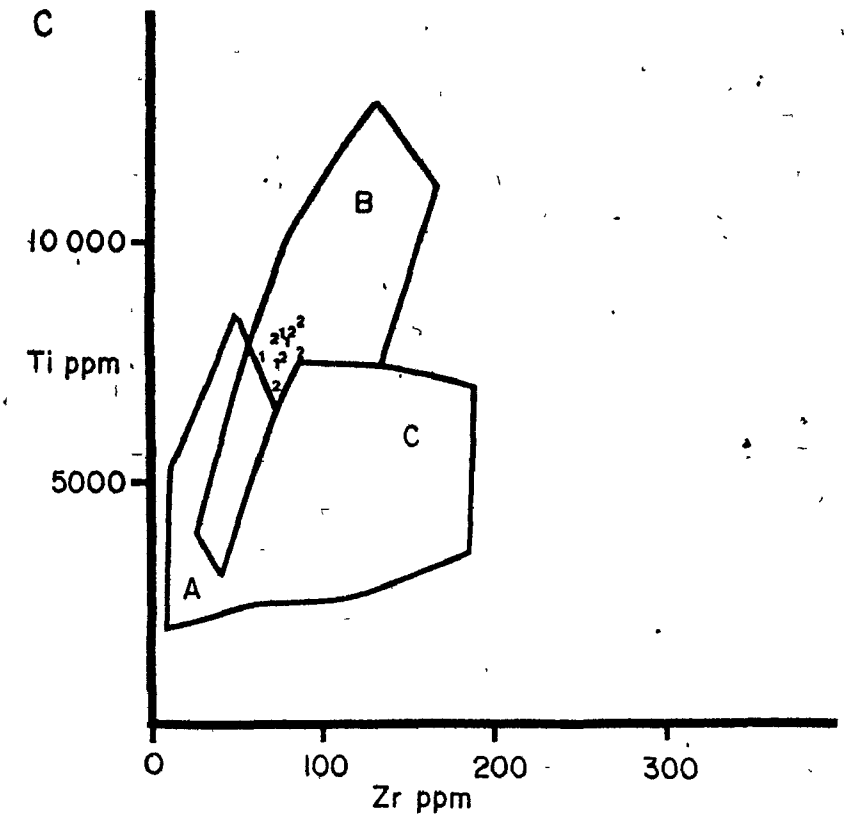

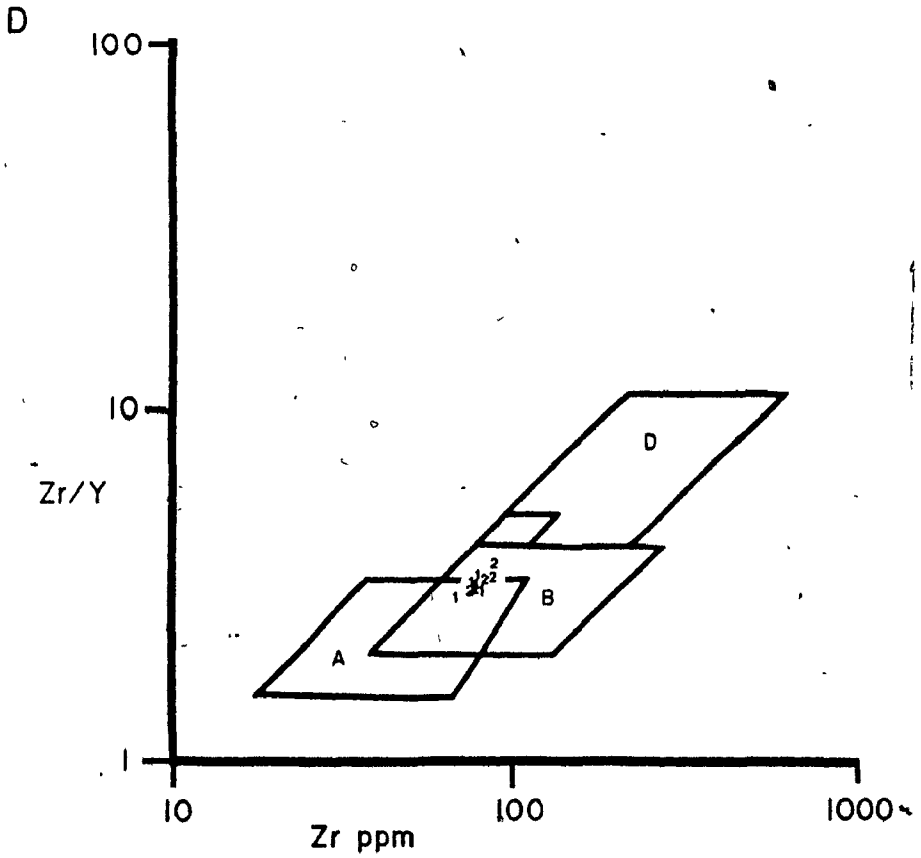

Fig. 27 c,d Tectonic discriminate diagrams (Pearce and Cann, 1973; Pearce and Norry, 1979). Note the restriction of gabbro chilled margins (1) and Menihek basalts (2) to the ocean floor basalt field (B).

within the ocean floor basalt fields in such diagrams (Fig. 27).

Previous extensive studies of the "basaltic" rocks of the Labrador Trough (Baragar, 1960; 1967) have demonstrated both the tholeiitic nature of the Montagnais Group and the derivation of intrusives and extrusives of this Group from a common parental liquid. The limited data base of this study confirms the chemical similarity of the chilled margins of the ordinary gabbros to the basalts of the Menihek Formation.

4.2 Chemical Variation in Ordinary Gabbro Sills

One 500 metre-thick ordinary gabbro sill in the Frederickson Lake area was selected for detailed chemical study (Fig. 11). From bottom to top, this sill shows an overall increase in Si, Ti, Fe and P, and a corresponding decrease in Al, Mg and Ca (Fig. 28). The fluctuations in composition are caused by small scale layering, and, in upper regions of the sills, variable amounts of pegmatitic veining. A reversal in some elemental trends towards the base of the sill suggests that clinopyroxene and orthopyroxene crystals in this part of the sill represent crystal cumulates. Despite minor fluctuations, the overall chemical trends are compatible with in-situ differentiation of a single injection of magma. This is further supported by the similarity of the average composition of the entire sill to its chilled margins (Table 5).

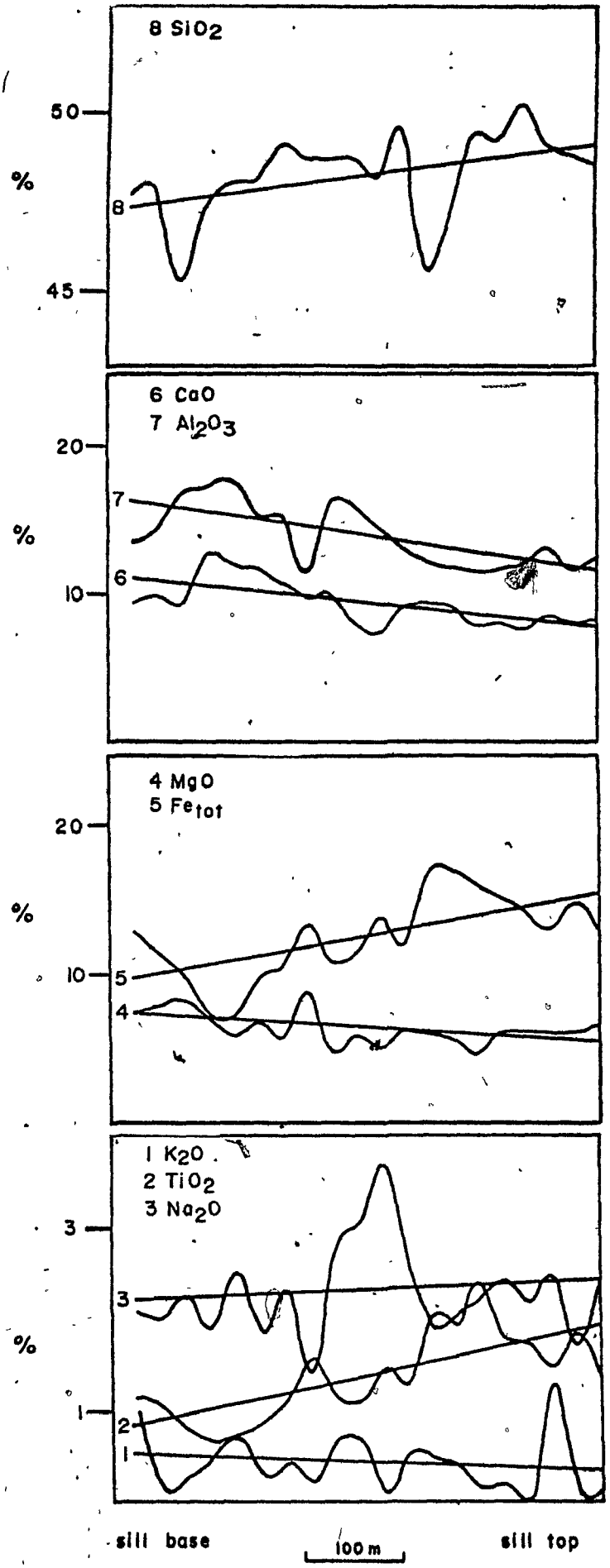

Fig. 28 Chemical cross sections through a 500 m-thick ordinary gabbro sill. Straight lines represent linear regressions of the data.

Table 5 Average Composition of Igneous Rocks (SD = Standard Deviation)

	Ord. Gabbro	SD	Basalt Menih	SD	Volcan Murd	SD	Glom. Gabbro	SD	Gabbro Chill	SD	Basalt Doub	SD
SiO2	48.3	1.21	48.7	1.21	43.4	2.38	45.9	1.12	49.2	1.24	48.0	1.31
Al2O3	14.0	2.00	13.8	0.26	9.21	2.34	15.7	2.00	13.7	0.41	13.9	0.57
Fe tot	14.0	3.02	13.9	1.17	14.9	1.75	13.5	2.06	13.9	1.02	13.3	0.71
MgO	6.40	1.12	6.93	0.55	15.5	5.07	8.01	1.31	7.34	0.29	6.12	0.32
CaO	9.57	1.45	9.20	1.51	7.80	0.88	9.85	1.07	8.67	1.41	10.8	0.49
Na2O	2.33	0.49	2.22	0.66	1.66	1.73	1.69	0.36	2.52	0.50	1.90	0.65
K2O	0.44	0.32	0.31	0.19	0.08	0.06	0.36	0.23	0.78	0.50	0.08	0.03
TiO2	1.37	0.47	1.28	0.09	2.44	0.84	0.97	0.13	1.23	0.07	1.30	0.15
MnO	0.19	0.04	0.21	0.02	0.14	0.03	0.17	0.03	0.30	0.07	0.17	0.02
P2O5	0.10	0.03	0.09	0.01	0.21	0.11	0.08	0.02	0.08	0.01	0.10	0.02
LOI	2.54	0.43	3.30	1.16	3.89	1.24	3.15	0.41	2.29	0.42	3.79	1.23
TOTALS:	99.24	10.58	99.94	6.83	99.23	16.43	99.38	8.74	100.01	5.94	99.46	5.50
Ba	88.4	56.1	101	58.4			58.3	33.1	196	131		
Be	2.00	0.77	0.38	0.70			1.00	0.00	0.43	0.73		
Cd												
Ce	16.8	5.13	22.5	4.61			12.1	0.99	15.7	7.78		
Co	48.6	8.64	42.5	7.50			69.1	22.9	41.0	9.02		
Cr	69.9	81.8	70.0	121			127	92.9	127	113		
Cu	187	91.0	173	66.4			615	454	115	61.4		
Dy	5.80	2.18	1.13	1.96			2.71	0.70	3.86	3.76		
Eu	4.80	1.08	2.63	1.11			4.00	0.53	2.86	1.36		
La	6.90	10.0	3.13	4.99			4.71	3.37	2.43	2.13		
Li	10.2	3.06	12.4	8.09			10.9	2.59	11.0	3.21		
Mo												
Nd	89.0	24.1	54.4	20.7			67.1	6.47	69.3	19.0		
Ni	82.4	50.0	104	6.10			315	159	116	31.0		
Pb									6.57	16.1		
Pr												
Sc	45.9	3.94	42.63	2.39			32.1	5.84	46.1	3.80		
Sm	0.30	0.90										
V	455	199	378	13.7			269	44.5	376	12.7		
Zn	72.6	20.7	96.5	30.9			112	83.2	92.9	16.5		
Ga	19.5	0.50	16.3	6.85			18.0	2.45	10.4	9.26		
Nb	2.50	2.50	0.38	0.99								
Rb	8.00	2.00	10.0	6.60			12.7	10.1	17.0	24.1		
Sr	135	15.0	147	53.5			107	23.3	71.7	71.4		
Ta	4.50	4.50	0.71	1.75			1.67	2.36	1.43	2.26		
Th	1.50	1.50	6.86	1.46			6.00	1.41	4.00	3.63		
U	2.00	2.00	2.00	1.77			1.00	1.41	0.57	1.40		
Y	30.5	8.50	22.9	6.10			19.0	0.00	14.1	12.3		
Zr	97.5	32.5	83.6	4.40			67.3	4.78	43.4	37.8		

major elements in Wt% trace elements in ppm nd = not detected blank space = not analyzed

4.3 Glomeroporphyritic Gabbros

As a result of the mechanical concentration of plagioclase phenocrysts, it was difficult to obtain glomeroporphyritic gabbro samples that were representative of the original liquid compositions. In terms of major element chemistry, some samples from the centres of glomeroporphyritic sills were different from the chilled margin reflecting the mechanical concentration of phenocrysts (for example sample 99411 from the sill interior contains 19.2% Al_2O_3 while the chilled margin sample 99417 contains only 13.6% Al_2O_3). However, glomeroporphyritic chilled margins are similar to those of ordinary gabbros (Table 5, Fig. 26), suggesting a common parental magma. Minor differences in concentrations of Co, Cu, Cr, V and Zn between the chilled margin and the centers of glomeroporphyritic gabbro sills could also reflect the effects of flow differentiation.

Plagioclase compositions reflect the composition of the parental magma from which the plagioclase crystallizes. However, the common saussuritization of glomerophenocrysts in the Frederickson Lake area precludes a simple estimation of their An content. In order to circumvent this problem, a normative calculation was carried out based on chemical analyses of the most feldspar-rich glomeroporphyritic gabbro (sample 99411). This calculation yielded a bulk rock plagioclase composition of An 75, which represents the average of the plagioclase in the groundmass (An 55) and that in the glomerophenocrysts. Thus the composition of the plagioclase glomerophenocrysts is inferred to be greater than

An 75. Corroboration of this is provided by microprobe analyses of small 0.01 mm patches of unsaussuritized plagioclase, which are present in the cores of some plagioclase glomerophenocrysts. These patches yield an average composition of An 82. Theoretically (Nielsen and Duagan, 1983), the chilled margin of the glomeroporphyritic gabbro should crystallize plagioclase with a maximum An content in the range 67-70 not An 75-82. The plagioclase glomerophenocrysts, therefore appear to be too calcic to have formed from a liquid with the composition of the chilled margin.

4.4 Rare Earth Element Analyses

Two basalts of the Menihek Formation, two ordinary gabbro chilled margins, and a glomeroporphyritic chill margin (J-8) have similar, relatively flat patterns with overall abundances approximately ten times chondrite (Fig. 29 a,b,c). As shown earlier, trace element discrimination diagrams place the rocks of the Montagnais Group mainly within the ocean floor basalt field. However the flat REE patterns of these rocks contrast with the LREE depletion of most modern MORBs.

REE data also were obtained for plagioclase phenocryst separates ("plag" and "matrix" in Fig. 29 d,e) and the accompanying groundmass from both the glomeroporphyritic and anorthositic gabbros. The purpose was to determine if the plagioclase glomerophenocrysts were geochemically related to the accompanying matrix. In the anorthositic gabbro, the strong positive Eu anomaly of the phenocrysts and mirror-image

TABLE 6 Rare earth element analyses of igneous rocks from the Central Labrador Trough

	J-7 Gabbro Chill	J-8 Glom Chill	J-11 Menihek Basalt	J-12 Menihek Basalt	J-17 Gabbro Chill	J-19 Glom Chill	J-30 Glom Plag	J-31 Glom Matrix	J-32 An Gab Plag	J-33 An Gab Matrix
La	3.45	2.81	3.54	3.59	3.89	19.3	1.39	3.22	1.65	4.20
Ce	7.80	6.80	8.90	8.90	8.80	35.6	2.20	7.50	4.00	10.0
Nd	5.70	5.00	5.80	6.90	6.80	16.0	1.00	5.10	2.60	9.20
Sm	2.53	2.45	2.69	2.71	2.49	3.65	0.34	1.97	0.98	3.37
Eu	0.82	0.63	1.11	1.13	0.98	1.17	0.37	0.61	0.72	0.79
Tb	0.52	0.56	0.53	0.55	0.58	0.63	0.04	0.38	0.19	0.74
Ho	0.98	0.94	1.08	0.94	0.91	1.08	0.18	0.70	0.24	1.46
Tm	0.31	0.27	0.35	0.49	0.34	0.43	0.07	0.27	0.10	0.46
Yb	2.35	2.29	2.55	2.66	2.58	2.76	0.15	1.92	0.65	3.74
Lu	0.42	0.38	0.39	0.46	0.36	0.34	0.04	0.27	0.10	0.42
Sc	42.5	43.9	42.3	47.0	42.9	31.2	0.19	30.2	2.37	62.4
Cr	161	186	182	187	168	97.2	4.10	116	1.56	76.5
Co	48.1	51.1	44.6	44.3	38.6	18.8	11.1	71.6	5.61	54.2
As	1.62	0.53	0.30	nd	3.77	0.53	nd	nd	nd	nd
Sb	0.10	0.40	0.10	0.10	0.50	0.45	nd	nd	nd	nd
Cs	0.92	1.39	0.76	0.48	1.24	1.23	2.03	1.76	0.87	0.24
Ba	207	33.0	119	188	337	241	244	nd	nd	nd
Hf	1.66	1.28	1.90	2.04	2.13	3.41	0.20	1.45	0.67	2.72
Ta	0.24	0.26	0.14	0.16	0.13	0.53	0.04	0.12	nd	0.64
W	5.18	6.07	7.25	7.72	6.43	6.15	1.34	nd	nd	nd
Th	0.30	0.40	0.40	0.30	0.30	5.40	0.10	0.50	0.20	0.40
U	0.30	0.20	0.10	0.10	0.10	0.90	0.10	0.20	0.10	0.10
Na (%)	1.72	1.61	1.60	1.66	1.73	2.30	1.15	nd	nd	nd

Neutron activation analyses (in ppm) provided by the Geochemistry Laboratory, U. de M.

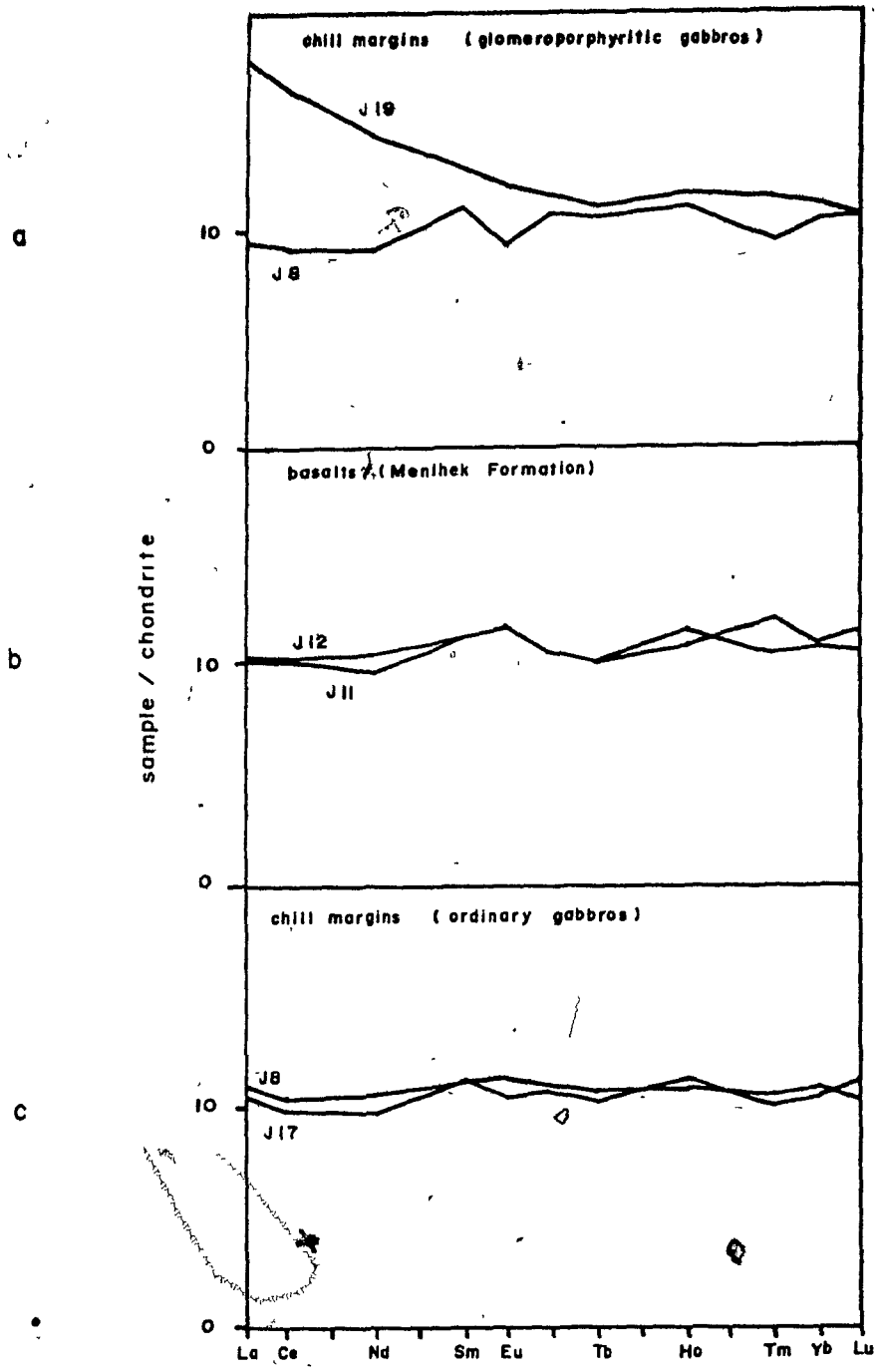

Fig. 29 Chondrite-normalized rare earth element diagrams.

a. Glomeroporphyritic gabbro chilled margins. Note the distinctive LREE enrichment in sample J-19.
b. Basalts of the Menihek Formation
c. Ordinary gabbro chill margins. Patterns are similar to the basalts of the Menihek Formation.

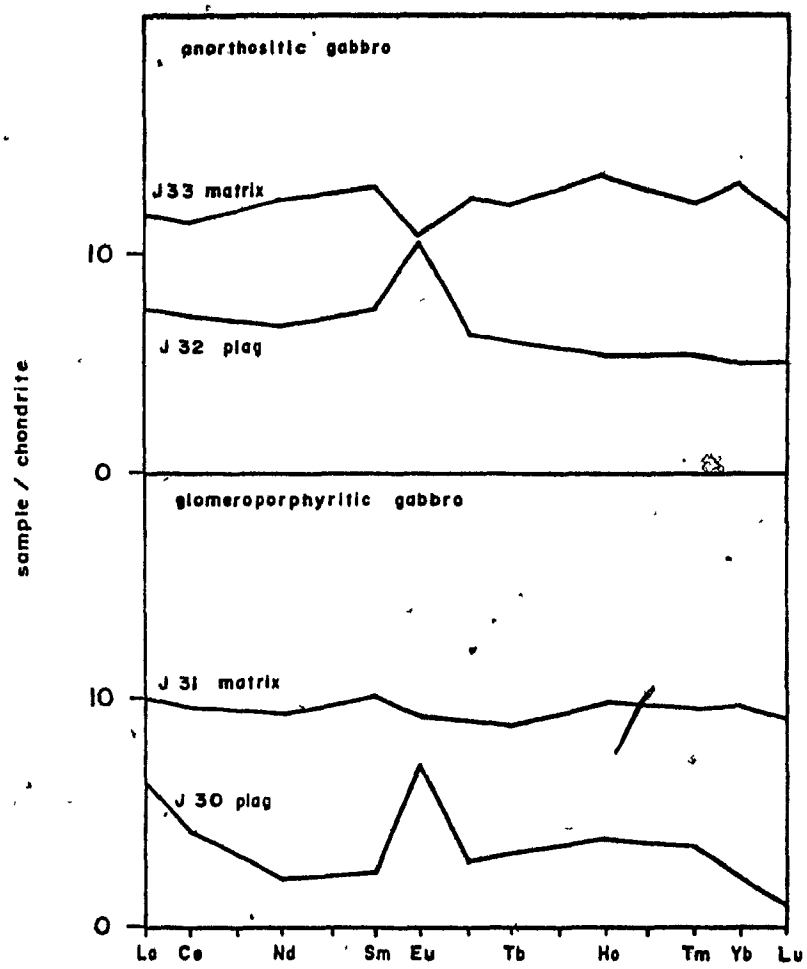

d

e

Fig. 29 Chondrite-normalized (Talyor and Gorton, 1977) rare earth element diagrams.

d. Anorthositic gabbro. Note the mirror image patterns of the matrix and plagioclase separates.

e. Glomeroporphyritic gabbro. The matrix of sample J-31 lacks a Eu anomaly.

pattern of the matrix suggest that the matrix liquid could have precipitated the phenocryst assemblage. The Eu anomaly in this gabbro also may have been enhanced by its high plagioclase phenocryst-matrix ratio (3:1). Growth rims on plagioclase phenocrysts demonstrate the late stage precipitation of plagioclase, which may account for the negative Eu anomaly in the residual matrix. Patterns for the glomeroporphyritic gabbro are harder to interpret because there is no Eu anomaly in the matrix. This suggests, but does not prove, that the glomerophenocrysts were not precipitated from the matrix in which they now reside.

CHAPTER 5 PETROGRAPHY AND GEOCHEMISTRY OF THE SULPHIDE SHOWINGS

5.1 Descriptions of Showings

5.1.1 Frederickson Lake South Showing (glomeroporphyritic gabbro-hosted Cu-Ni deposit)

Stratigraphic relationships for this area (Fig. 30) were determined from old diamond drill logs obtained from the Hollinger North Shore Exploration Company (HNS); surface exposure was poor. North of this showing, a thin band of black argillite containing sulphide-facies iron formation is intruded along its western contact by a 50 metre-thick sill of glomeroporphyritic gabbro. To the east, the argillite is intruded by a thicker ordinary gabbro sill. The eastern ordinary gabbro sill exhibits partial transformation of clinopyroxene to actinolite, a texture also observed in lower regions of other ordinary gabbro sills. The eastern band of argillite pinches out along strike to the south, leaving the glomeroporphyritic gabbro in direct contact with the ordinary gabbro sill close to the zone of mineralization (Fig. 30; Map 2). Xenoliths of sedimentary rock within the glomeroporphyritic gabbro, and dykes of glomeroporphyritic gabbro, which crosscut the ordinary gabbro where the pinching out occurs (Fig. 15), suggest that the sedimentary band here has been removed by the intrusion of the younger glomeroporphyritic gabbro.

A layer of massive Cu-Ni-bearing sulphides, about 200 m in length and 1.5 m in thickness, occurs near the centre of the glomeroporphyritic sill and is oriented parallel both to sill margins and to internal flow banding (Fig. 30). The

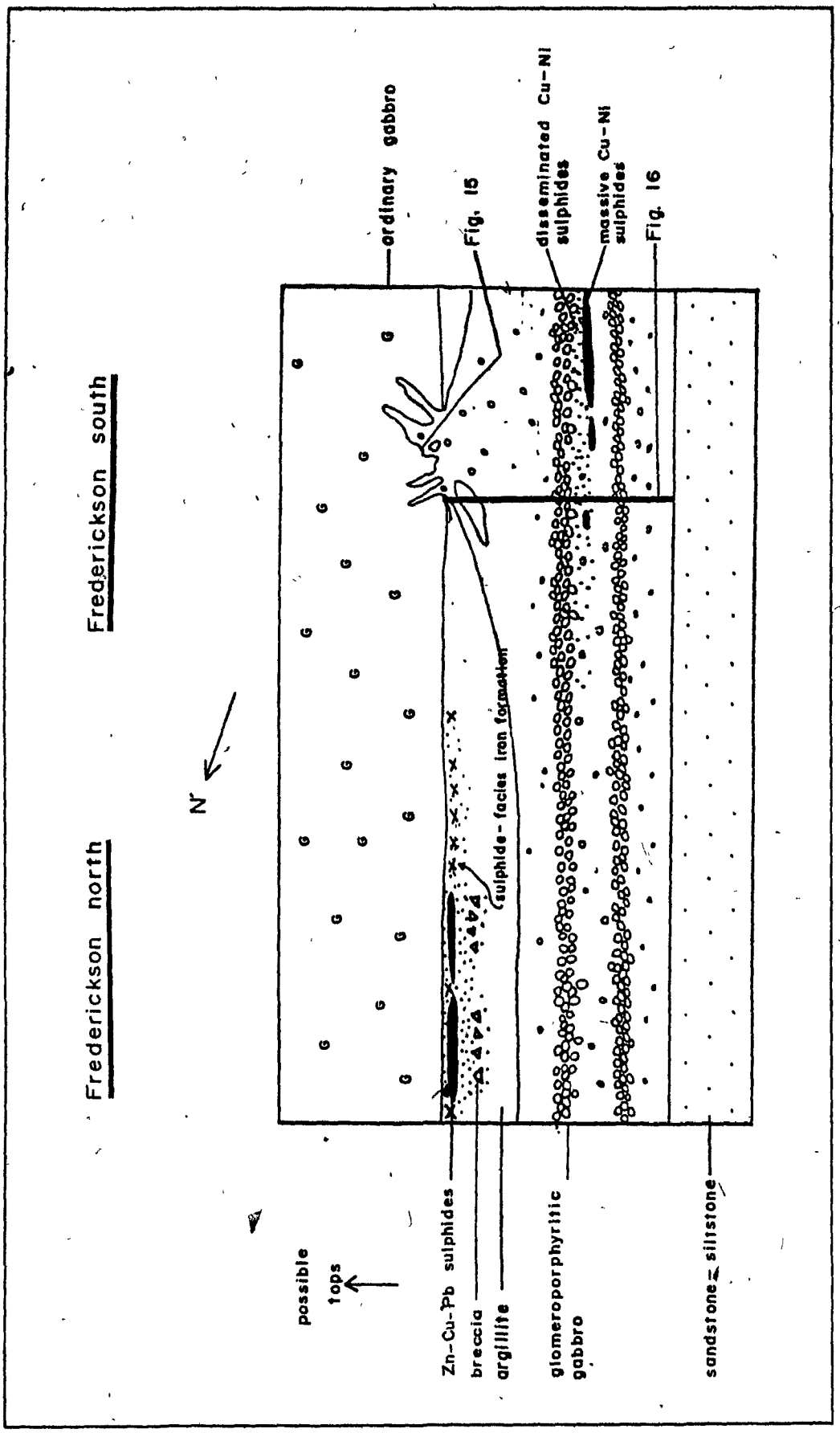

Fig. 30 Generalized cross section through the Frederickson Lake showings. Note the localization of the Zn-Cu-Pb lens to the contact with an ordinary gabbro sill, and the abrupt termination of its host sedimentary band near the south showing. The two showings are separated by 2 000 metres.

western contact of the sulphide body is sharp; its eastern contact is diffuse; the percentage of sulphides decreases upwards to form net-textured sulphide mineralization. This texture suggests that sill tops are towards the east. Although the tabular nature of the sulphide body led early workers to describe it as a vein (Griffis, 1945), the asymmetry of the sulphide lens and the absence of metasomatic alteration at its margins suggests that it is syngenetic rather than epigenetic.

As noted by Fournier (1983), the upper portion of the sulphide lens appears to be richer in Ni and Cu (0.81% and 4.19% respectively) than the lower part (0.23% and 0.61%). Disseminated sulphides 4 m above the massive zone assayed 0.66% Cu and 0.14% Ni (Appendix 1). The overall grade of the deposit, however, is low, 1.5% Cu and 0.5% Ni. Three samples of Cu-Ni mineralization were analyzed for the platinum group elements Pt, Pd and Rh; one sample assayed 0.73 g/t Pd.

Disseminated sulphides consisting mainly of pyrrhotite are present within the matrix of the glomeroporphyritic gabbro along strike from the main ore lens. The largest of these occurrences is located 500 m northwest of the main sulphide showing.

5.1.2 Frederickson Lake North (sediment-hosted Zn-Cu-Pb deposit)

Although exposure is poor, this showing appears to occur stratigraphically above (i.e. to the east of) the glomeroporphyritic gabbro hosting the Southern deposit. Fournier (1983) suggested that this showing is bounded to the

east by a glomeroporphyritic gabbro; however, it is suggested here that the glomeroporphyritic gabbro lies to the west of the showing (Fig. 30). The contact zone of the eastern gabbro is again marked by incomplete alteration of pyroxene to amphibole as seen in other gabbro chilled margins.

Drilling by HNS in 1944 indicated that a massive Zn-Cu-Pb-rich sulphide lens about 2 meters thick occurs within black argillite and extends for 200 m parallel to the ordinary gabbro contact. The best assays obtained by HNS were from DDH-7, which returned 14.1% Zn, 2.25% Cu, 1.76% Pb and 10.1 oz/ton Ag over 1.3 meters. Drill logs indicate that disseminated sulphides and quartz-carbonate veins with pyrite and minor chalcopyrite lie west of the massive lens (i.e. probably beneath it). Sulphide-facies iron formation occurs along strike from the sulphide lens, but its contact relation with the lens is unknown. The drill logs also indicate that the host black argillite is siliceous around the ore lens and that two breccia zones are present. The first zone occurs within the massive sulphide ore; the second zone, which is several meters in thickness, occurs 40 m below the massive ore (Hogg, 1957). Breccia fragments are described as volcanic, but this could not be confirmed during the present study; only a few surface blocks of sulphide-rich breccia were located.

5.1.3 Other Showings in the Frederickson Lake Region

Other glomeroporphyritic, gabbro-hosted Cu-Ni showings in the region include the Gossan 1 and Connolly showings (Map 1; Fig. 2). Both of these occur adjacent to sulphide-facies iron formation. The glomeroporphyritic gabbro of the Connolly showing contains several sedimentary xenoliths of sulphide-facies iron formation. Sulphide mineralization in the gabbros at both localities consists only of disseminated pyrrhotite and chalcopyrite.

Sediment-hosted sulphides in the area are present at the Jimmick Lake, Gossan Lake and Faute showings. At Jimmick Lake, sulphides occur close to the nose of a major antiformal syncline; this is the only showing which has any visible relation to structure. Sulphide-facies iron formation from the eastern limb of the syncline displays local re-crystallization of iron sulphides. The Gossan Lake and Faute Lake showings are essentially sulphide-facies iron formation with rare disseminated chalcopyrite.

5.2 Sulphide Petrology

5.2.1 Cu-Ni Deposits

In these deposits pyrrhotite is the most abundant phase and forms the matrix for other sulphides (Fig. 31). The occurrence of many sub-grain boundaries suggests recrystallization. Pentlandite is present as exsolution flames up to 0.5 mm in length in pyrrhotite and as coarser euhedral grains up to 2 mm in diameter along pyrrhotite grain boundaries. Chalcopyrite occurs as anhedral crystals and as

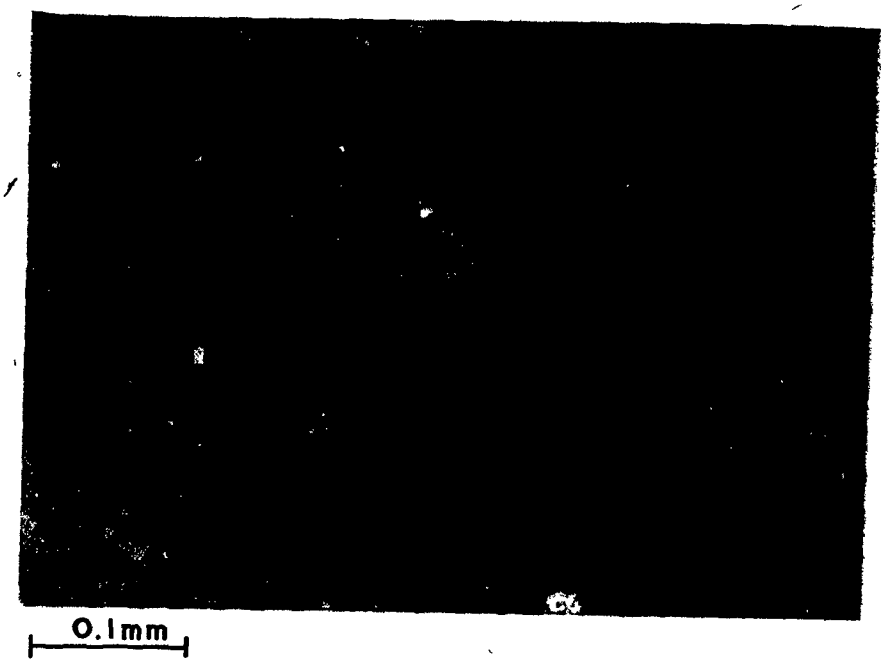

Fig. 31 Microphotograph of a polished section of Cu-Ni mineralization from the Frederickson Lake South showing. (po=pyrrhotite, py=pyrite, mag=magnetite, cpy=chalcopyrite, gan=gangue)

exsolution lamellae within the massive pyrrhotite. Magnetite is present as rounded grains and only rarely contains exsolution lamellae of ilmenite. Pyrite is rare, occurring both as small cubes (0.05 mm) within the pyrrhotite matrix and as larger annealed grains (0.1 mm). Quartz is the dominant gangue mineral in the zone of massive mineralization. Towards the top of the sulphide lens, where a net-texture is developed, chlorite and epidote after clinopyroxene become more common.

5.2.2 Zn-Cu-Pb Deposits (Frederickson Lake North)

Megascopically, the massive mineralization at Frederickson Lake North has a layered appearance resulting from alternating sphalerite-galena-rich and iron sulphide-chalcopyrite-rich bands (Fig. 32). Deformation of the sulphide lens was not evident in outcrop, but cut specimens of massive ore exhibited minor folding (Fig. 32). The pyrrhotite-rich layers contain abundant anhedral masses of chalcopyrite and large pyrite cubes. Sphalerite occurs as anhedral masses surrounding anhedral grains of galena. Small, oriented and unoriented inclusions of chalcopyrite are common within sphalerite (Fig. 33). Trace amounts of arsenopyrite occur as euhedral, diamond-shaped crystals. A similar mineral assemblage is present in the breccia horizon of the ore lens, where it forms the matrix to cherty argillite clasts up to 5 cm in diameter.

On the basis of the anhedral nature of the galena and chalcopyrite in the massive mineralization, Fournier (1983) proposed that these were the last-formed sulphide minerals.

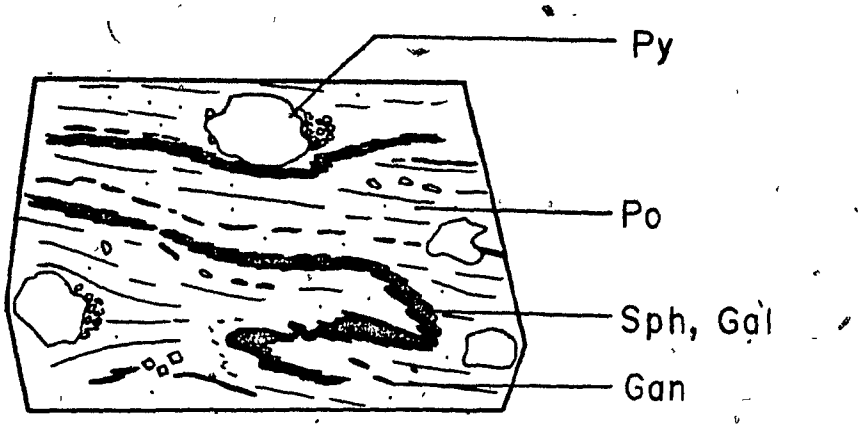

Fig. 32 Hand sample tracing of Zn-Cu-Pb mineralization from the Frederickson Lake North showing (actual size). Note the deformation of bedding by minor folds and the development of large pyrite porphyroblasts. Refer to Figure 31 for symbols.

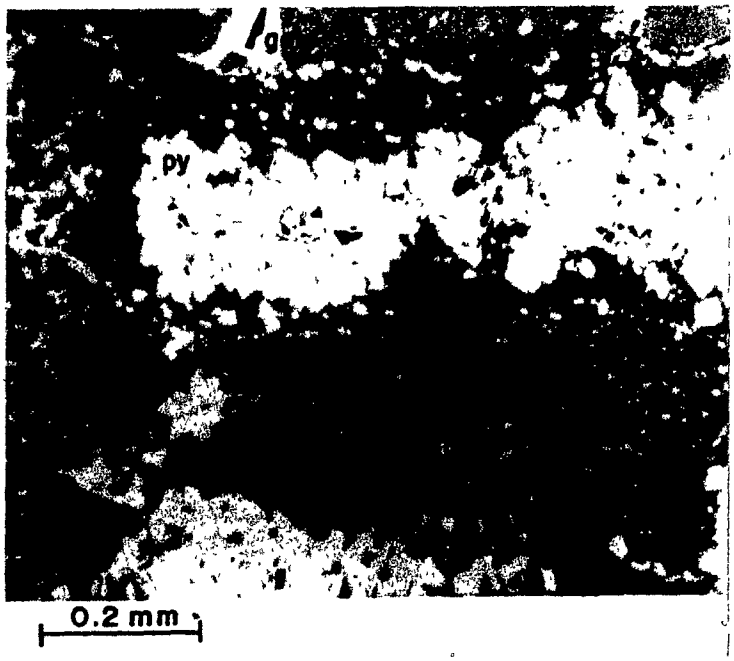

Fig. 33 Microphotograph of polished section of Zn-Cu-Pb mineralization from the Frederickson Lake North showing. Note inclusions of chalcopyrite in sphalerite. Refer to Figure 31 for symbols.

However, anhedral textures for these sulphides also commonly result from metamorphism (Volkes, 1969). In any case, the lack of primary textures in the Zn-Cu-Pb deposits makes it impossible to determine the original mineral paragenesis.

5.2.3 Po-Py rich sediments

These sediments were classified in the field as sulphide-facies iron formation. Such sediments commonly contain ~50% iron sulphides, mainly as pyrrhotite, with minor pyrite. The pyrrhotite is recrystallized and intergrown with silicate grains (Fig. 8). Pyrrhotite-rich boulders of sulphide-facies iron formation on the eastern flank of the Jimmick Lake antiformal syncline exhibit schistocity parallel to bedding and recrystallization of pyrrhotite. Base metal and gold concentrations in po-py rich sediments are low (Appendix 1).

5.3 Geochemistry of the Showings

5.4.1 Ni/Cu ratios of Gabbro-Hosted Mineralization.

Ni/Cu ratios have been applied to magmatic Cu-Ni sulphide deposits to infer parental magma compositions and the timing of sulphide liquid immiscibility with respect to olivine fractionation. Olivine fractionation rapidly depletes a magma of Ni but increases the amount of Cu in the residual liquid. A low Ni/Cu ratio of 0.35 for the Frederickson Lake South showing, and similar ratios for other glomeroporphyritic gabbro-hosted Cu-Ni deposits of the Labrador Trough (Fournier, 1983), indicate that olivine fractionation may have depleted the magma in Ni prior to

sulphide liquid immiscibility. By contrast, komatiite-hosted Ni-Cu deposits, with Ni/Cu ratios of up to 15, are inferred to reflect early sulphide liquid immiscibility relative to olivine fractionation (Naldrett, 1981). It is interesting to note that the ultramafic-hosted Cu-Ni sulphide deposits of the Montagnais Group (type 1) have Ni/Cu ratios that are similar to the glomeroporphyritic gabbro-hosted deposits (type 2). This suggests that the ultramafic rocks are cumulates that formed from a gabbroic parental magma.

5.3.2 Magma-Sulphide Ratios

Syngenetic magmatic sulphide deposits are generally attributed to the separation of an immiscible sulphide liquid from a silicate melt (Vogt, 1893). Elements enter the sulphide liquid in proportion to their sulphide-silicate partition coefficients (Table 7: MacLean and Shimazaki, 1976; Naldrett, 1981). For the economically important elements Cu, Ni and PGE, the coefficients are >>1, thus sulphide liquids are able to scavenge and concentrate these elements from co-existing silicate liquids. If the initial concentration, final concentration, and partition coefficient for any element are known, then the proportion of silicate liquid that has equilibrated with a given sulphide liquid, its R value, can be calculated (Table 7b). Large R values (up to 10 000) imply that the sulphide liquid has equilibrated with a large volume of silicate liquid, whereas small values (below 500) indicate the opposite (Campbell and Naldrett, 1979).

Table 7

Partition coefficients between silicate and sulphide liquids for selected elements.

	1 Ni	1 Cu	1 Pt	1 Pd	2 Zn	3 Pb
Komatiitic liquids						
27 % MgO	100	250	1 000	1.500		
19 % MgO	175	250	1 000	1 500		
Basaltic liquids	275	250	1 000	1 500	.1-.5	10

Sources: 1 - Naldrett (1981)
2 - MacLean and Shimazaki (1976)
2 - Shimazaki and MacLean (1976)

Note: Campbell and Barnes (1984) suggested that the partition coefficients for the PGE are as high as 1 000 000.

Table 7b Formula for R value

$$Yi = \frac{Di * Xi * (R + 1)}{(R + Di)}$$

where:

R=silicate-sulphide ratio
Yi=final concentration of element in sulphide liquid
Xi=initial concentration of element in silicate liquid
Di=partition coefficient

Magma-sulphide ratios have been used to argue that the Pipe nickel deposit of the Manitoba Nickel Belt formed through the assimilation of sulphur (Naldrett et al., 1979). An R value of 43 for this deposit was interpreted as indicating an excess of sulphur above that which could be dissolved in the parental magma. This excess sulphur was considered to reflect assimilation of sulphide-rich sediments.

R values were calculated for the Frederickson Lake Cu-Ni showing, using initial values of 110 ppm Ni and 300 ppm Cu (values for the chilled margin of the host glomeroporphyritic gabbro; sample 99417, Appendix 1). The resulting R values range between 53 for Ni and 57 for Cu, suggesting that the sulphide liquid which formed the deposit did not equilibrate with large volumes of silicate liquid. This may indicate that sulphide liquid immiscibility occurred late in the magmatic history of the host glomeroporphyritic gabbros.

5.3.3 Zn-Cu-Pb ratios in sediment-hosted mineralization

On the ternary plot of Gustafson and Williams (1981), data from the Frederickson Lake Zn-Cu-Pb showing fall in both the sediment-hosted and volcanogenic massive sulphide fields (Fig. 34). Sediment-hosted stratiform sulphide deposits can be divided into two generally separate classes, Cu-rich and Pb-Zn-rich (Gustafson and Williams, 1981). The Frederickson Lake sulphides are similar to the Zn-Pb class because of the dominance of (Zn+Pb) over Cu, but in general contain too much copper to be directly analogous. They have Zn-Cu-Pb values similar to the Koke showing (Fig. 1, showing #8) of the

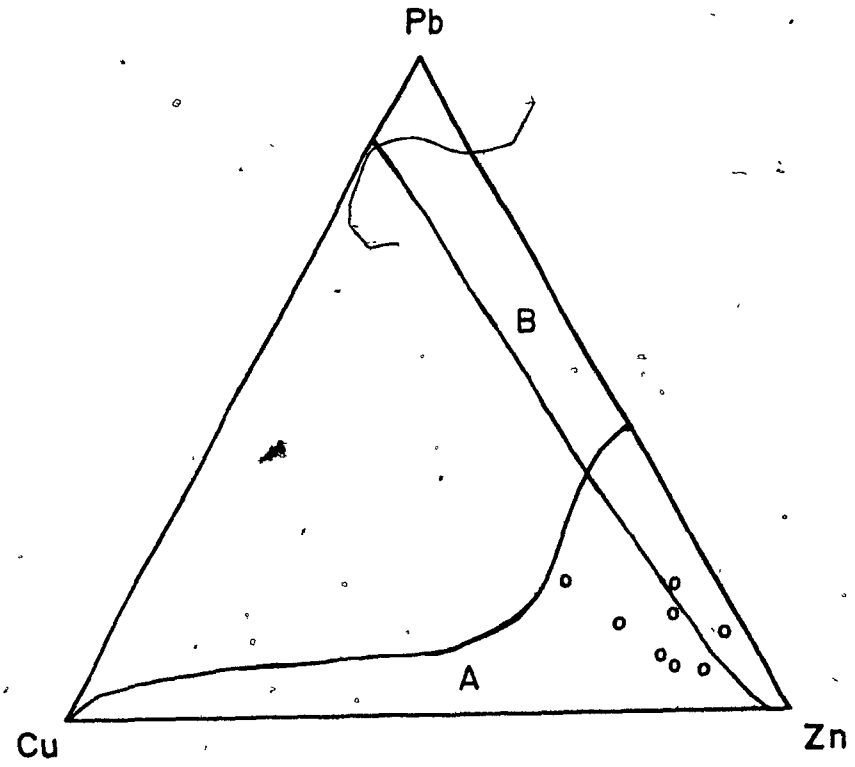

Fig. 34 Cu-Zn-Pb diagram for massive sulphides at the Frederickson Lake North showing.

A. volcanogenic massive sulphide field (from Pélissonnier, 1972)
B. sediment hosted Pb-Zn massive sulphide field (estimated from Gustafson and Williams, 1981)

Northern Labrador Trough (R. Wares; pers. comm., 1987).

5.3.4 Sulphur-Selenium Ratios

S/Se ratios for two samples of each of the three main types of mineralization are given in Table 8. The S/Se ratio has been proposed as a possible discriminant between magmatic and sedimentary ore deposits (Goldschmidt and Strock, 1935). Mineralization with S/Se ratios below 10 000 (cosmic ratio 7 000; Cameron, 1968) have been interpreted as magmatic in origin while those with higher ratios have been considered as synsedimentary deposits. However, not all sedimentary rocks are depleted in Se, and seleniferous sedimentary provinces are known to exist (Stanton, 1972). Although S/Se ratios have been employed as discriminators by Naldrett (1981), Thompson and Naldrett (1984), and Eckstrand and Hulbert (1987), their use recently has been criticized by Auclair et al., (1987) because the behaviour of both selenium and sulphur in hydrothermal systems is variably affected by pH and fO2.

Notwithstanding, this method still appears valid for purely magmatic deposits. The average ratio of 5000 for the two samples of glomeroporphyritic gabbro-hosted Cu-Ni ore is compatible with a magmatic origin for the ore. The low S/Se ratios also imply that the glomeroporphyritic gabbros have not assimilated large volumes of sedimentary sulphides, as this would increase the ratio. The average ratio of 30 000 for the Zn-Cu-Pb sediment-hosted sulphides is compatible with a sedimentary origin for the sulphides.

Table 8

Analyses of sulphur and selenium

sample	type	S %	Se ppm	S/Se
1	argillite rich in po-py	32.7	20	16 450
2	argillite rich in po-py	15.9	10	15 900
3	Zn-Cu-Pb (Frederickson N.)	42.5	10	42 500
4	Zn-Cu-Pb (Frederickson N.)	38.5	20	19 250
5	Cu-Ni (Frederickson S.)	35.2	70	5 030
6	Cu-Ni (Frederickson S.)	25.0	50	5 000

Analyst: D. Toye - Acme Analytical Laboratories Ltd

lower limit of detection S: 0.01%
Se: 1 ppm

NOTE:
In order for sample 6 to equal the average value S/Se of the Zn-Cu-Pb mineralization (~30 000) the Se value would have to be reduced by 85%. Thus even with an analytical error of 20% with respect to the Se value, the S/Se ratio would still reflect magmatic values.

5.3.5 Sulphur Isotopes

Contamination of gabbroic magmas with crustal sulphur was proposed by Sullivan (1959) to explain the Cu-Ni deposits of the Thompson Belt. Later sulphur isotope studies invoked this mechanism for a variety of gabbro-hosted deposits (Noril'sk: Godlevski and Grinenko, 1963; Duluth Complex: Naldrett and Mainwaring, 1977; Ripley, 1981; Rao and Ripley, 1983; Thompson and Naldrett, 1984; Ripley and Alawi, 1986; Ripley and Al-Jassar, 1987; Bushveld (Potgietersrus Limb): Buchanan and Rouse, 1984). Early work on the Water Hen deposit (Duluth Complex) suggested that sulphur was incorporated into the Water Hen intrusion by the assimilation and melting of local sulphur-rich sedimentary rocks (Naldrett and Mainwaring, 1977). Later studies of the Dunka Road deposit (Duluth Complex) proposed that sulphur was transferred to the melt as a vapour phase produced by contact metamorphic breakdown of pyrite in wall rocks and sedimentary xenoliths (Ripley, 1981; Rao and Ripley, 1983). In contrast, a study of the Babbitt deposit of the Duluth complex (Ripley and Al-Jassar, 1987) demonstrated that sulphur incorporation took place in auxiliary magma chambers at depth rather than at the presently exposed level of the Duluth complex.

Although fractionation of sulphur isotopes during regional or contact metamorphism potentially complicates the interpretation of sulphur isotopic data, metamorphosed deposits are thought to retain their initial sulphur isotopic ratios up to amphibolite facies if there is no change in mineralogy (Ohmoto and Rye, 1979). However, experimental

work by Kajiwara et al., (1981) detected significant sulphur isotope fractionation during the thermal decomposition of pyrite to pyrrhotite and sulphur at 600 C. In their study, the initial sulphur vapour was 12 per mil lower than the source pyrite, and the final pyrrhotite residue was enriched by 4.5 per mil. These large degrees of fractionation are, however, somewhat controversial because of the high temperature at which fractionation took place. Ripley and Al-Jassar (1987) found no evidence for such S-isotope fractionation between pyrrhotite and pyrite in the Babbitt gabbro-hosted deposit.

In the Frederickson Lake area, glomeroporphyritic gabbros have intruded sulphur-rich sediments. In order to assess whether mixing of magmatic and sedimentary sulphur has occurred, the sulphur isotopic composition of pyrrhotite was determined for pyrrhotite separates from glomeroporphyritic gabbro-hosted Cu-Ni deposits, sediment-hosted Zn-Cu-Pb deposits, and sulphide-facies iron formation (Table 9). In addition the isotopic composition of whole rock sulphur from the ordinary gabbro sills was measured.

Six pyrrhotites from the Frederickson Lake South Cu-Ni deposit had an average d S34 value of +3.7 per mil (Fig. 35). Two pyrrhotites from a disseminated Cu-Ni sulphide occurrence, 500 m northwest and along strike of the main showing, had an average d S34 value of +19.6 per mil. Three pyrrhotites from separate locations at the Frederickson Lake North Zn-Cu-Pb showing yielded a tight clustering of d S34 values at +9.2 per

Table 9

Sulphur isotope analyses of pyrrhotite mineral separates from the Frederickson Lake area

Sample	Showing and Type of Mineralization	d S34 (+/- 0.2)
S1	Frederickson S. (Cu-Ni)	3.4 per mil
S2	Frederickson S. (Cu-Ni)	3.6
S3	Frederickson S. (Cu-Ni)	3.6
S4	Frederickson N. (Zn-Cu-Pb)	9.2
S5	Frederickson N. (Zn-Cu-Pb)	9.3
S6	Frederickson N. (Zn-Cu-Pb)	9.3
S7	Frederickson N. (Po-Py)	3.9
S8	Secalar Lake (Po-Py)	2.4
S9	Gossan-1 (Po-Py	4.1
S10	Frederickson S. (Cu-Ni)	3.8
S11	Frederickson S. (Cu-Ni)	4.0
S12	Frederickson S. (Cu-Ni)	3.7
S13	Disseminated Po NE of Frederickson S.(Cu-Ni)	18.9
S14	Disseminated Po NE of Frederickson S.(Cu-Ni)	20.4
S15	Ordinary Gabbro bulk rock sulphur	*2.2 +/- 0.5

Deposit Type	average value	standard deviation	# of samples
Frederickson South (Cu-Ni)	3.7	0.2	6
Frederickson North (Zn-Cu-Pb)	9.2	0.05	3
Sulphide-Facies Iron Formation	3.5	0.9	3
Menihek Formation (Cameron, 1983)	3.7	0.9	12

* Kiba extraction - higher analytical uncertainty is due to the low sulphur content of the sample

S1-S9 analyzed at Universite du Quebec a Montreal by C. Gariepy
S10-S15 analyzed at the University of Ottawa by J. St-Jean

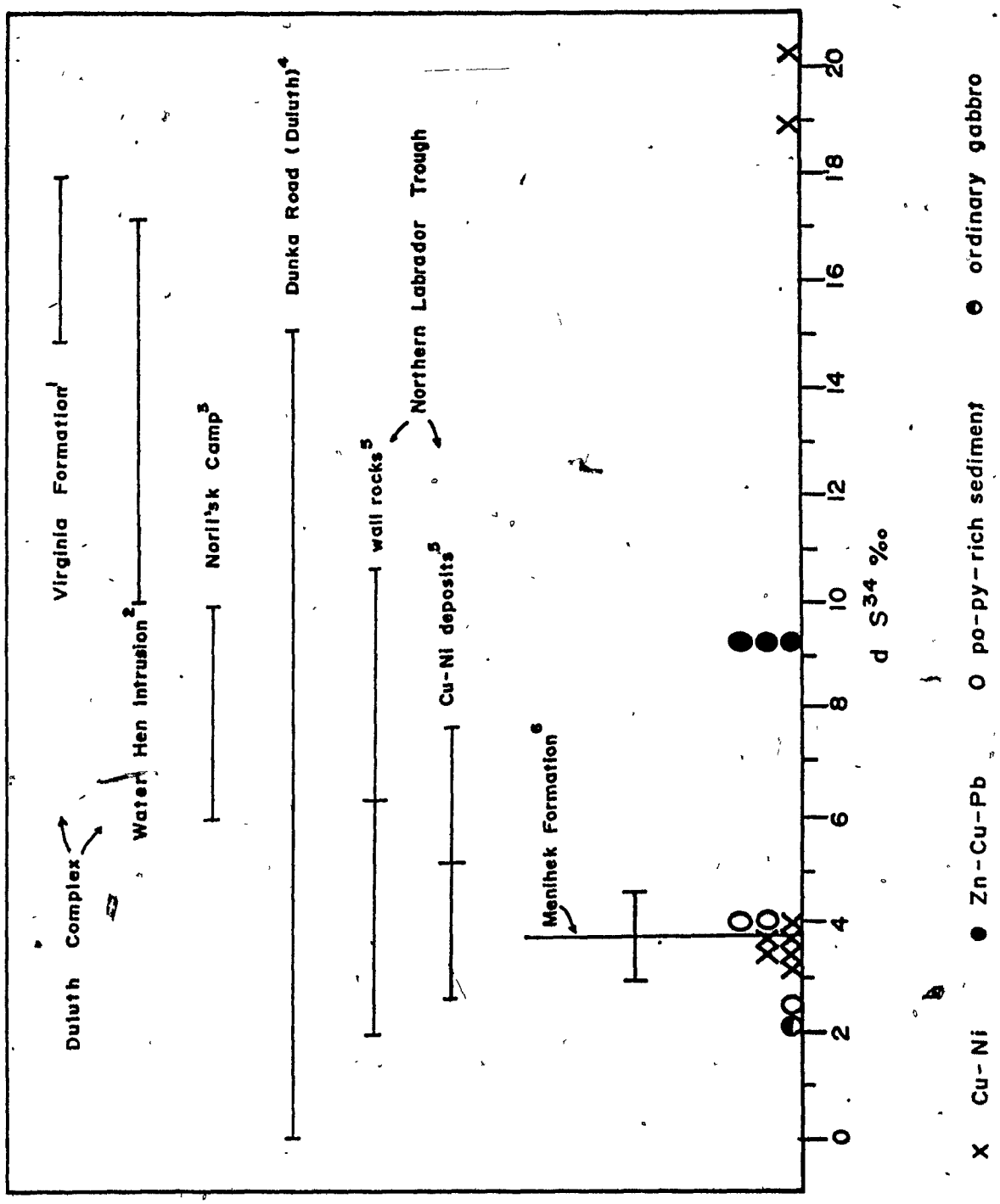

Fig. 35 Sulphur isotope data from the Frederickson Lake region and from other selected deposits. 1, 2 Mainwaring and Naldrett (1977), 3 Godlevski and Grinenko (1963), 4 Ripley (1981), 5 Eckstrand (1983), 6 Cameron (1983).

mil. The d S34 values of pyrrhotites from three widely separated occurrences of sulphide-facies iron formation ranged from +2.4 to +4.1 per mil, with an average of +3.5. per mil. Regionally, over a 77 km interval, the sulphide-facies iron formation of the Menihek Formation has a similar average d S34 value of +3.7 +/- 0.9 per mil (Cameron, 1983). A sample of bulk rock sulphur from an ordinary gabbro sill had a value of +2.2 +/- 0.5 per mil.

The d S34 value of primary magmatic minerals in mafic to ultramafic rocks depends on the temperature and fO2 of the magma, but is believed to be between -1.0 and +2.0 with an average value of +1.3 per mil (Ohmoto and Rye, 1979). However, magmatic sulphides in the Bushveld complex range from -0.6 to +3.5 per mil (Buchanan and Rouse, 1984). By contrast, sulphides within the Water Hen intrusion of the Duluth Complex had an average d S34 value of +15 per mil (Mainwaring and Naldrett, 1977). Adjacent sediments had an average sulphur isotopic value of +18 per mil. Because of the extreme difference between the isotopic composition of sulphides in the Water Hen intrusion and the ideal magmatic value of zero, a significant addition of sedimentary sulphur to the Water Hen intrusion could be demonstrated. In the Frederickson Lake area, the value of +3.5 per mil for the probable assimilant (sulphide-facies iron formation) is too close to the possible range of natural magmatic values to conclusively demonstrate mixing. The value of +3.7 per mil for the Frederickson Lake South showing may reflect a minor component of non-magmatic sulphur.

Pyrrhotites from the sediment-hosted Zn-Cu-Pb showing have an isotopic value (+9.2 per mil) which is significantly higher than those from sulphide-facies iron formation of the Menihek Formation (+3.7 per mil; Cameron, 1983). If the former pyrrhotites are synsedimentary, the value of +9.2 would reflect the isotopic composition of sulphur deposited on the seafloor. The large difference in the d S34 values of the sediment and gabbro-hosted deposits makes it unlikely that both types of deposits formed as immiscible sulphide liquids, as suggested by Fournier (1983).

The average d S34 value of +19.7 per mil for the small disseminated sulphide showing in glomeroporphyritic gabbro is problematic. A normal magmatic source can be ruled out, as can assimilation of sediment (even the Zn-Cu-Pb sulphide lens only has an average value of +9.2 per mil).

CHAPTER 6 DISCUSSION

6.1 Evolution of the Labrador Trough - Upper Cycle II

Regionally, the Menihek Formation overlies shallow water shelf sediments. It was deposited following the flooding of an epicontinental shelf wedge during the second major marine transgression identified in the Labrador Trough (Cycle II). Wardle and Bailey (1981) have proposed a turbidite origin for the bulk of the Menihek Formation; Baragar (1967) emphasized that both volcanic terrains and basement gneisses were important in supplying detritus.

Within the Frederickson Lake area, limited sediment preservation precludes a complete stratigraphic reconstruction, although a few inferences about the original depositional environment can be made. The extremely fine-grained laminations preserved within the sulphide-rich argillites indicate deposition in quiet water. The interlaminated sandstones and siltstones are reminiscent of distal turbidites, although complete Bouma sequences with grading and parallel laminations are absent. The compositional maturity of the quartzite beds that occur with the interlaminated sandstones and siltstones appears to conflict with a deep water origin, although fine-grained quartz sands from shelf environments conceivably could have been transported by mass flow mechanisms into deep water settings (c.f. Sarnthein and Diester-Haass, 1977). Limited volcanism during Menihek deposition is indicated by the presence of minor, intermediate tuff horizons within the

sandstone-siltstone layers and by thin basaltic flows in its upper stratigraphic levels.

The Menihek Formation has been correlated with the Doublet Group (Wardle and Bailey, 1981; Fournier, 1983). It appears that the Menihek Formation was deposited during the transition of the Labrador Trough from a relatively deep water, sediment-dominated environment to a volcanic-dominated, environment. Baragar (1967) proposed that gabbro sills of the Montagnais Group are most likely the subvolcanic equivalent of the extrusive rocks of the Doublet Group. This relationship is supported by the chemical similarity between gabbroic chilled margins and basalts of the Menihek Formation (Figs. 25, 26).

6.2 Genesis of Glomeroporphyritic Gabbros

Glomeroporphyritic gabbros are a minor but consistent component of mafic magmatic environments ranging from Archean greenstone belts (Green, 1975; Phinney and Morrison, 1982; 1984) to Proterozoic volcano-sedimentary belts (Baragar, 1967), and modern ocean-floor basalt terrains (Flower, 1980; Cullen et al., in press). Nevertheless, their genesis is poorly understood. Green (1975) and Phinney and Morrison (1982, 1984, 1985) have suggested that these gabbros result from the fractional crystallization of plagioclase from primitive magmas at deep crustal levels. Ashwal et al. (1983) and Phinney and Morrison (1983) have pointed out a possible genetic link between glomeroporphyritic gabbros and anorthosite complexes.

Phenocrysts in the glomeroporphyritic gabbros are more calcic than normative values calculated for the chilled margins (section 4.3). Such calcic phenocrysts could have been produced either from a more primitive mafic magma or from a gabbroic magma contaminated by continental crust. Models favouring a parental magma of primitive composition for Archean glomeroporphyritic gabbros with calcic phenocrysts have been developed by Phinney and Morrison (1982, 1984, 1985). In these models, it is assumed that primitive magmas are trapped at the crust-mantle boundary where they fractionated Mg-rich olivine and calcic plagioclase. Calcic plagioclase phenocrysts are later entrained in upwelling magmas. Such models are difficult to verify in the field because the requisite mafic cumulates would have been retained at low levels in the crust that are not presently exposed. Calcic plagioclase phenocrysts (An 85-91.5) which are present in MORBs may have formed in this manner (Wilkinson, 1982). The occurrence of calcic plagioclase phenocrysts in oceanic basalts far removed from continental crust (e.g. Galapagos Archipelago; Cullen et al., in press) suggests that such phenocrysts can form in the absence of contamination by continental crust.

Assimilation of continental crust can effect the An content of plagioclase in gabbroic bodies by modifying the Al-Si ratio of the melt. However, models favouring assimilation are constrained by the small amount of continental crust that a mafic magma can assimilate before the latent heat of crystallization is consumed and the magma

solidifies (c.f. Bowen, 1928). It is unlikely that thin, subvolcanic glomeroporphyritic sills could assimilate much sediment, although assimilation is possible at deeper crustal levels.

Figure 36 illustrates the effects of variable amounts of upper crustal contamination on the REE pattern of the average gabbro chilled margin liquid. A composite sample of Post Archean Australian Shales (PAAS) was chosen as the assimilant (Taylor and McLennan, 1985) because of its similarity to the argillites of the Menihek Formation (Fig. 37). The lowermost line on Figure 36 represents the average of gabbro chilled margins and basalts of the Menihek Formation but excludes LREE enriched sample J-19. Although contamination of the gabbroic liquid by as little as 5-10% PAAS should be detectable using such a plot, there is no way of verifying that the liquid itself was not previously contaminated.

The LREE enriched sample J-19 was taken from the same glomeroporphyritic sill as sample J-8 (Fig. 29a) which has a flat REE pattern. It is unlikely that one portion of the chilled margin could assimilate greater than 10% of the surrounding sediment. Thus, sample J-19 may reflect a local, selective contamination of LREE; no other explanation is obvious.

The chemical similarity of the glomeroporphyritic and ordinary gabbro chilled margins in the study area and the unlikelihood that the original magma could produce very calcic plagioclase phenocrysts suggest that such phenocrysts may

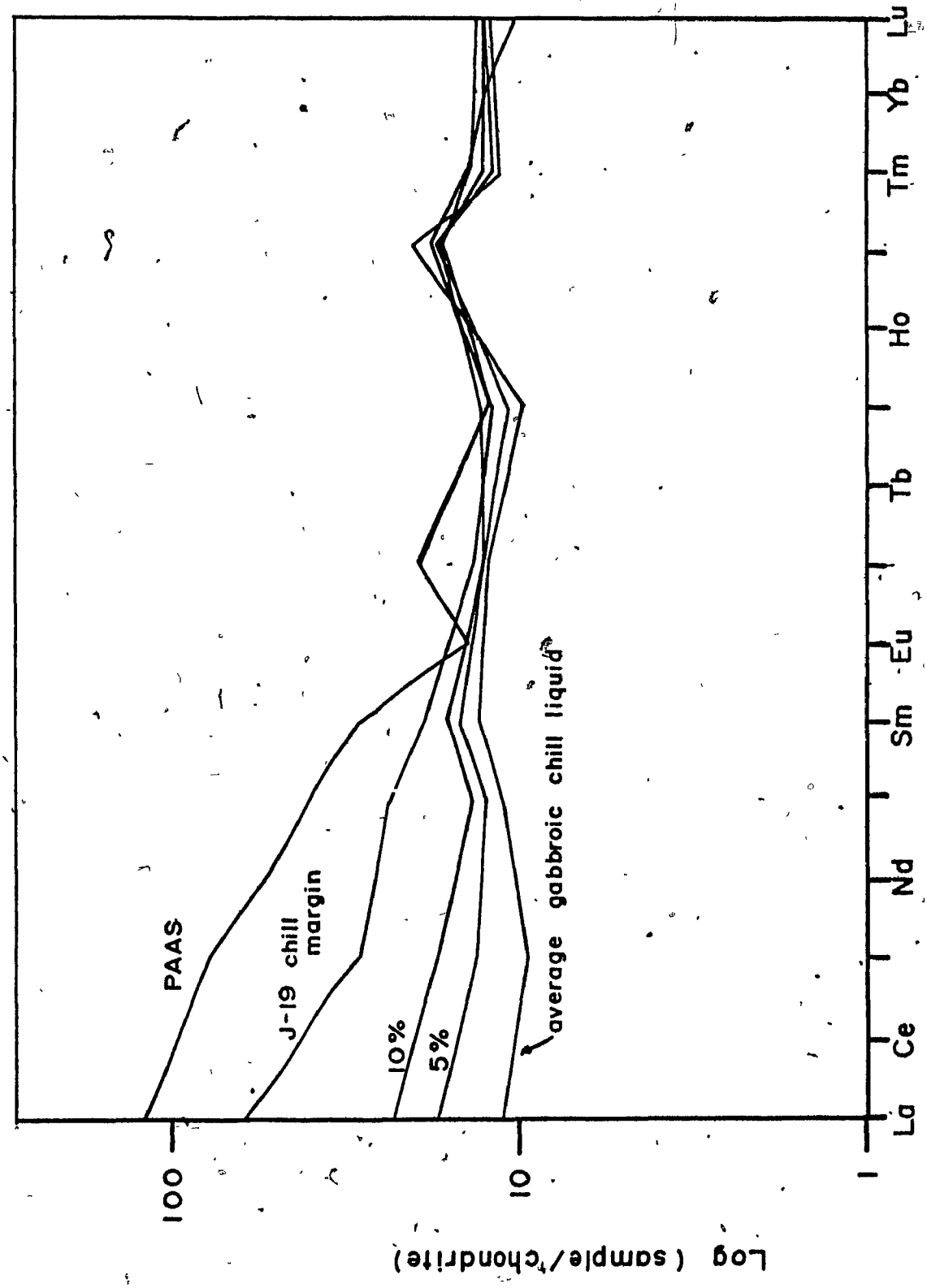

Fig. 36 Diagram illustrating the effect of contaminating the average gabbroic liquid of the Frederickson Lake area with upper continental crust. Upper continental crust is represented by PAAS (Taylor and McLennan, 1985). The average gabbroic liquid represents the average of gabbro chilled margins (excluding LREE enriched sample J-19) and basalts of the Menihek Formation. The lines labelled 5% and 10% represent the patterns which would result from contamination of average chill liquid by 5% and 10% PAAS.

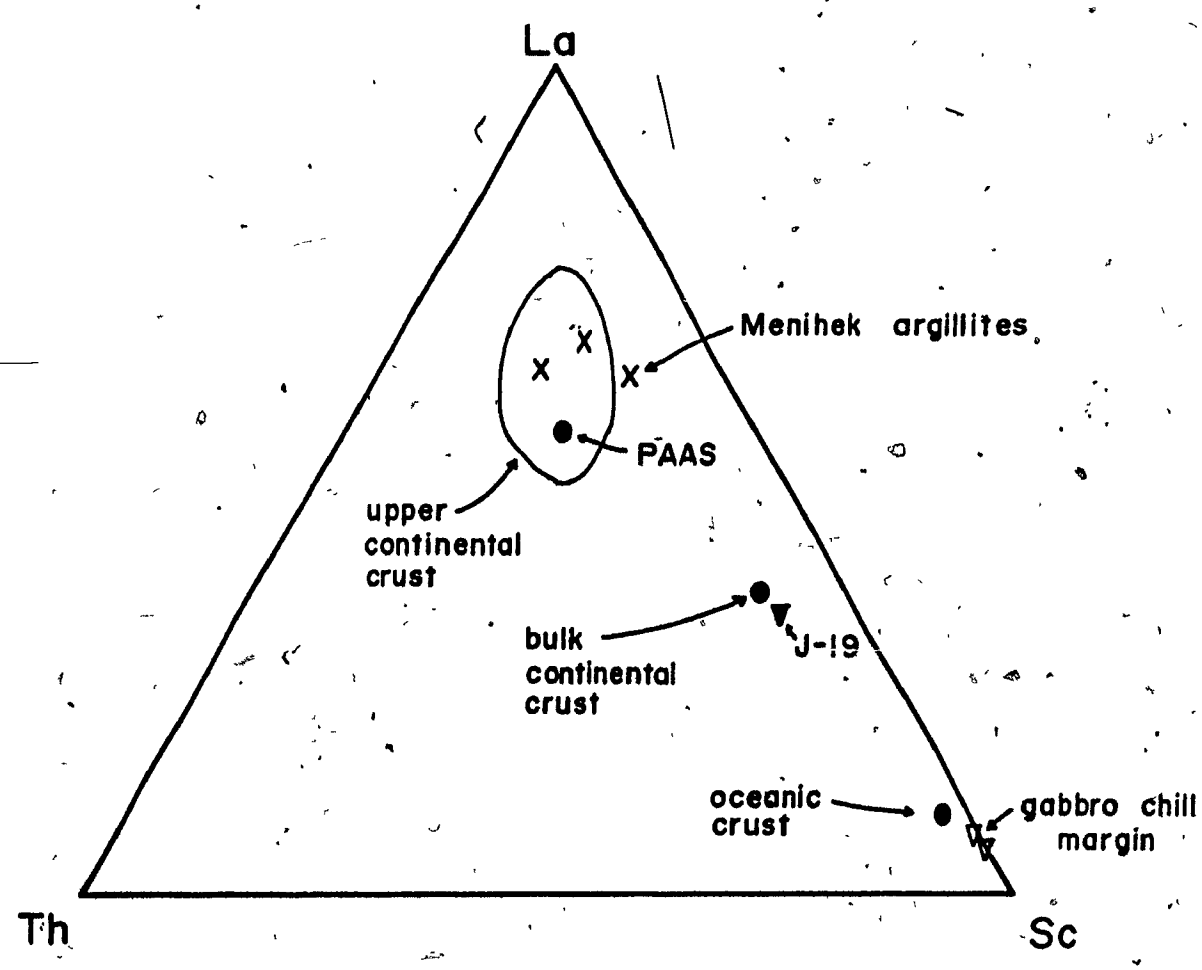

Fig. 37 Th-La-Sc diagram (Taylor and McLennan, I985). The argillites of the Menihek Formation (X) plot within or close to the upper continental crust field. Two gabbro chilled margins, but not sample J-19, plot close to oceanic crust.

have been introduced into an ordinary gabbro magma. Subsequent clustering of phenocrysts and their alignment within the glomeroporphyritic gabbros sills may have resulted from magmatic flow during sill emplacement. Growth rims around plagioclase glomerophenocrysts indicate that cementing of previously united phenocrysts took place during flow. Negative Eu anomalies for a glomeroporphyritic gabbro chilled margin (sample J-8) and an anorthositic gabbro matrix (sample J-33) suggest an earlier phase of plagioclase fractionation. The lack of a significant Eu anomaly in the matrix of the glomeroporphyritic gabbro (sample J-31) suggests that the plagioclase glomerophenocrysts were not precipitated from the matrix liquid, but were incorporated and concentrated by mechanical processes.

Glomeroporphyritic gabbros of the Labrador Trough occur at a specific stratigraphic horizon: the boundary between Cycle II sediments and the volcanics of the Doublet-Hellancourt Group. This suggests that these gabbros were produced during a restricted interval in the tectonic evolution of the Trough. Models attempting to relate glomeroporphyritic gabbros to tectonic parameters such as spreading rates have been proposed by Flower (1980) and by Cullen et al., (in press). Flower has suggested that the existence of thick oceanic crust beneath slow-spreading ridges would favour the ponding of magmas in lower crustal reservoirs, wherein slow, uninterrupted crystallization could produce large calcic phenocrysts. Cullen et al. (in press) believe that the presence of thick oceanic crust would serves

to retard the upward movement of calcic phenocrysts; they postulate that such phenocrysts form under thin oceanic crust, and at slow spreading rates.

Wardle and Bailey (1981) proposed that the extrusion of the Doublet Group occurred in response to rapid rifting which accompanied a second phase of opening of the Labrador Trough. It is suggested here that prior to rapid rifting, mafic melts may have accumulated plagioclase glomerophenocrysts due to extensive plagioclase fractionation at depth (Fig 38-1). These melts were intruded as glomeroporphyritic sills into the upper stratigraphic levels of the Menihek Formation (Fig. 38-2). Later rapid rifting led to short residence times for new batches of gabbroic melt, which gave rise to the ordinary gabbro sills (Fig. 38-3). In this fashion, a single parental magma type could produce both glomeroporphyritic and ordinary gabbros in response to different rates of crustal rifting, without invoking deep-level crustal contamination.

6.3 Genesis of Cu-Ni Deposits in Glomeroporphyritic Gabbros

The association of Cu-Ni sulphide bodies and glomeroporphyritic gabbros in the Labrador Trough is unusual. Many other gabbro-hosted Cu-Ni deposits occur instead within the lower mafic cumulate zones of differentiated intrusions (i.e. the Sudbury and Duluth Complexes). In any deposit formed by

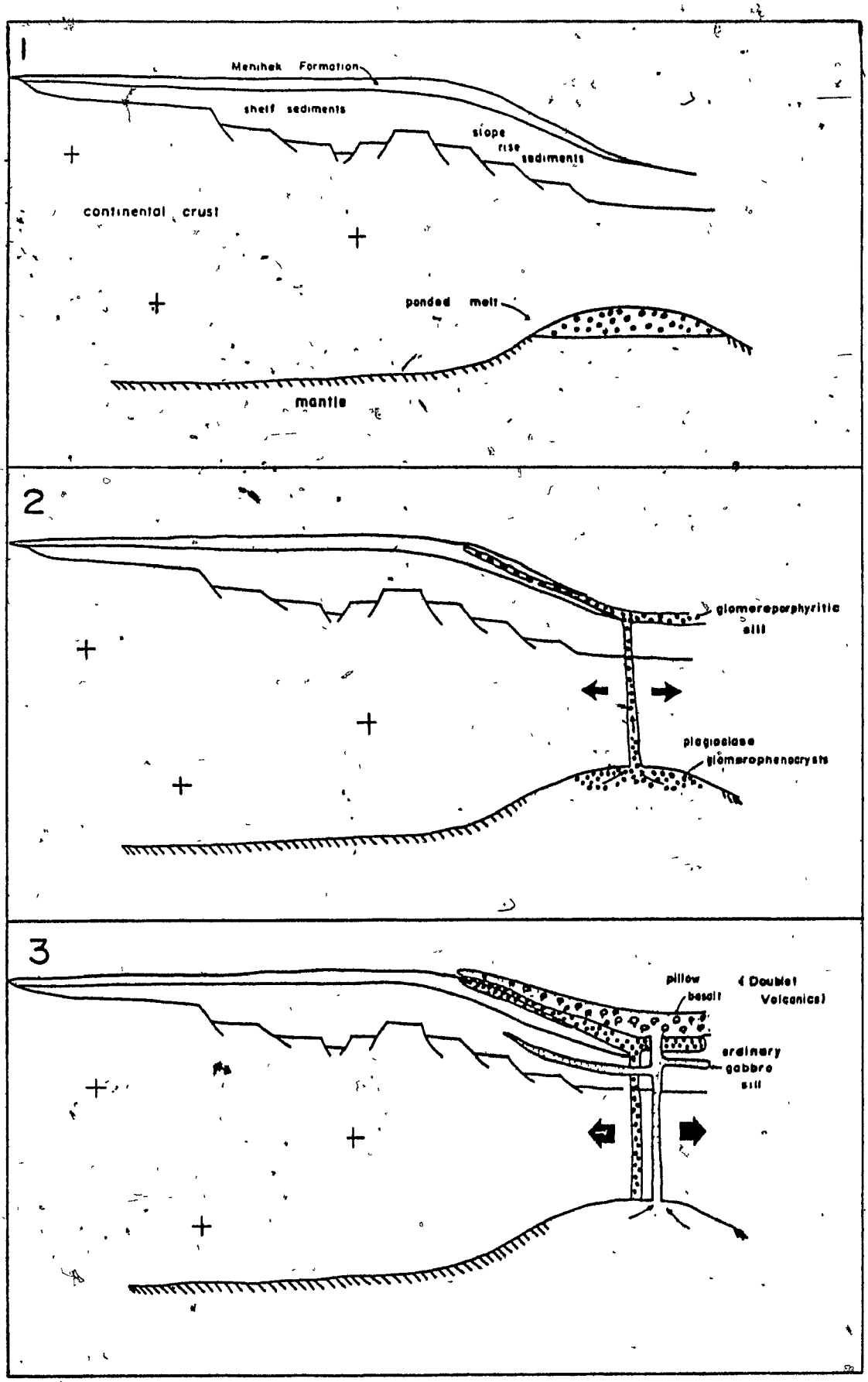

Fig. 38 Schematic diagram illustrating the transformation of the Labrador Trough from a sediment-dominanted to a volcanic-dominated environment. In (1) mafic melts are ponded at depth before rapid rifting; plagioclase phenocrysts are produced at this time. The onset of rifting (2) releases glomeroporphyritic magmas to a specific stratigraphic horizon. Later rapid rifting (3) produces non-porphyritic magmas.

sulphide liquid immiscibility, the availability and behavior of sulphur is critical. A brief review therefore follows on the controls on sulphide liquid immiscibility in tholeiitic melts.

Experimental evidence indicates that sulphur solubility in silicate melts increases with pressure and temperature. Most importantly, sulphur solubility increases with the ferrous iron content of the melt (MacLean, 1969; Haughton et al., 1974; Buchanan and Nolan, 1979), probably reflecting the complexing of sulphur with reduced iron in the melt. The ability of a fractionating mafic melt to achieve sulphur saturation within a closed system depends on the crystallization history of its silicate and oxide phases. As a magma fractionates, sulphur behaves incompatibly, and its concentration in the melt will increase until a sulphur-bearing phase appears. Initial fractionation of tholeiitic melts is usually controlled by olivine and clinopyroxene, which removes minor amounts of reduced iron (i.e. Stolper and Walker, 1980). When plagioclase joins olivine on the liquidus, the amount of reduced iron in the melt rises rapidly to produce the iron-enrichment trend characteristic of tholeiitic magmas. Calculations by Czamanske and Moore (1977) suggest that sulphide liquid immiscibility at this stage is unlikely. A small increase in the activity of silica during plagioclase fractionation, which favours immiscibility (Irvine, 1975), will be more than offset by the increase in ferrous iron content of the melt, which increases sulphur solubility. Thus, extensive plagioclase

fractionation should inhibit rather than favour sulphide liquid immiscibility. Eventually, iron enrichment trends are reversed by crystallization of iron-oxide phases, at which time an immiscible sulphide phase may also be produced.

Although most tholeiitic magmas should be close to sulphur saturation after first stage melting of the mantle (Helz, 1977; McGoldrick et al., 1979; Mitchell and Keays, 1981; Roedder, 1981; Wendlandt, 1982; Hamlyn et al., 1985) and upon emplacement into higher levels of the crust (Mathez, 1976; MacLean, 1977), this does not imply that large volumes of immiscible sulphide liquids can be produced. Indeed, the the low initial sulphur content of tholeiites (300 ppm: Ringwood, 1966; 800 +/- 150 ppm at mantle source: Moore and Fabbi, 1971) implies that even with fractionation, only small amounts of sulphur will be available for liquid immiscibility. Gross sulphur oversaturation may be required to produce immiscible sulphide liquids of sufficient volume to form an economic ore body (c.f. McCarthy et al., 1984).

Because of the tendency of tholeiitic melts to remain close to, but not exceed sulphur saturation until late stages of crystallization (i.e. the appearance of magnetite), many models for the generation of Cu-Ni deposits invoke the addition of sulphur from external sources (Sullivan, 1959, Godlevski and Grinenko, 1963; Mainwaring and Naldrett, 1977; Ripley, 1981; and Thompson and Naldrett, 1984). Such models are supported by sulphur isotopic data, which suggest components of nonmagmatic sulphur.

The low R-values, low metal grades and low Ni-Cu ratios of the Frederickson Lake South showing suggest that sulphide liquid immiscibility was a late stage event, which occurred within the glomeroporphyritic gabbro sills at high crustal levels. Fournier (1983) proposed that sulphide liquid immiscibility took place in deep-level crustal magma chambers during the precipitation of plagioclase phenocrysts. Sulphide droplets were assumed to have adhered to plagioclase phenocrysts, causing them to sink, and concentrating both plagioclase and Cu-Ni sulphides. Fournier proposed that Cu-Ni sulphides and plagioclase phenocrysts were later extracted from the deep level chambers and emplaced into higher crustal levels as sills.

It is unlikely that sulphide liquid immiscibility took place during plagioclase fractionation because plagioclase fractionation would increase sulphur solubility. Even if the immiscible sulphide liquid formed at depth, as proposed by Fournier (1983), it would tend to separate from plagioclase because of their contrasting densities. Furthermore, the early production of a sulphide melt at depth would have allowed a longer period for equilibration of this melt with a co-existing silicate liquid. As discussed in section 5.3.2, this would produce sulphide deposits with high R values and increased metal grades, and high Ni-Cu ratios. Thompson and Naldrett (1984) suggest that the grade of the Katahdin Cu-Ni deposit was diluted by late stage addition of crustal sulphur during emplacement of the gabbro host. Thus, although sulphur assimilation will increase the probability of sulphide

liquid immiscibility, excess sulphur may lower metal grades.

Sulphur isotopic data from the glomeroporphyritic gabbros (section 5.3.5) suggests a contribution of non-magmatic sulphur, although the results are not conclusive. In the Northern Trough, Cu-Ni deposits within glomeroporphyritic gabbros have a more convincing non-magmatic component, with sulphur isotopic values up to 6 per mil (Eckstrand, 1983; R. Wares, pers. comm., 1987). In the Frederickson Lake area, sulphide-facies iron formation adjacent to the gabbro-hosted Cu-Ni deposits commonly contains more than 40% pyrrhotite, although the original iron-sulphide was probably pyrite. Previous arguments suggest that large volumes of sediment were not assimilated by the high level glomeroporphyritic sills. Xenoliths of sulphide-facies iron formation at the Connolly Cu-Ni showing show no evidence of assimilation. Nevertheless, it is possible that sulphur was volatilized from these xenoliths through the breakdown of pyrite to pyrrhotite during contact metamorphism. Experimental studies show that this reaction occurs at 743C, well below the liquidus temperature of a gabbroic melt (Kullerud and Yoder, 1959). Incorporation of sulphur as a volatile phase, without large scale melting of sediment or country rocks, also has been proposed by Ripley (1981)* for the Duluth Complex. Figure 39 shows the amount of sulphur that can be liberated from the metamorphic conversion of pyrite to pyrrhotite, assuming that all pyrite is converted to pyrrhotite plus sulphur gas. This diagram indicates that the incorporation of 0.25% xenoliths

* also Mainwaring and Naldrett (1977)

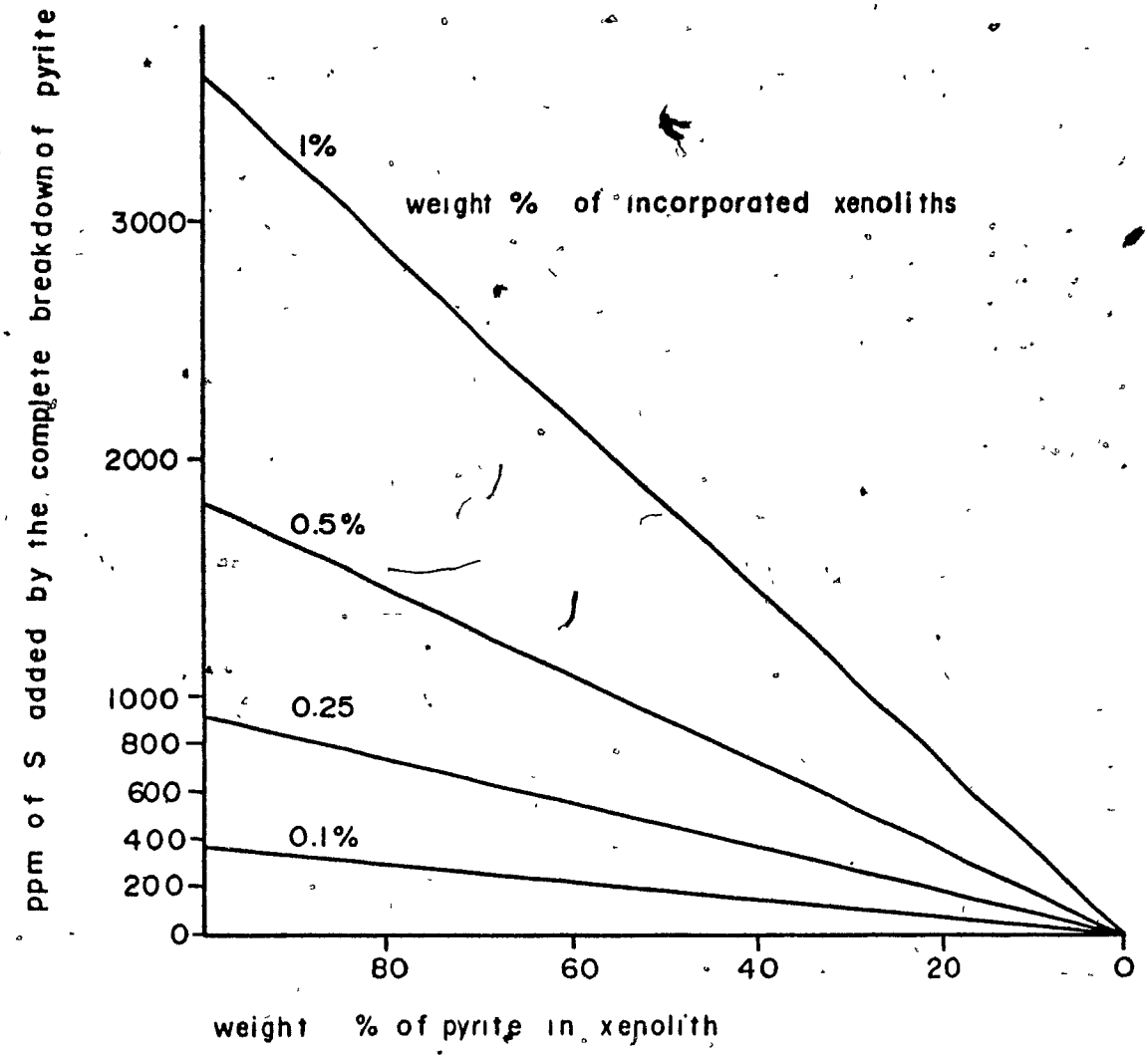

Fig. 39 Diagram showing the maximum amount of sulphur which can be released to a melt by the metamorphic breakdown of pyrite to pyrrhotite. Very low contents of sulphide-facies iron formation xenoliths can release significant quantities of sulphur to the melt.

containing 50% pyrite should release 500 ppm of sulphur to the melt. Experimental curves of Haughton et al., (1974) suggest that about 1000 ppm sulphur is required to saturate a tholeiitic melt. Thus, incorporation of a very small proportion of sulphide-facies iron formation into a tholeiitic melt, followed by volalitization of the sulphur, could provide enough excess sulphur to cause sulphide liquid immiscibility.

Addition of sulphur by the contact metamorphism of xenoliths does not explain why glomeroporphyritic gabbros are mineralized, and ordinary and anorthositic gabbros are barren, as all gabbros intrude the same sulphur-rich sediments. However, the effect of sulphur incorporation in the thinner glomeroporphyritic sills would be greater because the incorporated sulphur would be diluted by lower volumes of gabbroic magma. The glomeroporphyritic gabbros of the Frederickson Lake region are an order of magnitude thinner than the ordinary gabbro sills (50 m versus 500 m).

The timing of sulphide liquid immiscibility is one factor affecting the potential of the glomeroporphyritic gabbros to host platinum group element (PGE) mineralization. Rapid, late stage sulphide liquid immiscibility would not allow the sulphide liquid time to equilibrate with the silicate liquid and concentrate PGE elements. This effect can be seen in the Babbitt deposit of the Duluth Complex, for which early sulphide liquid immiscibility has been proposed. PGE concentrations in the Babbitt deposit are four times higher than in the Dunka deposit, for which late stage immiscibility has been proposed (Ripley and Al-Jassar, 1987).

6.4 Genesis of Sediment-Hosted Zn-Cu-Pb deposits

The close association of some sediment-hosted Zn-Cu-Pb deposits with glomeroporphyritic gabbros has led to speculation that they are genetically related to the gabbros. Fournier (1983) proposed two possible relationships between Zn-Cu-Pb deposits and glomeroporphyritic gabbros: i) glomeroporphyritic gabbro magmas produced Zn-Cu-Pb-rich immiscible sulphide liquids, which were injected into structurally favourable sites such as gabbro-sediment contacts; and ii) Zn-Cu-Pb-rich residual solutions produced from the cooling glomeroporphyritic sill were injected into sulphide-rich sediments, where they reacted with sedimentary sulphur to form Zn-Cu-Pb sulphide deposits.

There are several lines of evidence, however, that conflict with these magmatic models. Zn-Cu-Pb deposits, although occurring close to the contacts of gabbro sills, are always within sediments; proximity to contacts may largely reflect the thinness of most sedimentary units in the Frederickson Lake area . Furthermore, at the Frederickson Lake North and the Jimmick Lake showings, the nearest gabbro is of ordinary type. Thus, Zn-Cu-Pb deposits also occur in the absence of glomeroporphyritic gabbros. In addition, studies of gabbro-hosted sulphide deposits formed by sulphide liquid immiscibility indicate that these deposits are enriched in Cu and Ni but rarely contain Zn (Naldrett, 1981). Those deposits that are enriched in Zn, for example the Zenith mine (Kite, 1981) and the Obrazek deposit (Watkinson

et al., 1978), are thought to represent volcanogenic massive sulphides that were mechanically incorporated into the magma chamber as large xenoliths. Finally, Fournier (1983) postulated that glomeroporphyritic gabbros could give rise to immiscible sulphide liquids of both Cu-Ni and Zn-Cu-Pb types; the former in association with early magmatic cumulate phases, and the latter with residual magmatic phases. However, there is no apparent explanation for why these two independently evolved liquids should ultimately form deposits in close spatial association, and in particular why the Cu-Ni liquids should remain trapped within the sills whereas the Zn-Cu-Pb liquids are expelled to form replacement deposits in the sediments.

These various factors, in conjunction with the S/Se ratios and sulphur isotope values at Frederickson Lake North suggest that sediment-hosted mineralization is not magmatic but syngenetic. More convincing documentation of such an origin is impossible due to the lack of exposure. However, a few broad inferences can be made based on the regional geology and on similar deposits found elsewhere.

On a world-wide basis, most syngenetic base metal deposits hosted solely by sediments can be classified into Cu-rich and Zn-Pb-rich groups (Gustafson and Williams, 1981; Russell et al., 1981). The Frederickson Lake North deposit does not fall clearly into either of these classes. Zn and Cu more commonly are important ore constituents in mixed volcanic-sedimentary deposits (Besshi Type) or in volcanic-dominated environments (Polymetallic Type) (Hutchison, 1980).

On the basis of depositional environment and associated rock types, the Frederickson Lake Zn-Cu-Pb deposits appear more similar to the Besshi type, which occurs in deep marine settings in association with tholeiitic volcanism. The occurrence of all three metals in the former deposits may in part reflect the mixed sedimentary and volcanic source rocks. The polymetallic type, by contrast, occurs in shallow water in association with calc-alkaline to alkaline marine or continental volcanism.

A possible analogous deposit is present at Ankarvattnet in the Northern Swedish Caledonides. This deposit is hosted by Ordovician calcareous turbidites which have been intruded by thick, tholeiitic gabbro sills (Sundblad, 1981). Stephens (1980) interpreted the regional geology of the Ankarvattnet area in terms of a rifted continental margin, similar to the model proposed for the Labrador Trough by Wardle and Bailey (1981). The Ankarvattnet mine (750 000 tonnes; 5.5% Zn, 0.45% Cu, 0.37% Pb) is also similar in grade and tonnage to the Frederickson Lake North Deposit (279 400 tonnes; 4.38% Zn, 0.77% Cu, 0.50% Pb). In the Southern Caledonides, the Roros district contains numerous Zn-Cu-Pb sulphide deposits within a gabbro-intruded metagreywacke sequence (Rui and Bakke, 1975; Sundblad and Stevens, 1983). A similar gabbro-intruded sedimentary sequence characterizes the Ducktown district in the Appalachians (Magee, 1968; Gair and Slack, 1980)

Sediments of the Menihek Formation appear to be partly

coeval with more distal volcanism of the Doublet Group (Wardle and Bailey, 1981; Fournier, 1983). Prior to volcanism, basaltic magmas chambers may have existed which increased heat flow within the sediments of the Cycle II basin. This would have led to circulation of heated formational fluids, which may have leached metals from the sediments. Structures such as the Walsh Lake Fault, which Dimroth (1972) proposed was an original basinal growth fault, could have been influential in focusing the discharge of metal-bearing fluids through the sediments and localizing the deposits. If so, the common brecciated intervals with sulphide matrices in drill core from the Frederickson Lake North showing conceivably could represent fault scarp mineralization. Unfortunately, stratigraphic relations in the study area have been disrupted by the intrusion of thick gabbro sills, and fluid pathways cannot be traced. Nevertheless, the proximity of most Zn-Cu-Pb deposits in the upper levels of the Menihek Formation to the Walsh Lake Fault suggests this structure was influential in their formation.

The closest modern analog of the Frederickson Lake area can found in the Guaymas basin in the Gulf of California (Einsele et al., 1980; Koski et al., 1985). High sedimentation rates in the Guaymas basin have led to burial of a segment of the spreading axis of the East Pacific Rise. As a result, mafic magmas intrude into unconsolidated sediment as sills rather than forming normally layered oceanic crust. Sediment layers are 10 to 100 metres in thickness (Einsele et al., 1980), a range similar to that of the Frederickson Lake

area. Sediments in contact with the sills have been altered by the circulation of pore water fluids driven by the heat of the gabbro sills (Kastner, 1982). Polymetallic sulphide deposits (po-py-sph-cpy-gal) are forming at the sediment-seawater interface as fluids at 200-300°C discharge into seawater (Peter, 1986).

CHAPTER 7 CONCLUSIONS

Although the metallogeny of the Frederickson Lake area remains problematic, arguments presented in this study allow modifications to be made to previous models, as well as allowing constraints to be placed on the genesis of glomeroporphyritic gabbros. The calcic plagioclase glomerophenocrysts of the glomeroporphyritic gabbros could not have been precipitiated from the liquids in which they now reside, which suggests that plagioclase precipitation took place at depth. This is also supported by the textures of glomeroporphyritic gabbros which show that plagioclase glomerophencrysts were only concentrated in the high level glomeroporphyritic sills. It is speculated that prior to rapid rifting, less evolved mafic magmas underwent prolonged fractional crystallization at depth to produce calcic plagioclase phenocrysts. Later rapid rifting released glomeroporphyritic magmas to a specific near-surface stratigraphic interval. Continued rapid rifting, which limited the residence times of magma at depth, led to the formation of ordinary gabbro sills. Such a model therefore relates glomeroporphyritic gabbros to tectonic factors. As such, the assimilation of continental crust is not required to explain the genesis of the plagioclase glomerophenocrysts, although minor assimilation would be undetectable.

Cu-Ni sulphide deposits occurring within glomeroporphyritic gabbros are interpreted as magmatic deposits formed by sulphide liquid immiscibility. The average sulphur isotopic composition of pyrrhotites from the

Frederickson Lake South Cu-Ni showing (+3.7 per mil) is consistent with a component of non-magmatic sulphur. Low metal grades, which reflect low magma/sulphide ratios, suggest that sulphide liquid immiscibility took place within high-level sills rather than within gabbro magma chambers at depth. The contact metamorphism of sulphide-facies iron formation could have provided enough sulphur to saturate the melt and induce sulphide liquid immiscibility. The exclusion of Cu-Ni deposits from anorthositic and ordinary gabbro sills may reflect the dilution of any incorporated sulphur by these thicker sills.

The Zn-Cu-Pb deposits of the Frederickson Lake area are interpreted as synsedimentary in origin, rather than magmatic. This is supported by the occurrence of these deposits in sediments of the Menihek Formation and by arguments relating to the inability of gabbroic magmas to segregate sulphide liquids enriched in lead and zinc. Metals may have been acquired during circulation of heated formational fluids through sediments prior to and during the high level, synsedimentary intrusion of Montagnais Group sills; faults may have focused discharge of these fluids on the seafloor to produce syngenetic massive sulphide deposits. Later gabbro sills invaded the sediments of the Menihek Formation, further enclosing the sediments and sulphide deposits within a sequence of thick gabbro sills. The sulphides seem to represent an uncommon class of syngenetic, sediment-hosted deposits enriched in Zn-Cu-Pb that form in deep water marine settings during tholeiitic volcanism.

REFERENCES

Albarede, F., and Juteau, M., 1984, Unscrambling the lead model ages: Geochim. Cosmochim. Acta, v. 48, p. 207-212.

Ashwal, L.D., Morrison, D.A., Phinney, W.C., and Wood, J., 1983, Origin of Archean anorthosites: evidence from the Bad Vermillion Lake Anorthosite Complex, Ontario: Contr. Mineral. Petrol., v. 82, p. 259-273.

Avramtchev, L., and LeBel-Drolet, S., 1979, Inventaire des gisements minéraux du Quebec, au 30 septembre 1979: Ministère des Richesses Naturelles du Québec, DPV-707.

Auclair, G., Fouquet, Y., and Bohn, N., 1987, Distribution of selenium in high-temperature hydrothermal sulphide deposits at 13 north, East Pacific Rise: Can. Mineral., in press.

Auger, P.E., 1950, Report on detailed geological mapping in the Frederickson-Faute-Martin Lake area, Base metal zone: Labrador Mining and Explor. Comp. Ltd.: Ministère de l'Energie et des Ressources du Québec, GM-6844, 20p.

Baragar, W.R.A., 1960, Petrology of basaltic rocks in part of the Labrador Trough: Bull. Geol. Soc. Am., v. 77, p. 1589-1644.

Baragar, W.R.A., 1967, Wakuach map area, Quebec-Labrador: Geol. Sur. Can., Memoir 344. 174 p.

Bowen, N., 1928, The Evolution of Igneous Rocks. Dover Press: New York, 332 p.

Buchanan, D.L., and Nolan, J., 1979, Solubility of sulphur and sulphide immiscibility in synthetic tholeiitic melts and their relevance to Bushveld Complex rocks: Can. Mineral., v. 17, p. 483-494.

Buchanan, D.L., and Rouse, J.E., 1984, Role of contamination in the precipitation of sulphides in the Platreef of the Bushveld Complex: in: M.J. Jones (ed.), Sulphide Deposits in Mafic and Ultramafic Rocks, p.141-146.

Campbell, I.H., and Naldrett, A.J., 1979, The influence of silicate:sulphide ratios on the geochemistry of magmatic sulphides: Econ. Geol., v. 74, p. 1503-1505.

Campbell, I.H., and Barnes, S.J., 1984, A model for the geochemistry of the platinum-group elements in magmatic sulphide deposits: Can. Mineral., v. 22, p. 151-160.

Cameron, A.W.G., 1968, A new table of solar abundances of the elements in the solar system: in: L.H. Ahrens (ed.), Origin and Distribution of the Elements: Pergammon Press: Oxford.

Cameron, E.M., 1983, Genesis of Proterozoic iron-formation: Sulphur isotope evidence: Geochim. Cosmochim. Acta, v. 47, p. 1069-1074.

Clark, T., 1987, Platinum group element occurrences of the Labrador Trough: Minsitère des Richesses Naturelles du Québec, Document de promotion no. 18.

Clark, T., and Thorpe, R., 1987 Lead isotope galena ages from the Labrador Trough: (abs.) In: GAC-MAC joint annual meeting Saskatoon 1987, p. 37.

Cullen, A., Vicenzi, E., and McBirney, A.R., 1985, Abingdonites, plagioclase ultraphyric basalts of the Galapagos Archipelago: in press.

Czamanske, G.K., and Moore, J.G., 1977, Composition and phase chemistry of sulphide globules in basalt from the mid-Atlantic ridge rift valley near 37 lat: Geol. Soc. Am. Bull., v. 88, p.587-599.

Dimroth, E., 1970, Evolution of the Labrador Geosyncline: Geol. Soc. Am. Bull., v. 81, p. 2717-2742.

Dimroth, E., Baragar, W.R.A., Bergeron, R., and Jackson, G.D., 1970, The filling of the Circum-Ungava Geosyncline: In: A.J. Baer, (ed.), Symposium on Basins and Geosynclines of the Canadian Shield, Geol. Sur. Can., Paper 70-40, p. 45-142.

Dimroth, E., 1972, The Labrador Geosyncline revisited: Am. J. Sci., v. 272, p. 487-506.

Dimroth, E., 1978, Région de la Fosse du Labrador (54 30 - 56 30): Ministère des Richesses Naturelles du Québec, Geology Report 193, 396 p.

Dimroth, E., and Dressler, B., 1978, Metamorphism of the Labrador Trough. In: Metamorphism of the Canadian Shield. Geol. Sur. Can., Report 78-10, p. 215-236.

Dimroth, E., 1981, Labrador Geosyncline: type example of early Proterozoic cratonic reactivation: In: A. Kroner (ed.), Precambrian Plate Tectonics, Elsevier: Amsterdam, p. 332-352.

Doe, B.R., and Stacey, J.S., 1974, The application of lead isotopes to the problem of ore genesis and ore prospect evaluation: A review: Econ. Geol., v. 69, p. 757-776.

Doe, B.R. and Zartman, R.E., 1979 Plumbotectonics I, the Phanerozoic: In: H. L. Barnes (ed.), Geochemistry of Hydrothermal Ore Deposits, 2nd edition, Wiley Interscience: New York, p. 22-70.

Eckstrand, O.R., 1983, Sulphur isotope data for selected nickel deposits of the Labrador Trough and Thompson Belt: Notes accompanying a poster display, Geol. Sur. Can., Current Activities Fourm, unpublished.

Eckstrand, O.R., and Hulbert, L.J., 1987, Selenium and the source of sulphur in magmatic nickel and platinum deposits: (abs.) In: GAC-MAC joint annual meeting, Saskatoon 1987, p. 40.

Einsele, G., Gieskes, J.M., Curray, J., Moore, D.M., Aguayo, E., Aubury, M., Fornari, D., Guerrero, J., Kastner, M., Kelts, K., Lyle, M., Matoba, Y., Molina-Cruz, A., Niemitz, J., Rueda, J., Saunders, A., Schrader, H., Simoneit, B., and Vacquier, V., 1980, Intrusion of basaltic sills into highly porous sediments, and resulting hydrothermal activity: Nature, v. 283, p. 441-445.

Flower, M.F., 1980 Accumulation of calcic plagioclase in ocean-ridge tholeiites: an indication of spreading rate?: Nature v. 285, p. 530-532.

Fournier, D., 1983, Les Indices de Cu-Ni et de Zn-Cu, Fosse du Labrador: unpublished Phd Thesis, Université de Pierre et Marie Curie, Paris, 209 p.

Franklin, J.M., Roscoe, S.M., Loveridge, W.D., and Sangster, D.F., 1983, Lead isotope studies in Superior and Southern Provinces: Geol. Sur. Can., Bull. no. 351, 60 p.

Frarey M.J., and Duffell, S,. 1964, Revised stratigraphic nomenclature for the central part of the Labrador Trough: Geol. Sur. Can., Paper 64-25, p. 1-13.

Frarey, M.J., 1967, Willbob Lake and Thompson Lake map area, Quebec and Newfoundland: Geol. Sur. Can., Memoir 348, 73 p.

Fryer, B.J., 1972, Age determination in the Circum - Ungava geosyncline and the evolution of Precambrian banded iron-formations: Can. J. Earth Sci., v. 9, p. 652-663.

Gair, J., and Slack, J.F., 1980, Stratabound massive sulphide deposits of the U.S. Appalachians. in: F.M. Volkes and E. Zackrisson (eds.), Review of Caledonian-Appalachian Stratabound Sulphides: Geol. Sur. Ireland, Special Paper 5, p. 67-81.

Godlevski, M.N., and Grinenko, L.N., 1963, Some data on the isotopic composition of the sulphides from the Noril'sk deposit: Geochemistry v. 1, p. 35-41.

Goldschmidt, V.M., and Strock, L.W., 1935, Zur geochemie des selens II: Ges. Wiss. Gottingen, Nachr., mat-phys. Kl., Geol. U. Miner. N.F. Bd. 1, no. 11, p. 123-142.

Goulet, N., Gariépy, C., and Mareschal, J.C., 1987, Structure, geochronology, gravity and tectonic evolution of the Northern Labrador Trough: (abs.) In: GAC-MAC joint annual meeting, Saskatoon 1987, p. 48.

Green, N.L., 1975, Archean glomeroporphyritic basalts: Can. J. Earth Sci., v. 12, p. 1770-1784.

Griffis, A.T., 1943, The Geology of the Attikamagen-George River area, 1942: Labrador Mining and Explor. Comp. Ltd: Ministère de l'Energie et des Ressources du Québec, GM-1212, 26 p.

Griffis, A.T., 1945, The Frederickson-Jimmick-Walsh Lake area, 1944: Hollinger North Shore Explor. Comp. Ltd: Ministère de l'Energie et des Ressources du Québec, GM-8394B, 39 p.

Gulson, B.L., and Porritt, P.M., 1987, Base metal exploration of the Mount Read volcanics, Western Tasmania: pt. II. Lead isotope signatures and genetic implications: Econ. Geol., v. 82, p. 291-307.

Gulson, B.L., Large, R.R., and Porritt, P.M., 1987, Base metal exploration of the Mount Read volcanics, Western Tasmania: pt. III. Application of lead isotopes at Elliott Bay: Econ. Geol., v. 82, p. 308-327.

Gustafson, L. B., and Williams, N., 1981, Sediment-hosted stratiform deposits of copper, lead and zinc. In: B. J. Skinner (ed.), Economic Geology 75th Anniversary Volume, p. 139-178.

Harrison, J.M., 1952, The Quebec-Labrador iron belt, Quebec and Newfoundland (preliminary report): Geol. Sur. Can., Report 52-20.

Harrison, J.M., Howell, J.E., and Farhig, W.F., 1972, A geological cross section of the Labrador Trough miogeosyncline near Schefferville, Quebec: Geol. Sur. Can., Report 70-37.

Haughton, D.R., Roedder, P.L., and Skinner, B.J., 1974, Solubility of sulphur in mafic magmas: Econ. Geol., v. 69, p. 451-461.

Hamlyn, P.R., Keays, R.R., Cameron, W.E., Crawford, A. J., and Waldron, H.M., 1985, Precious metals in magnesian low-Ti lavas: implications for metallogenesis and sulphur saturation in primary magmas: Geochim. Cosmochim. Acta, v. 49, p. 1797-1811.

Helz, R.T., 1977, Determination of P-T dependance of the first appearance of Fe-S-rich liquids in natural basalts to 20 kb: (abs.) EOS, v. 58, p.523.

Hobbs, B.E., Means, W.P., and Williams, P.F., 1976, An Outline of Structural Geology: John Wiley and Sons: Toronto, 571 p.

Hogg, G.M., 1957, Report on the Frederickson Prospect: Hollinger North Shore Explor. Comp. Ltd, Ministère de l'Energie et des Ressources du Québec, GM-5200.

Hutchison, R.W., 1980, Massive base metal sulphide deposits as guides to tectonic evolution. in: D.W. Strangeway (ed.), Continental Crust and Its Mineral Deposits: Geological Association of Canada, Special Paper 20, p. 659-684.

Irvine, T.N., and Baragar, W.R.A., 1971, A guide to the chemical classification of common volcanic rocks: Can. J. Earth Sci., v. 8, p. 523-548.

Irvine, T.N., 1975, Crystallization sequences of the Muskox intrusion and other layered intrusions II. Origin of chromite layers and other similar deposits of other magmatic ores: Geochim. Cosmochim. Acta, v. 39, p. 991-1020.

Jensen, L.S., 1976, A new cation plot for classifying subalkalic volcanic rocks: Ont. Dept. Mines, Misc. Paper 66.

Kajiwara, Y., Sasaki, A., and Matsubaya, O., 1981, Kinetic sulphur isotopic effects in the thermal decomposition of pyrite: Geochem. Jour., v. 15, p. 193-197.

Kastner, M., 1982, Evidence for two distinct hydrothermal systems in the Guaymas Basin: In: J.R. Curray and D.G. Moore et al., (eds.), Initial Reports of the Deep Sea Drilling Project, v. 64, Washington (U.S. Govt. Printing Office), p. 1143-1157.

Kavanagh, P.M., 1953, Geology of the Hyland Lake area, New Quebec: Labrador Mining and Explor. Comp. Ltd: Ministère de l'Energie et des Ressources du Québec, GM-2757.

Kirkland, R.W., 1950, The Connolly-Walsh Lake area, New Quebec: Ministère de l'Energie et des Ressources du Québec, GM-6847, 9 p.

Kite, B.T., 1981, The Geology of the Zenith Zinc deposit near Schreiber Ontario: B.Sc. Thesis, Lakehead University, Unpublished.

Koski, R.A., Lonsdale, P.F., Shanks, W.C., Berndt, M.E., and Howe, S.S., 1985, Mineralogy and geochemistry of a sediment-hosted hydrothermal sulphide deposit from the Southern Trough of the Guaymas Basin, Gulf of California: J. Geophys. Res., v. 90, no. B8, p. 6695-6707.

Kullerud G., and Yoder, H.S., 1959, Pyrite stability relations in the Fe-S system: Econ. Geol., v. 54, p. 533-572.

Lavergne, C., 1985, Gîtes minéraux à tonnage évalué et production minérale du Québec: Ministère de l'Energie et Des Ressources, Québec, DV-85-08.

LeGallais, C.J., and LaVoie, S., 1982, Basin evolution of the Lower Proterozoic Kaniapiskau Supergroup, central Labrador miogeocline (Trough), Quebec: Bull. Can. Soc. Pet. Geol., v. 30, p. 150-166.

Low, A.P., 1898, Report on a traverse of the Northern part of the Labrador Peninsula from Richmond Gulf to Ungava Bay: Geol. Sur. Can., Annu. Rept. 9, part L.

MacLean, W.H., 1969, Liquidus phase relationships in the FeS-FeO-Fe2O3-SiO2 system, and their application in geology: Econ. Geol., v. 64, p. 865-884.

MacLean, W.H., 1977, Sulphides in Leg 37 drill cores from the mid-Atlantic: Can. J. Earth Sci., v. 14, p. 677-683.

MacLean W,H., and Shimazaki, H., 1976, The partition of Co, Ni, Cu and Zn in silicate liquids: Econ. Geol., v. 74, p. 1049-1057.

Magee, M., 1968, Geology and ore deposits of the Ducktown district, Tennessee. in: J.D. Ridge (ed.), Ore Deposits of the United States, 1933-1967: AIME, p. 208-241.

Mainwaring, P.R., and Naldrett, A.J., 1977, Country-rock assimilation and the genesis of Cu-Ni sulfides in the Water Hen intrusion, Duluth Complex, Minnesota: Econ. Geol., v. 72, p. 1269-1284.

Mathez, E.A., 1976, Sulphur solubility and magmatic sulphides in submarine basaltic glass: J. Geophy. Res., v. 81, p. 4269-4276.

McCarthy, T.S., Lee, C.A., Fesq, H.W., Kable, E.J.D., and Erasmus, C.S., 1984, Sulphur saturation in the lower and critical zones of the Eastern Bushveld Complex: Geochim. Cosmochim. Acta, v. 48, p. 1005-1019.

McGoldrick, P.J., Keays, R.R., and Scott, B.S., 1979, Thallium: a sensitive indicator of rock/seawater interaction and of sulphur saturation in silicate melts: Geochim. Cosmochim. Acta., v. 43, p. 1303-1311.

Mitchell, R.H., and Keays, R.R., 1981, Abundance and distribution of gold, palladium, and iridium in some spinel and garnet ilherolites: Implications for the nature and origin of precious metal-rich intergranular components in the upper mantle: Geochim. Cosmochim. Acta, v. 45, p. 2425-2442.

Ministère de L'Energie de Des Ressources Quebec, 1985, Map # 2001, DV 85-09.

Moore, J.G., and Fabbi, B.P., 1971, An estimate of the juvenile sulphur content of basalt: Contr. Mineral. Petrol., v. 33, p. 118-127.

Naldrett, A.J., Hoffman, E.L., Green, A.H., Chou, C.L., and Naldrett, S.R., 1979, The composition of Ni-sulphide ores, with particular reference to their content of PGE and Au: Can. Mineral., v. 17, p. 403-415.

Naldrett, A.J., 1981, Nickel sulphide deposits: classification, composition and genesis. In: B. J. Skinner (ed.), Economic Geology 75th Anniversary Volume, p. 628-685.

Nielsen, R.L., and Dungan, M.A., 1983, Low pressure mineral-melt equilibria in natural anhydrous mafic systems: Contr. Mineral. Petrol., v. 84, p. 310-326.

Ohomto, H., and Rye, R.O., 1979, Isotopes of sulphur and carbon: In: H.L. Barnes (ed.), Geochemistry of Hydrothermal Ore Deposits, second edition. John Wiley and Sons: Interscience, p. 509-567.

Pearce, J.A., and Cann, J.R., 1973, Tectonic setting of basic volcanic rocks determined using trace element analyses: Earth Planet. Sci. Lett., v. 19, 290-300.

Pearce, J.A., and Norry, M.J., 1979, Petrogenetic implications of Ti, Zr, and Nb variations in volcanic rocks: Contr. Mineral. Petrol., v. 69, p. 33-47.

Pélissonnier, H., 1972, Les dimensions des gisements de cuivre du monde. Essai de métallogénie quantitative: Bur. Recherche Géol. Minière. Memoir 57, 405 p.

Peter, J.M., 1986, Genesis of hydrothermal vent deposits in the Southern Trough of the Guaymas Basin, Gulf of California: A mineralogical and geochemical study: MSc. Thesis, University of Toronto, Unpublished.

Phinney, W.C., and Morrison, D.A., 1982, Archean megacrystic plagioclase units and the tectonic setting of greenstones: Lunar Planet. Sci. Inst., Report 82-01, Houston, p. 121-124.

Phinney, W.C., and Morrison, D.A., 1984, Calcic plagioclase megacrysts: implications for widespread formation of cumulates in Archean crust: Precambrian Geochemistry Field Conference, 1984, p. 115.

Phinney, W.C., and Morrison, D.A., 1985, Alteration in Archean anorthosites, Lunar Planet. Sci. Conf. XVII, Houston, p. 589-590.

Rao, B.V., and Ripley, E.M., 1983, Petrochemical studies of the Dunka Road Cu-Ni deposit, Duluth Complex, Minnesota: Econ. Geol., v. 78, p. 1222-1238.

Ringwood, A.E., 1966, The Chemical composition and the origin of the earth: In: P.M. Hurley (ed.), Advances in Earth Science. MIT Press: Cambridge Mass.

Ripley, E.M., 1981, Sulphur isotopic studies of the Dunka Road Cu-Ni deposit, Duluth Complex, Minnesota: Econ. Geol., v. 76, p. 610-620.

Ripley, E.M., and Alawi, J.A., 1986, Sulphide mineralogy and chemical evolution of the Babbitt Cu-Ni deposit, Duluth Complex, Minnesota: Can. Mineral., v. 24, p. 347-368.

Ripley, E.M., and Al-Jassair, T.J., 1987, Sulphur and oxygen isotope studies of melt-country rock interaction, Babbit Cu-Ni deposit, Duluth Complex, Minnesota: Econ Geol., v. 82, p. 87-107.

Roedder, P.L., 1981, CO2-sulphide melt and silicate melt inclusions in olivine nodules from the Loihi Seamount, Hawaii: (abs.) EOS, v. 62, p. 1083.

Rui, J.I., and Bakke, I., 1975, Stratabound sulphide mineralization in the Kjoli area, Roros District, Norwegian Caledonides: Norsk Geologisk Tidsskrift, v. 55, p. 51-57.

Russell, M.J., Solomon, M., and Walshe, J.L., 1981, The genesis of sediment-hosted, exhalative zinc + lead deposits: Mineral. Deposita, v. 16, p. 113-127.

Sarnthein, M., and Diester-Haass, L., 1977, Eolian-sand turbidites: J. Sed. Petrol., v. 47, no. 2, p. 868-890.

Sasaki, A., Arikawa and Foinsbee, R., 1979, Kiba reagent method of sulphur extraction applied to isotopic work: Bull. Geol. Sur. Japan, v. 30, p. 241-245.

Sauvé, P., and Bergeron, R., 1965, Region des lacs Gerido et Thevenet: Ministère des Richesses Naturelles du Québec, Geology Report 104, 110 p.

Shimazaki, H., and MacLean, W,H., 1976, An experimental study on the partition of lead and zinc between silicate and sulphide liquids: Mineral. Deposita, v. 11, p. 125-132.

Stacey, J.S., and Krämers, J.D., 1976, Approximation of terrestrial lead by a two stage model: Earth Sci. Plan. Lett., v. 26, p. 207-221.

Stanton, R.L., 1972, Ore Petrology. McGraw Hill: New York, 713 p.

Stephens, M.B., 1980, Occurrence, nature and tectonic significance of volcanic and high-level intrusive rocks within the Swedish Caledonides: In: D.R. Wones (ed.), The Caledonides in the USA. Viriginia Polytechnic Institute and State University, Blacksburg, p. 289-298.

Stolper, E.M., and Walker, D., 1980, Melt density and the average composition of basalt: Contr. Mineral. Petrol., v. 74, p. 7-12.

Sullivan, C.J., 1959, The origin of massive sulphide ores: CIM Bull., v. 52, p. 613-619.

Sundblad, K., 1981, Chemical evidence for, and implication of, a primary FeS phase in the Ankarvattnet Zn-Cu-Pb massive sulphide deposit, Central Swedish Caledonides: Mineral. Deposita, v. 16, p. 129-146.

Sundblad, K., and Stephen, M.B., 1983, Lead Isotope systematics of strata-bound sulphide deposits in the Higher Nappe Complexes of the Swedish Caledonides: Econ. Geol., v. 78, p. 1090-1107.

Taylor, S.R., and Gorton, M.P., 1977, Geochemical application of spark source spectrography III, element sensitivity, precision and accuracy: Geochim. Cosmochim. Acta, v. 41, p. 1375-1380.

Taylor, S.R., and McLennan, S.M., 1985, The Continental Crust: Its Composition and Evolution: Blackwell Scientific Publications: London.

Thompson, J.F.H., and Naldrett, A.J., 1984, Sulphide-silicate reactions as a guide to Ni-Cu-Co mineralization in central Maine USA. in: D.L. Buchanan and M.J. Jones (eds.), Sulphide deposits in Mafic and Ultramafic Rocks. p. 103-113.

Volkes, F.M., 1969, A review of the metamorphism of sulphide deposits: Earth Sci. Rev., v. 5, p. 99-143.

Vogt , J.H.L., 1893, Bildung von Erzlagerstatten durch differentiationprocesse in basischen Eruptivmagmata. II. z. prakt. Geol., p. 125-143.

Wardle, R.J., and Bailey, D.G., 1981, Early Proterozoic sequences in Labrador: Geol. Sur. Can., Report, 81-10, p. 331-395.

Watkinson, D.H., Mainwaring, P.R., and Pertold, Z., 1978, The Cu-Zn Obrazak deposit, Czechoslovakia, a volcanogenic deposit invaded in the Ransko Intrusive Complex: Mineral. Deposita, v. 13, p. 151-163.

Wendlandt, R.F., 1982, Sulphide saturation of basalt and andesite melts at high pressures and temperatures: Am. Mineral., v. 67, p. 877-885.

Wilkinson, J.F.G., 1982, The genesis of mid-ocean ridge basalt: Earth Sci. Rev., v. 18, p. 1-57.

Winchester, J.A., and Floyd, P.A., 1976, Geochemical magma type discrimination: application to altered and metamorphosed basic igneous rocks: Earth Planet. Sci, Lett., v. 28, p. 459-469.

Yamamoto, M., 1976, Relationship between Se/S and sulphur isotope ratios of hydrothermal sulphide minerals: Mineral. Deposita, v. 11, p. 197-209.

York, D., 1969, Least squares fitting of a straight line with correlated errors: Earth Planet. Sci. Lett., v. 5, p. 320-324.

APPENDIX 1 Chemical Analyses

	99391 Gabbro	99392 Gabbro	99393 Gabbro	99394 Gabbro	99395 Gabbro	99396 Gabbro	99397 Gabbro	99398 Gabbro	99399 Gabbro	99400 Gabbro	99401 Gabbro	99402 Gabbro
SiO2	48.6	48.5	49.2	50.3	49.3	49.4	47.1	45.7	49.6	48.6	48.7	48.7
Al2O3	12.7	11.8	13.3	12.2	11.9	11.6	11.9	12.1	13.3	14.4	15.8	16.2
Fe tot	14.5	16.5	14.5	15.9	16.9	17.8	18.9	18.8	13.4	15.5	12.8	12.1
MgO	6.63	6.04	6.14	6.10	6.04	4.68	5.61	6.07	6.26	5.12	5.81	4.77
CaO	8.49	8.22	8.70	7.81	8.25	8.09	9.47	9.57	9.29	7.62	8.16	10.2
Na2O	2.53	1.75	2.50	2.13	2.44	2.26	2.08	1.93	2.77	3.70	3.09	2.79
K2O	0.18	0.15	1.32	0.06	0.21	0.18	0.41	0.49	0.57	0.11	0.67	0.70
TiO2	1.39	1.86	1.51	1.74	1.82	2.41	1.99	2.06	1.32	1.49	1.21	1.16
MnO	0.22	0.20	0.19	0.21	0.21	0.22	0.23	0.23	0.20	0.17	0.16	0.16
P2O5	0.11	0.16	0.12	0.15	0.13	0.16	0.10	0.08	0.09	0.13	0.09	0.10
LOI	3.16	3.04	2.73	3.12	2.85	2.62	1.99	2.16	2.46	2.74	2.63	2.37
Total	98.51	98.22	100.21	99.72	100.05	99.42	99.78	99.19	99.26	99.58	99.12	100.35
Ba		38		22		61		142		30		112
Be		3		2		3		3		2		2
Cd		nd		nd		nd		nd		nd		nd
Ce		22		24		24		19		19		13
Co		51		50		53		62		49		40
Cr		19		30		12		10		25		18
Cu		224		78		237		407		78		199
Dy		9		8		9		6		6		5
Eu		6		6		6		6		5		4
La		5		6		36		nd		6		7
Li		17		14		10		10		8		8
Mo		nd		nd		nd		nd		nd		nd
Nd		105		115		130		105		100		75
Ni		49		54		37		86		51		51
Pb		nd		nd		nd		nd		nd		nd
Pr		nd		nd		nd		nd		nd		nd
Sc		48		49		48		54		44		42
Sm		3		nd		nd		nd		nd		nd
V		500		457		616		963		418		342
Zn		85		72		84		68		87		61
Ga						20						
Nb						5						
Rb						6						
Sr						120						
Ta						nd						
Th						3						
U						4						
Y						39						
Zr						130						

Gabbro = Montagnais gabbro

major elements in wt% trace elements in ppm nd=not detected blank space=not analyzed

APPENDIX 1 Chemical Analyses

	99403 Gabbro	99404 Gabbro	99405 Gabbro	99406 Gabbro	99407 Gabbro	99408 Gabbro	99409 Gabbro	99410 Gabbro Chill	99411 Gabbro Glom	99412 Gabbro Glom	99413 Gabbro Glom	99414 Gabbro Glom
SiO2	48.7	49.1	48.1	48.0	47.2	45.3	47.8	47.7	46.6	47.1	46.2	44.1
Al2O3	11.5	15.3	15.3	17.7	17.3	16.9	14.6	13.6	19.2	14.6	14.8	13.6
Fe tot	14.9	11.8	11.0	8.0	8.2	11.1	12.8	14.4	9.8	13.2	14.1	16.3
MgO	8.88	5.85	6.79	5.85	7.45	8.50	7.96	7.50	5.61	8.32	9.49	9.77
CaO	10.0	10.9	11.8	12.1	12.8	9.59	10.7	9.54	11.4	9.64	9.78	8.28
Na2O	1.44	2.34	1.89	2.52	1.92	2.28	2.04	2.11	2.16	2.16	1.35	1.29
K2O	0.24	0.44	0.30	0.72	0.50	0.30	0.16	1.01	0.85	0.18	0.15	0.13
TiO2	1.00	1.15	0.90	0.73	0.68	0.82	1.07	1.18	0.90	1.13	0.97	0.98
MnO	0.22	0.18	0.16	0.13	0.13	0.17	0.19	0.28	0.14	0.19	0.18	0.16
P2O5	0.07	0.08	0.07	0.06	0.04	0.12	0.09	0.08	0.08	0.10	0.08	0.08
LOI	2.59	2.13	2.54	2.49	2.40	3.31	1.65	1.89	3.35	2.93	2.65	3.92
Total	99.54	99.27	98.85	98.30	98.62	98.39	99.06	99.29	100.09	99.55	99.75	98.61
Ba		88		159			44	188	136	54	34	34
Be		1		1			1	2	1	1	1	1
Cd		nd		nd			nd	nd	nd	nd	nd	nd
Ce		13		10			11	13	11	13	12	14
Co		40		31			55	55	42	53	69	120
Cr		39		250			96	200	49	240	67	47
Cu		187		127			134	203	133	286	247	1400
Dy		4		2			4	5	2	3	3	3
Eu		4		3			4	4	3	4	4	5
La		2		3			nd	4	nd	2	4	9
Li		6		11			8	10	9	14	7	13
Mo		nd		nd			nd	nd	nd	nd	nd	nd
Nd		70		50			70	70	75	70	65	65
Ni		66		77			199	154	155	190	321	593
Pb		nd		nd			nd	nd	nd	nd	nd	nd
Pr		nd		nd			nd	nd	nd	nd	nd	nd
Sc		47		40			42	45	29	36	28	28
Sm		nd		nd			nd	nd	nd	nd	nd	nd
V		327		217			332	374	269	320	248	256
Zn		53		39			60	117	70	71	97	74
Ga		19								18		15
Nb		nd								nd		nd
Rb		10								6		5
Sr		150								140		95
Ta		9								nd		5
Th		nd								5		8
U		nd								nd		3
Y		22								19		19
Zr		65								74		63

Gabbro = Montagnais gabbro Gabbro Glom = glomeroporphyritic gabbro Chill = chilled margin

major elements in wt% trace elements in ppm nd=not detected blank space=not analyzed

APPENDIX 1 Chemical Analyses

	99415 Gabbro Glom	99416 Gabbro Glom	99417 Gabbro Glom	99418 Gabbro Chill	99419 Basalt Menih	99420 Basalt Menih	126 Basalt Doub	127 Basalt Doub	128 Basalt Doub	129 Volcan Murd	130 Volcan Murd	131 Volcan Murd
SiO2	45.2	45.0	47.4	47.6	48.7	46.4	49.5	46.3	48.2	47.4	44.0	45.3
Al2O3	18.1	15.5	13.8	14.0	13.5	14.1	14.6	13.8	13.2	11.7	9.4	13.6
Fe tot	12.4	12.6	15.8	13.0	13.5	14.7	12.3	13.9	13.7	12.8	18.1	15.3
MgO	7.47	8.16	7.27	7.64	6.79	7.42	6.51	5.73	6.13	10.3	11.0	8.18
CaO	10.3	11.0	8.57	10.7	10.1	8.78	10.2	10.7	11.4	6.97	7.62	6.31
Na2O	1.50	1.41	1.99	1.69	1.90	2.65	2.70	1.89	1.11	3.60	3.04	4.21
K2O	0.35	0.38	0.46	0.40	0.31	0.16	0.06	0.12	0.07	0.20	0.11	0.10
TiO2	0.77	0.88	1.15	1.09	1.38	1.33	1.19	1.51	1.21	2.34	3.79	3.65
MnO	0.13	0.15	0.24	0.19	0.20	0.20	0.16	0.19	0.15	0.15	0.11	0.08
P2O5	0.05	0.06	0.11	0.08	0.11	0.10	0.11	0.12	0.08	0.17	0.31	0.45
LOI	3.43	3.00	2.79	2.72	2.72	3.31	2.08	4.91	4.38	2.48	2.42	2.60
Total	99.70	98.14	99.58	99.11	99.21	99.15	99.41	99.17	99.43	98.11	99.90	99.71
Ba	62	46	42	40	158	50	17					
Be		1	1	1	2	1	1					
Cd	nd	nd	1	nd	nd	nd	nd					
Ce	11	12	12	15	15	15	15					
Co	73	61	66	49	40	47	40					
Cr	36	180	270	280	270	290	240					
Cu	1000	939	303	95	133	137	42					
Dy	2	2	4	4	5	4	4					
Eu	4	4	4	4	4	5	4					
La	3	5	10	5	4	6	3					
Li	14	9	10	13	19	6	6					
Mo	nd	nd	nd	nd	nd	nd	nd					
Nd	55	65	75	75	90	85	70					
Ni	417	411	118	168	95	108	94					
Pb	nd	nd	nd	nd	nd	nd	nd					
Pr	nd	nd	nd	nd	nd	nd	nd					
Sc	29	30	45	44	46	46	46					
Sm	nd	nd	nd	nd	nd	nd	nd					
V	200	248	343	348	391	381	348					
Zn	69	86	314	91	76	83	84					
Ga			21		16	19	17					
Nb			nd		3	nd	nd					
Rb			27		11	5	nd					
Sr			87		210	97	130					
Ta			nd		nd	nd	nd					
Th			5		5	8	5					
U			nd		4	nd	nd					
Y			19		25	25	24					
Zr			65		87	83	75					

Menih = Menihek Formation Doub = Doublet Formation Murd = Murdoch Formation

major elements in wt% trace elements in ppm nd=not detected blank space=not analyzed

APPENDIX 1 Chemical Analyses

	132 Volcan Murd	133 Volcan Murd	134 Volcan Murd	135 Volcan Murd	20464 Cu-Ni Fred S	20465 Cu-Ni Fred S	20466 Cu-Ni Gos-1	20467 Po-Py Faute	20468 Zn-Cu Fred N	20469 Zn-Cu Jimmic	20470 Po-Py Gos L.	20471 Cu-Ni Conn
SiO2	42.1	42.3	43.1	39.3								
Al2O3	7.3	7.1	7.5	7.8								
Fe tot	14.3	13.3	13.8	16.5								
MgO	19.7	21.2	18.3	20.1								
CaO	8.58	7.93	9.13	8.05								
Na2O	0.21	0.12	0.30	0.12								
K2O	0.05	0.02	0.03	0.02								
TiO2	2.06	1.57	1.87	1.77								
MnO	0.17	0.15	0.14	0.17								
P2O5	0.15	0.12	0.13	0.15								
LOI	4.73	5.12	4.42	5.47								
Total	99.35	98.93	98.72	99.45								
Ba				7	26	4	62	56	17	18	10	36
Be				2	nd	nd	nd	1	nd	nd	1	3
Cd				nd	nd	4	nd	4	175	8	nd	1
Ce				50	3	nd	6	19	27	nd	36	38
Co				92	279	934	120	38	35	91	24	50
Cr				2300	77	nd	330	31	44	nd	45	48
Cu				269	6000	41900	3000	563	2600	4600	208	235
Dy				3	5	3	5	4	9	1	7	4
Eu				5	7	16	4	14	7	10	5	8
La				95	2	nd	3	17	18	394	13	27
Li				13	10	nd	12	6	19	2	9	6
Mo				nd	nd	5	nd	22	59	4	nd	25
Nd				110	nd	nd	50	nd	nd	nd	60	35
Ni				1000	2300	8100	1200	256	38	33	36	186
Pb				nd	nd	nd	nd	59	7700	36	nd	17
Pr				nd	nd	nd	nd	nd	nd	nd	nd	nd
Sc				29	18	3	36	8	9	2	13	10
Sm				nd	nd	nd	nd	nd	nd	nd	nd	nd
V				293	103	83	280	99	169		156	352
Zn				46	129	119	92	76	>3	1600	81	61
Ga								25	230	44	11	20
Nb								31	13	22	5	54
Rb								36	5	nd	nd	3
Sr								3	3	nd	6	4
Ta								nd	nd	9	nd	nd
Th								17	nd	7	11	10
U								13	nd	nd	nd	7
Y								11	7	nd	20	18
Zr								56	76	8	61	180

Volcan = volcanic rock
Gos-1 = Gossan 1 Showing
Gos L. = Gossan Lake Showing
Fred S = Frederickson South Showing
Fred N = Frederickson North Showing
Faute = Faute Showing
Conn = Connolly Showing
Jimm = Jimmick Showing

major elements in wt% trace elements in ppm nd=not detected blank space=not analyzed

APPENDIX 1 Chemical Analyses

	200 Gabbro Glom	201 Gabbro Chill	202 Gabbro Chill	203 Gabbro Chill	204 Gabbro Chill	205 Tuff Menih	711 Argill Menih	712 Gabbro Chill	713 Argill Menih	714 Gabbro Chill	715 Argill Menih	716 Sand. Menih
SiO2	42.6	49.6	42.0	51.5	50.2	60.9	42.4	49.8	39.1	49.5	43.4	59.8
Al2O3	13.3	12.8	5.0	13.4	14.9	12.0	6.8	14.0	7.4	13.8	6.0	15.4
Fe tot	19.2	13.4	38.1	12.2	14.7	15.6	36.6	15.2	38.6	14.0	37.5	12.7
MgO	6.09	6.97	3.00	7.49	6.02	3.32	2.92	7.48	2.49	7.46	3.77	2.38
CaO	9.90	9.32	0.89	8.68	5.50	0.07	0.20	5.83	0.19	8.62	1.50	0.31
Na2O	1.49	3.22	1.14	2.94	2.00	0.30	0.50	2.85	2.50	2.21	0.79	2.20
K2O	0.09	0.18	0.04	0.63	0.73	2.68	2.14	0.79	0.30	1.84	0.06	3.75
TiO2	0.95	1.22	0.32	1.30	1.78	0.38	0.70	1.30	0.52	1.23	0.57	0.37
MnO	0.18	0.32	0.09	0.30	0.51	0.32	0.26	0.40	0.10	0.38	0.28	0.10
P2O5	0.07	0.07	0.15	0.09	0.16	0.03	0.15	0.07	0.07	0.08	0.12	0.05
LOI	4.41	2.04	8.08	1.85	3.61	4.45	8.12	3.03	8.41	2.05	6.08	3.02
Total	98.28	99.14	98.81	100.38	100.11	100.05	100.79	100.75	99.68	101.17	100.07	100.08
Ba	64	41	10	138	213	683	95	360	36	400	17	443
Be	nd	nd	1	nd	1	1	2	nd	2	nd	2	3
Cd	nd	nd	1	nd	nd	nd	nd	nd	nd	nd	nd	nd
Ce	2	5	nd	6	11	25	77	22	74	22	57	48
Co	136	41	25	49	5	19	34	51	40	37	16	
Cr	270	210	53	200	95	71	nd	nd	nd	nd	nd	nd
Cu	6600	84	382	76	228	252	266	57	231	70	140	50
Dy	6	9	5	9	13	5	nd	nd	nd	nd	nd	nd
Eu	6	4	10	4	5	4	4	1	4	2	2	1
La	5	4	nd	4	10	16	40	nd	40	nd	30	22
Li	11	9	21	10	28	26	11	18	13	9	7	14
Mo	nd	nd	26	nd	nd	nd	15	nd	22	nd	9	8
Nd	65	95	nd	95	120	35	40	50	30	55	30	30
Ni	1400	110	129	71	112	20	88	103	158	111	61	90
Pb	nd	nd	32	nd	nd	nd	22	46	22	nd	15	nd
Pr	nd	nd	nd	nd	nd	nd	nd	nd	nd	nd	nd	nd
Sc	46	51	12	52	52	9	11	47	12	41	13	12
Sm	nd	nd	nd	nd	nd	nd	nd	nd	nd	nd	nd	nd
V	275	376	300	387	450	113	184	390	226	381	212	297
Zn	188	61	8	99	132	234	45	103	60	81	50	195
Ga	25	14	40			16	33	18	23	20	22	21
Nb	4	nd	14			3	35	nd	20	nd	13	4
Rb	nd	5	nd			67	77	28	15	71	6	100
Sr	180	62	nd			28	10	110	6	140	12	15
Ta	16	nd	nd			nd	nd	nd	nd	5	nd	nd
Th	4	7	10			14	12	7	8	5	5	21
U	nd	nd	9			5	8	4	9	nd	nd	8
Y	15	24	16			8	21	24	14	24	17	13
Zr	66	68	68			61	140	79	91	76	77	87

Argill = argillite Sand = sandstone

major elements in wt% trace elements in ppm nd=not detected blank space=not analyzed

APPENDIX 1 Chemical Analyses

	717 Sand. Silt	718 Basalt Menih	719 Gabbro Chill	720 Basalt Menih	721 Basalt Menih	722 Basalt Menih	723 Basalt Menih	724 Basalt Menih	725 Gabbro Chill
SiO2	74.8	49.1	54.3	48.0	51.0	48.9	49.2	48.3	49.0
Al2O3	14.0	14.3	12.8	13.6	13.6	13.9	14.0	13.7	14.0
Fe tot	3.9	13.4	11.7	13.9	13.5	13.6	12.2	16.5	15.1
MgO	1.62	6.72	6.24	8.08	6.12	6.83	6.65	6.85	6.82
CaO		10.4	5.00	5.80	9.29	10.7	10.3	8.26	7.98
Na2O	0.13	1.98	2.78	2.84	3.41	2.00	1.85	1.13	2.60
K2O	3.64	0.42	0.11	0.51	0.07	0.65	0.17	0.15	0.60
TiO2	0.40	1.43	0.39	1.26	1.13	1.29	1.20	1.20	1.29
MnO		0.19	0.21	0.22	0.19	0.21	0.21	0.25	0.23
P2O5	0.04	0.10	0.07	0.10	0.09	0.08	0.08	0.09	0.10
LOI	2.73	2.60	7.42	6.29	2.84	2.45	2.96	3.26	2.42
Total	101.26	100.64	101.02	100.60	101.24	100.61	98.82	99.69	100.14
Ba	703	118	27	123	26	208	77	46	206
Be	nd	nd	2	nd	nd	nd	nd	nd	nd
Cd	nd	nd	nd	nd	nd	nd	nd	nd	nd
Ce	37	27	29	22	23	26	26	26	27
Co	4	50	13	29	55	38	41	40	43
Cr	nd	nd	nd	nd	nd	nd	nd	nd	nd
Cu	61	149	25	127	165	143	185	342	217
Dy	nd	nd	nd	nd	nd	nd	nd	nd	nd
Eu	nd	2	1	2	2	2	2	2	1
La	26	15	17	nd	nd	nd	nd	nd	nd
Li	10	11	31	31	8	7	6	11	8
Mo	nd	nd	nd	nd	nd	nd	nd	nd	nd
Nd	nd	45	25	40	45	30	40	60	45
Ni	14	93	37	105	112	102	107	106	98
Pb	15	nd	nd	nd	nd	nd	nd	nd	nd
Pr	nd	nd	nd	nd	nd	nd	nd	nd	nd
Sc	10	43	9	40	39	43	43	41	43
Sm	nd	nd	nd	nd	nd	nd	nd	nd	nd
V	70	380	174	398	359	383	374	355	375
Zn	21	93	62	106	69	68	169	108	98
Ga	20	21	20	18	nd	24	13	19	21
Nb	nd	nd	nd	nd	nd	nd	nd	nd	nd
Rb	120	16	3	15		21	8	4	15
Sr	10	160	23	70		230	130	130	190
Ta	5	nd	nd	nd		nd	nd	5	5
Th	21	9	13	6		5	7	8	9
U	4	3	3	nd		3	4	nd	nd
Y	13	27	13	8		25	25	25	27
Zr	240	88	63	83		77	78	89	81

Sand. Silt = finely laminated sandstone-siltstone

major elements in wt% trace elements in ppm nd=not detected blank space=not analyzed

APPENDIX 2 Analytical Techniques and Precision of Chemical Analyses

note: for some elements precision varies with concentration
LLD = lower limit of detection

Element	LLD	Precision Conc	+/-	Method
SiO2	0.10%	63.0%	0.8%	XRF
		49.0%	0.9%	XRF
		39.0%	0.9%	XRF
Al2O3	0.02%		2.0%	XRF
Fe2O3	0.10%	12.0%	2.0%	XRF
		10.0%	3.0%	XRF
		6.0%	4.0%	XRF
MgO	0.10%	20.0%	2.0%	XRF
		9.0%	2.0%	XRF
		5.0%	3.0%	XRF
CaO	0.02%		2.0%	XRF
Na2O	0.10%		5.0%	XRF
K2O	0.01%		5.0%	XRF
TiO2	0.01%	2.0%	3.0%	XRF
		0.5%	5.0%	XRF
MnO	0.01%	0.2%	6.0%	XRF
		0.1%	14.0%	XRF
P2O5	0.01%		10.0%	XRF
LOI	0.10%		4.0%	Gravimetric
Ba	1 ppm	130 ppm	8.0%	ICP
		150 ppm	5.0%	ICP
		420 ppm	6.0%	ICP
				ICP
Be	3 ppm		24.0%	ICP
Cd	2 ppm		74.0%	ICP
Ce	3 ppm	20 ppm	11.0%	ICP
		50 ppm	8.0%	ICP
Co	2 ppm	20 ppm	8.0%	ICP
		40 ppm	7.0%	ICP
		100 ppm	5.0%	ICP
Cr	2 ppm		12.0%	ICP
Cu	1 ppm	30 ppm	7.0%	ICP
		70 ppm	13.0%	ICP
Dy	1 ppm	2 ppm	50.0%	ICP
		20 ppm	12.0%	ICP
Eu	1 ppm		41.0%	ICP
La	2 ppm	10 ppm	15.0%	ICP
		40 ppm	11.0%	ICP
		90 ppm	12.0%	ICP
Li	1 ppm	10 ppm	9.0%	ICP

Element	LLD	Precision Conc	Precision +/-	Method
		20 ppm	11.0%	ICP
Nd	25 ppm	40 ppm	20.0%	ICP
		150 ppm	17.0%	ICP
Ni	1 ppm	10 ppm	38.0%	ICP
		70 ppm	8.0%	ICP
		2300 ppm	6.0%	ICP
Pb	12 ppm	30 ppm	22.0%	ICP
Pr	10 ppm			ICP
Sc	1 ppm	20 ppm	6.0%	ICP
		60 ppm	6.0%	ICP
Sm	2 ppm	25 ppm	28.0%	ICP
V	2 ppm	50 ppm	11.0%	ICP
		100 ppm	5.0%	ICP
		250 ppm	7.0%	ICP
Zn	2 ppm	60 ppm	15.0%	ICP
		100 ppm	7.0%	ICP
		150 ppm	11.0%	ICP
Ga	3 ppm	20 ppm	15.0%	XRF
		30 ppm	13.0%	XRF
Nb	3 ppm	10 ppm	30.0%	XRF
		25 ppm	20.0%	XRF
Rb	3 ppm	15 ppm	10.0%	XRF
		35 ppm	5.0%	XRF
		90 ppm	4.0%	XRF
		180 ppm	4.0%	XRF
Sr	3 ppm		4.0%	XRF
Ta	5 ppm			XRF
Th	3 ppm	5 ppm	30.0%	XRF
		30 ppm	12.0%	XRF
U	3 ppm	4 ppm	30.0%	XRF
Y	3 ppm	10 ppm	30.0%	XRF
		40 ppm	10.0%	XRF
		60 ppm	6.0%	XRF
Zr	3 ppm	40 ppm	10.0%	XRF
		200 ppm	4.0%	XRF
Au	15 ppb	30 ppb	50.0%	AA
		100 ppb	25.0%	AA
		200 ppb	10.0%	AA
Pd	0.07 ppm	0.13 ppm	40.0%	AA
		0.73 ppm	10.0%	AA
Pt	0.07 ppm			AA
Rh	0.03 ppm			AA

APPENDIX 3 Lead Isotopes

Lead isotopes potentially can be used in metallogenic studies to determine the age of mineralization and the source of the lead (c.f. Franklin et al., 1983; Gulson and Porritt, 1987; Gulson et al., 1987). Sediment-hosted Zn-Pb deposits such as Broken Hill, Mt. Isa, McArthur River and Sullivan plot close to the single-stage growth curve for lead on conventional Pb isotopic plots (Gustafson and Williams, 1981). However, dating these deposits by other techniques has revealed that the lead dates are inaccurate, and it is now recognized that single-stage growth models represent an oversimplication of lead isotopic evolution (op cit.). Ore leads from conformable, syngenetic deposits do not represent unmodified mantle values: because of their prior involvement in sedimentary or volcanic processes, such leads may represent mean values for large crustal segments (Albarede and Juteau, 1984). Multistage models such as those of Stacey and Krammers (1976), and Doe and Zartman (1979) have been developed to account for mixing in crustal and mantle reservoirs, but such models involve assumptions that cannot be directly verified.

Nevertheless, Pb isotopes were determined for a suite of samples from the Frederickson Lake region in order to assess whether crustal contamination had occurred, and to determine if a genetic relationship exists between the Pb in sediment-hosted and gabbro-hosted ore deposits. The sample suite consisted of pyrrhotites separated from two gabbro-hosted Cu-

Ni ores (Frederickson Lake, Connolly), one pyrrhotite from the sediment-hosted Zn-Cu-Pb deposit at Frederickson Lake North, and two pyrrhotite samples from sulphide-facies iron formation. The limited numbers of samples seemed justifiable, given the observation of Doe and Stacey (1974) that lead isotope ratios within individual conformable ore deposits are tightly constrained.

The data presented in Table 10 show a wide variation in lead isotopic ratios, with data points falling on and below the single stage growth curve of Doe and Stacey (1974) (Fig. 40). The data points were subjected to a linear regression analysis (York, 1969) to determine the model age. This treatment yielded an age of 2.06 +/- 0.3 Ga (two sigma). The large error is the result of data scatter. Pb isotope results from Clark and Thorpe (1987) suggest a possibly younger age of 1875 Ga for the Frederickson Lake deposits, although their data does fall within the error range of the present study (2.36 to 1.76 Ga.).

The isotopic heterogeneity of the sulphide suite could be produced by mixing of crustal and mantle leads, or by the in situ decay of uranium to increase the Pb206/Pb204 ratio. The dominant process is difficult to determine because both lead to similar end products. Since the lead isotopic data were obtained from iron sulphides, uranium decay could be a complicating factor because the ratio of uranium to Pb can be much higher in iron sulphides than in the galenas which are conventionally measured (Gulson and Porritt, 1987). Because of the various possible explanations of the lead isotopic

Table 10

Lead isotope analyses of iron sulphides from the Frederickson Lake area

sample	showing and type	Pb 206/204	207/204	208/204
(+/-)		(0.01)	(0.01)	(0.06)
Pb-1	Frederickson S. (Cu-Ni)	15.56	15.26	35.39
Pb-2	Frederickson N. (Zn-Cu-Pb)	15.32	15.25	35.27
Pb-3	Faute Lake (Po-Py)	17.62	15.54	35.54
Pb-4	Jimmick Lake (Po-Py)	15.74	15.34	35.23
Pb-5	Connolly Lake (Cu-Ni)	16.16	15.35	35.49

Analyst: R. Farquhar, Dept. of Physics, University of Toronto.

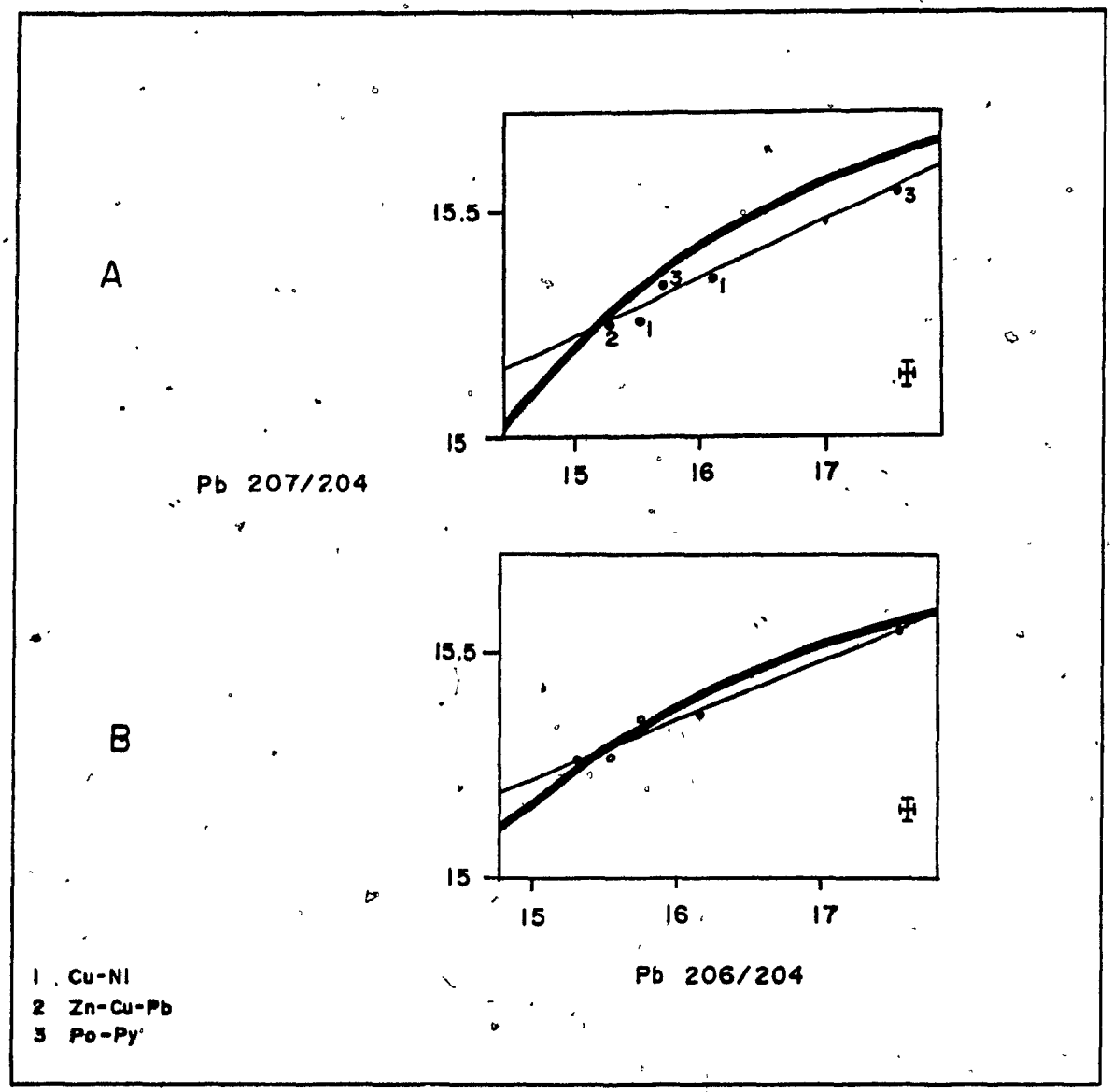

Fig. 40 Lead isotope data from the Frederickson Lake area plotted on growth curves from A: Doe and Stacey (1974) and from B: Stacey and Krammers (1976). Straight lines represent a linear regression through the data.

data, no genetic inferences could be made about the sulphide deposits. Franklin et al., (1983) also encountered interpretational problems in a Pb-isotope study of Labrador Trough sulphides.

MAP - I THE FRE

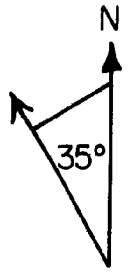

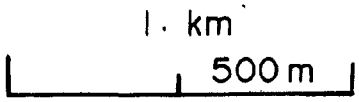

3g

FREDERICKSON LAKE NORTH SHOWING - DDH F-8

SW overburden

EDERICKSON LAKE AREA 1:20 000

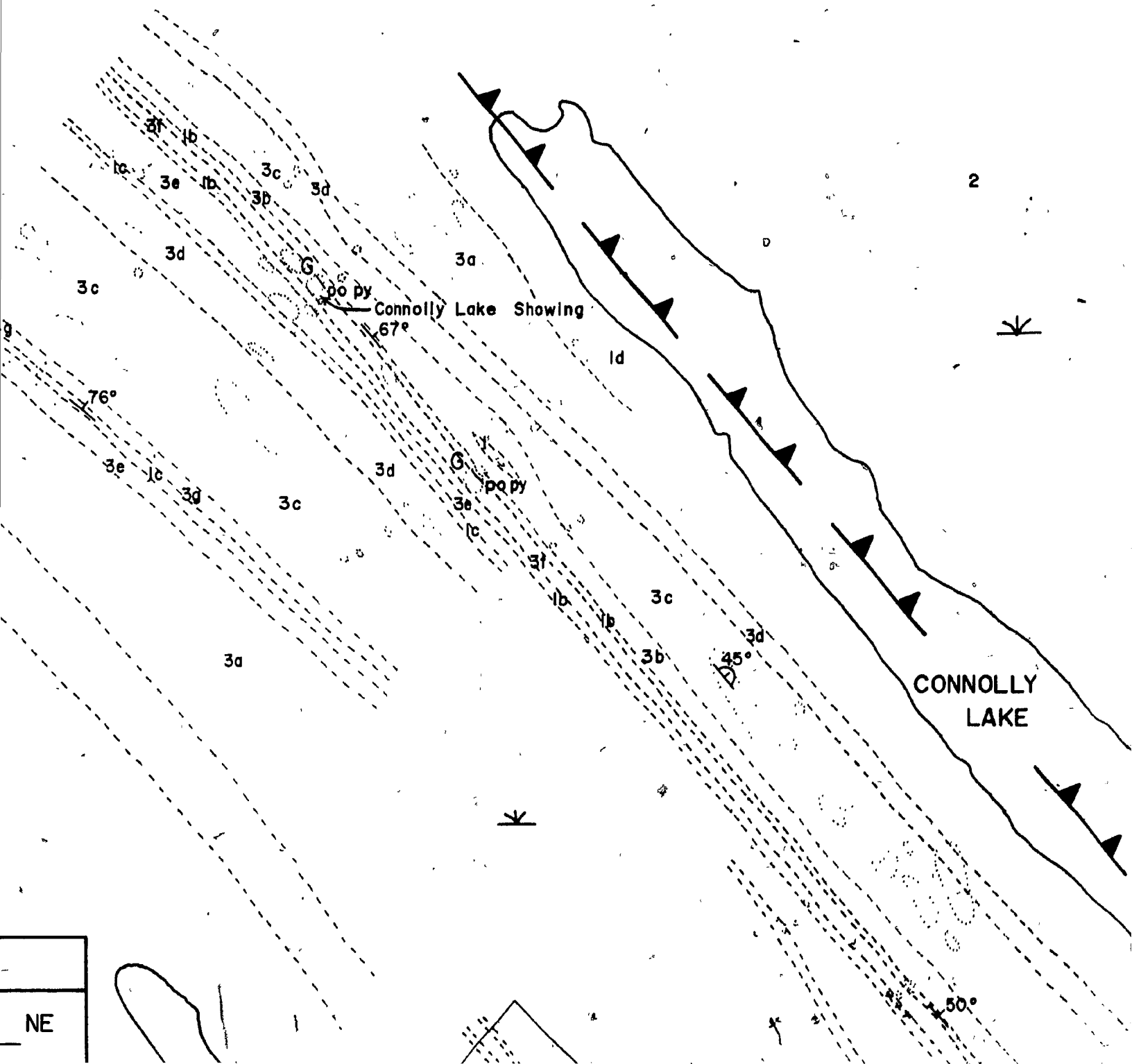

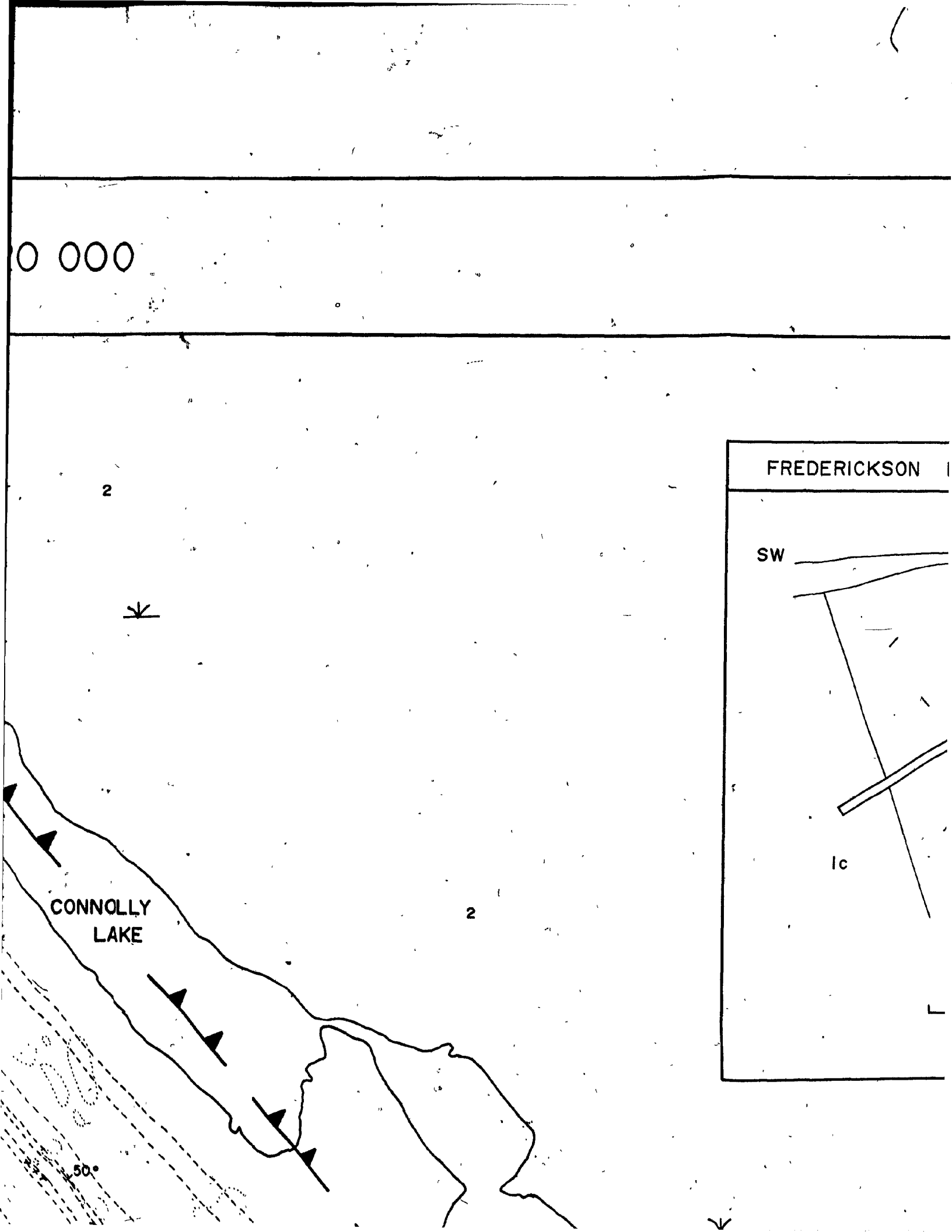
FREDERICKSON
SW
lc
2
2
CONNOLLY
LAKE
50°

J.S. GEBERT 1987

LAKE SOUTH SHOWING – DDH F-2, F-3

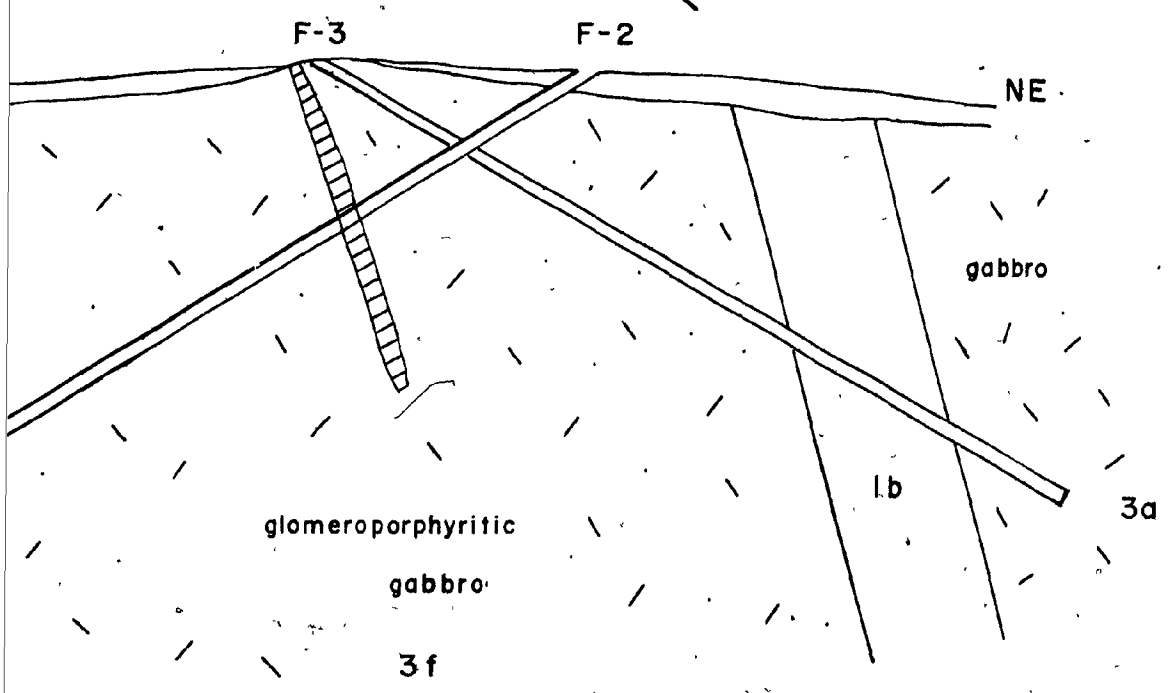

5m

mineralized zone is projected

from Griffis (1945)

FREDERICKSON LAKE NORTH SHOWING - DDH F-8

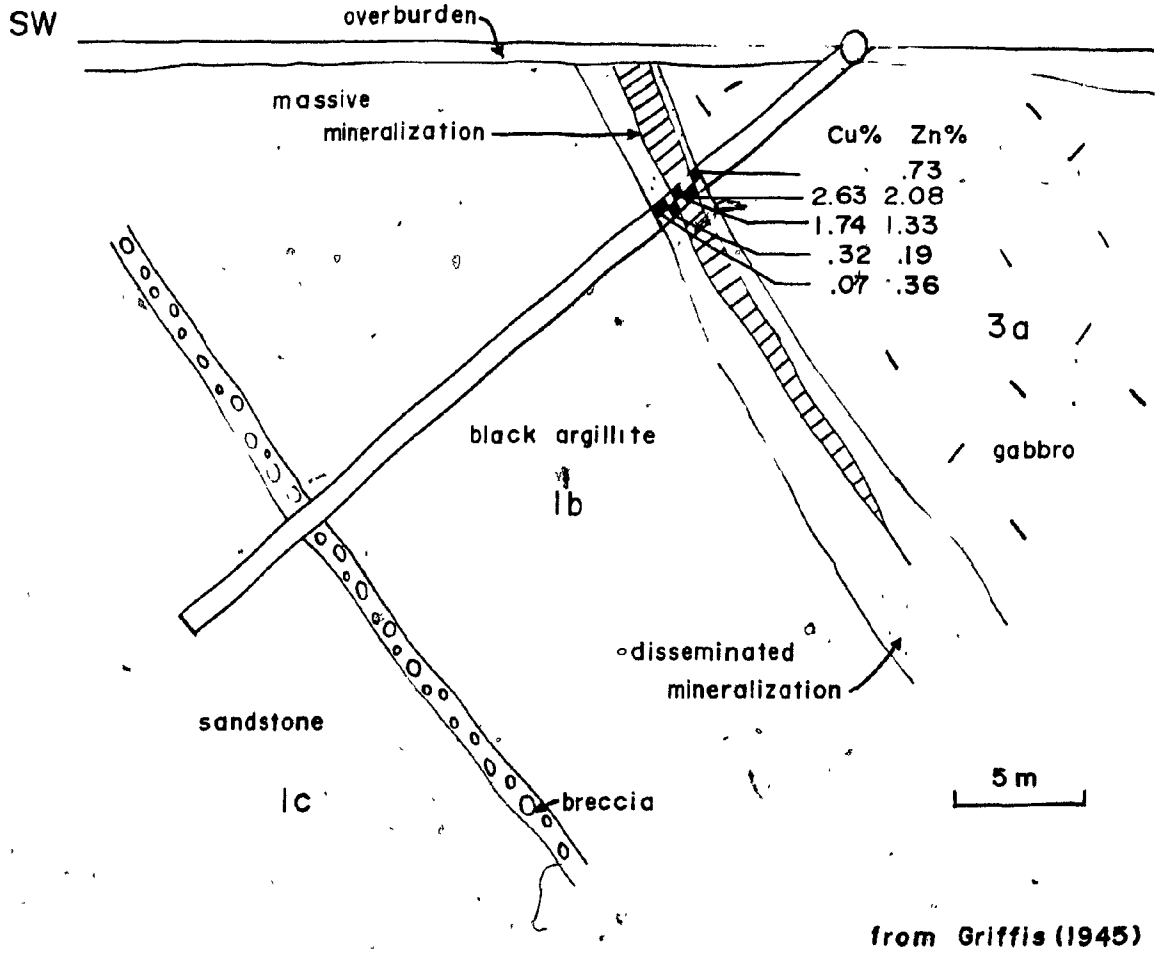

from Griffis (1945)

LEGEND

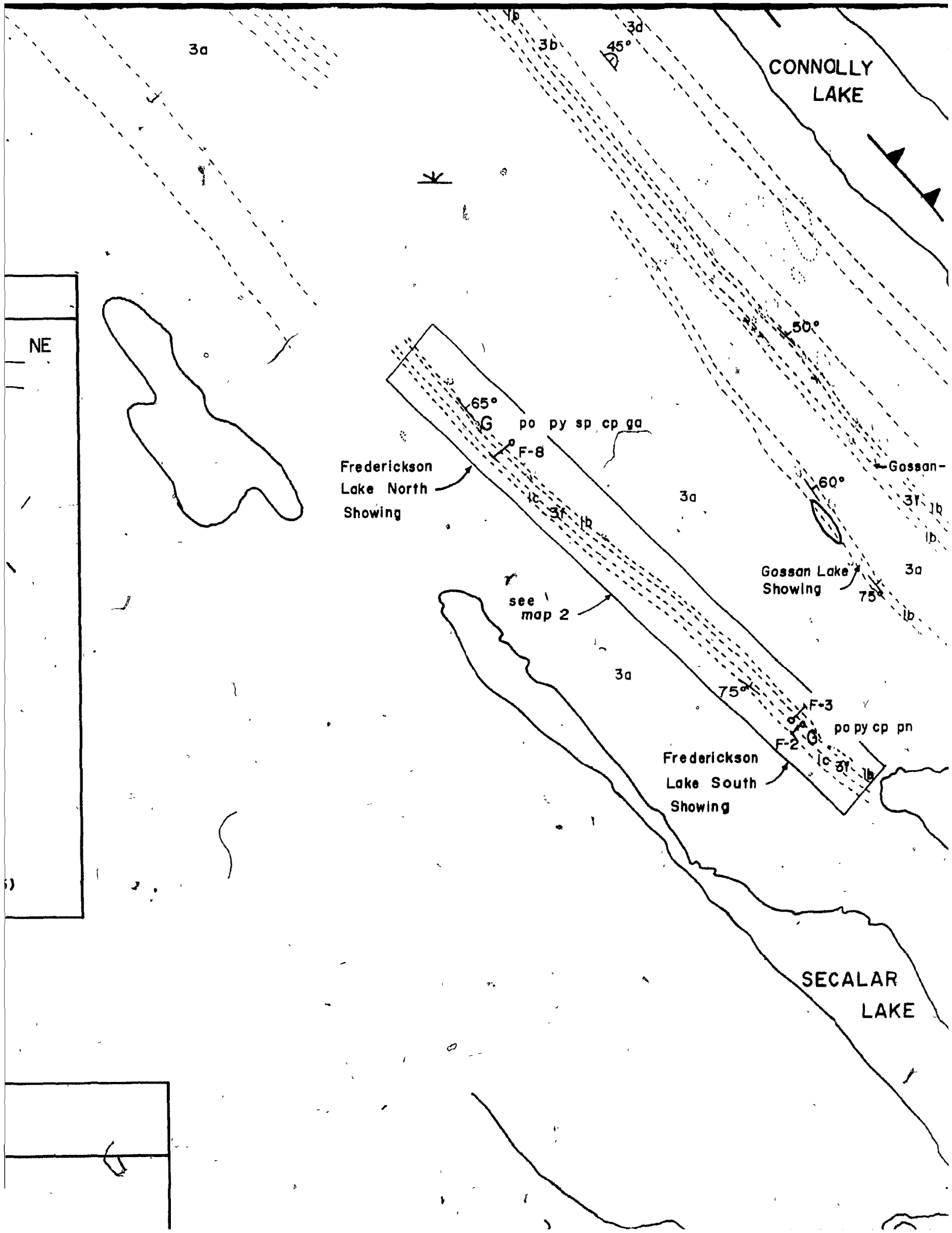
CONNOLLY LAKE
3a
3b
3d
45°
50°
65°
G
po py sp cp ga
F-8
Frederickson Lake North Showing
1c 3f 1b
3a
60°
Gossan-
3f 1b
1b
Gossan Lake Showing
3a
75°
1b
see map 2
3a
75°
F-3
F-4
G
po py cp pn
F-2
1c 3f 1b
Frederickson Lake South Showing
NE
SECALAR LAKE

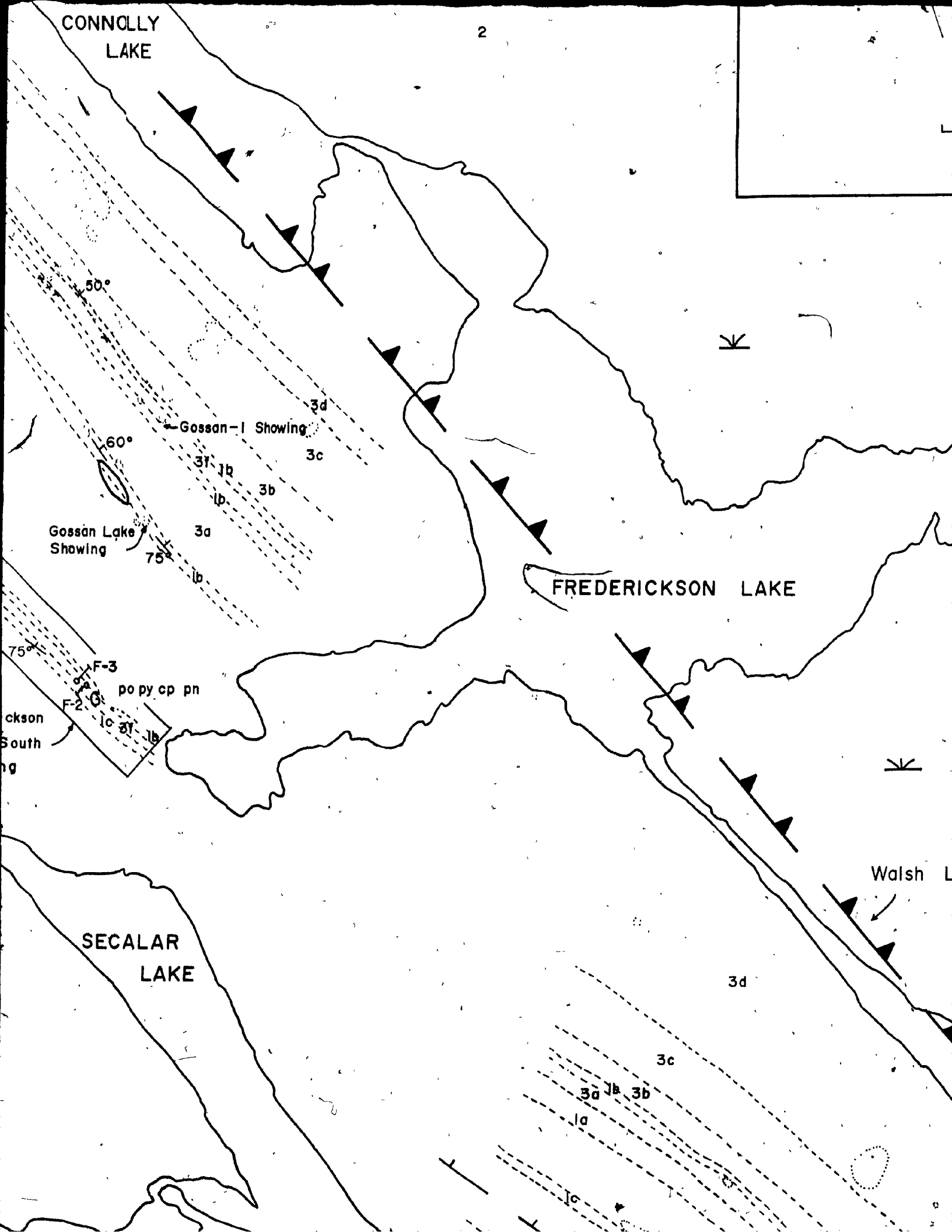
CONNOLLY LAKE
2
50°
60°
75°
Gossan-1 Showing
Gossan Lake Showing
3d
3c
3b
3a
1b
1a
1c
FREDERICKSON LAKE
F-3
F-2
po py cp pn
SECALAR LAKE
Walsh L

5m

mineralized zone is projected

from Griffis (1945)

2

Lake Fault

FAUTE
LAKE

MAP - 2

FREDERICKSON

FREDERICKSON LAKE

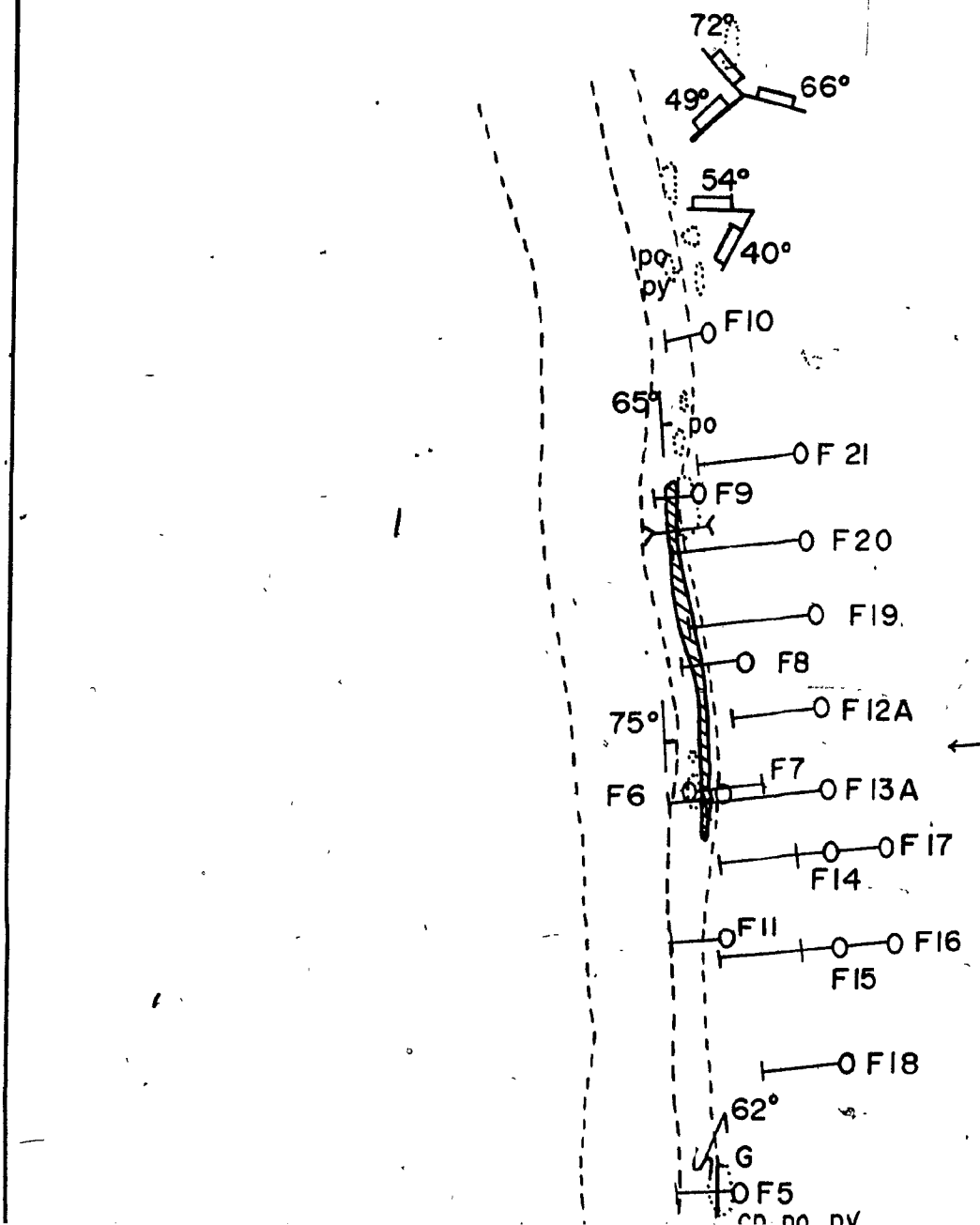

FREDERICKSON

← po, py, sp, cp, ga

N LAKE AND GOSSAN LAKE SULPHIDE

1:5 000

GOSSA

N LAKE NORTH

25 m

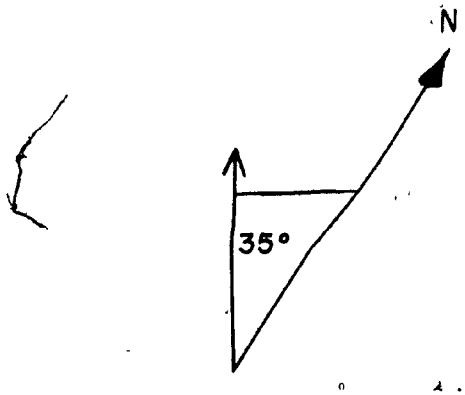

RICKSON LAKE AND GOSSAN LAKE SULPI

LAKE 1:5 000

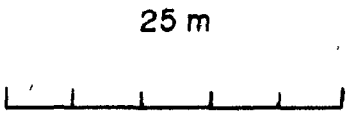

DERICKSON LAKE NORTH

, sp, cp, ga

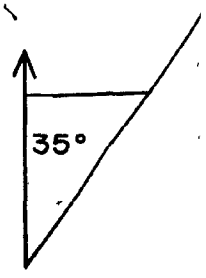

PHIDE SHOWINGS

J S GEBERT 1987

GOSSAN LAKE 1: 500

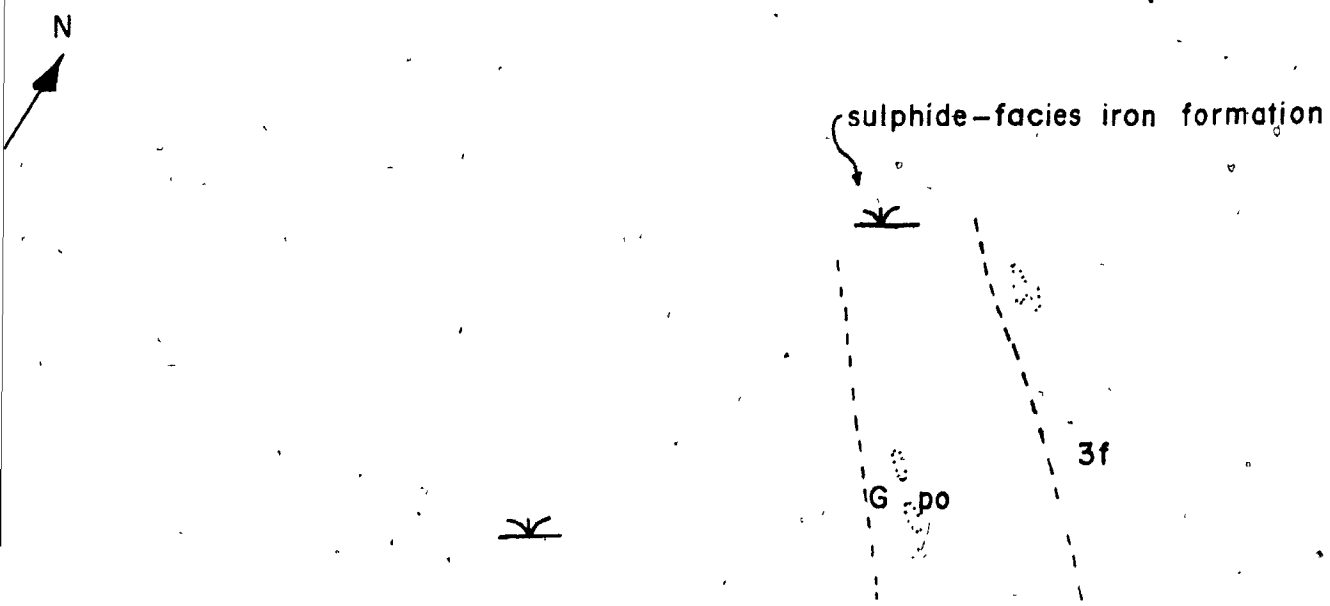

LEGEND

MONTAGNAIS GROUP

3 — Wakuach gabbro

- a gabbro (not divided)
- b porphyritic gabbro
- c ordinary gabbro
- d pegmatitic gabbro
- e fine-grained gabbro
- f glomeroporphyritic gabbro
- g anorthositic gabbro

KANIAPISKAU SUPERGROUP

KNOB LAKE GROUP

2 — Murdoch Formation

chlorite schist

1 — Menihek Formation

- a shale
- b argillite (po-py indicates sulphide
- c siltstone - sandstone
- d basalt
- e tuff

LAKE

SNOWSHOE LAKE

e facies)

JIMMICK LAKE SHOWING - DDH

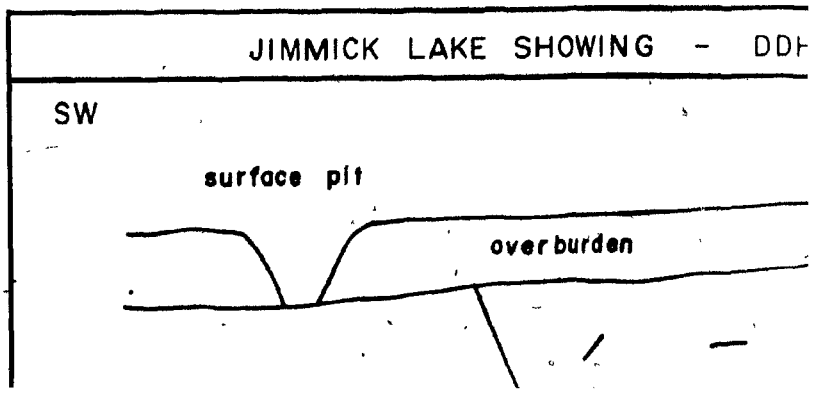

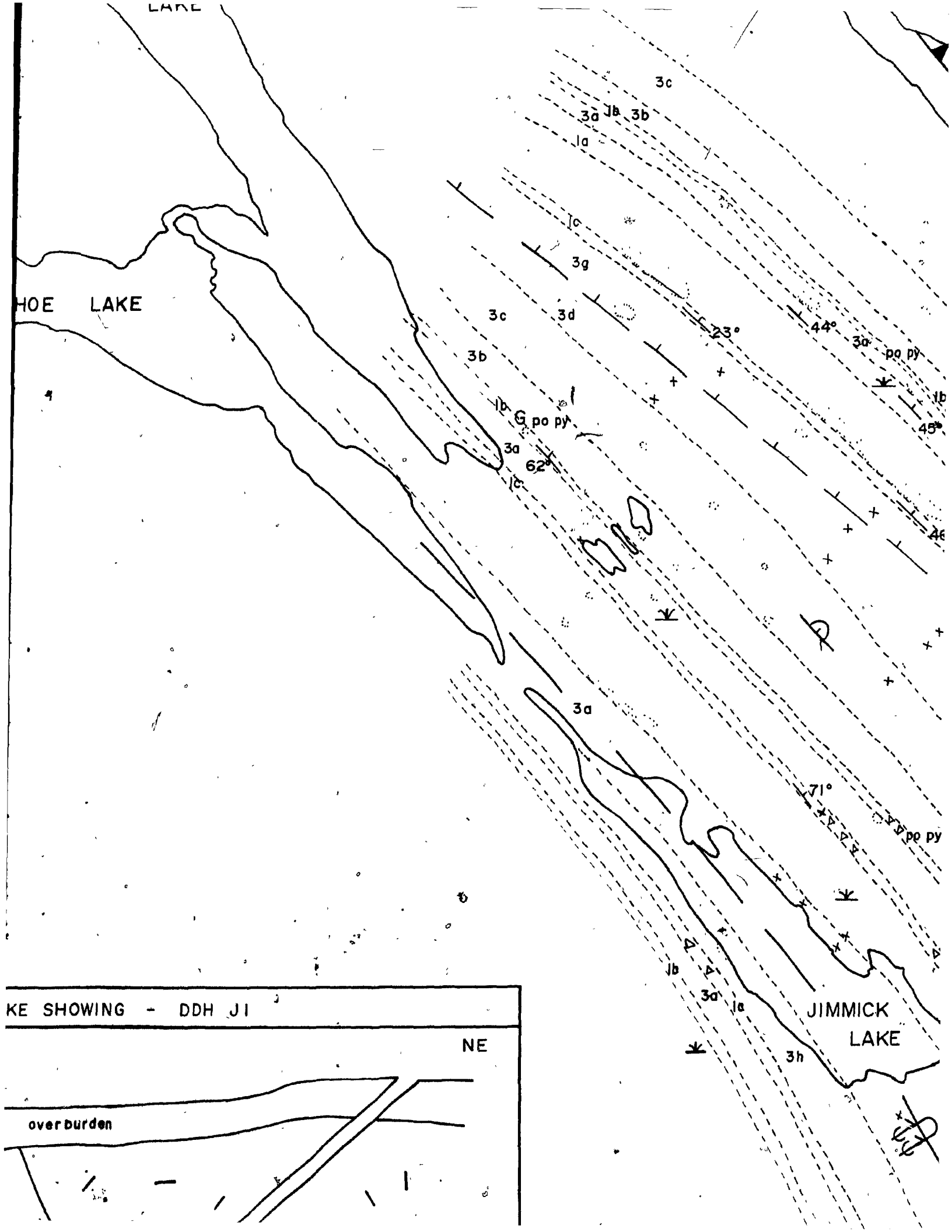
LAKE
HOE LAKE
3c
3a
1b
3b
1a
1c
3g
3c
3d
3b
23°
44°
3a
po py
1b
45°
1b
G po py
3a
62°
1c
46
3a
71°
po py
1b
3a
1a
JIMMICK
LAKE
3h
KE SHOWING - DDH J1
NE
over burden

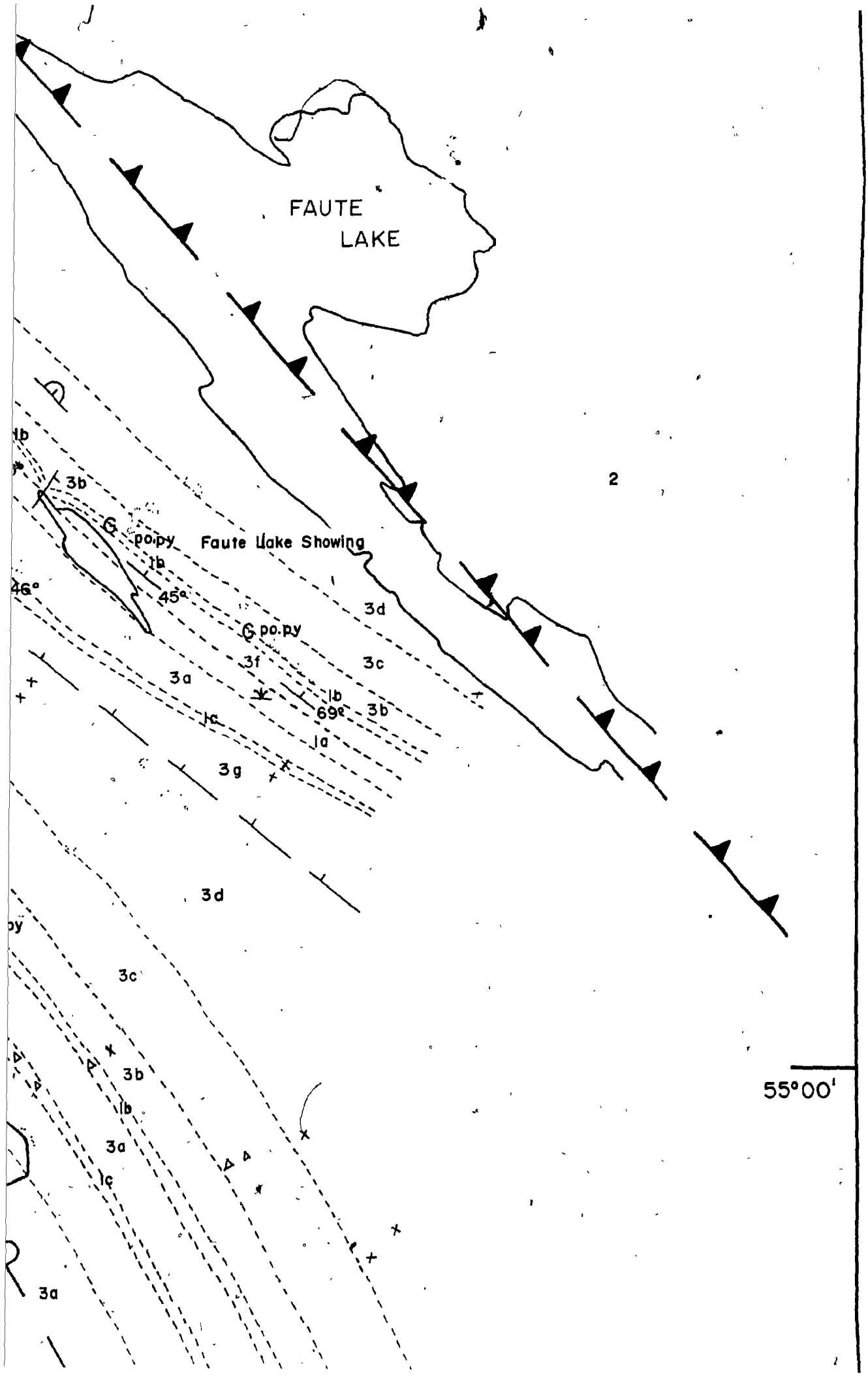
FAUTE
LAKE
2
3b
po.py
Faute Lake Showing
1b
45°
46°
3d
po.py
3f
3c
3a
1b
69°
3b
1c
1a
3g
3d
3c
3b
1b
3a
1c
3a
55°00'

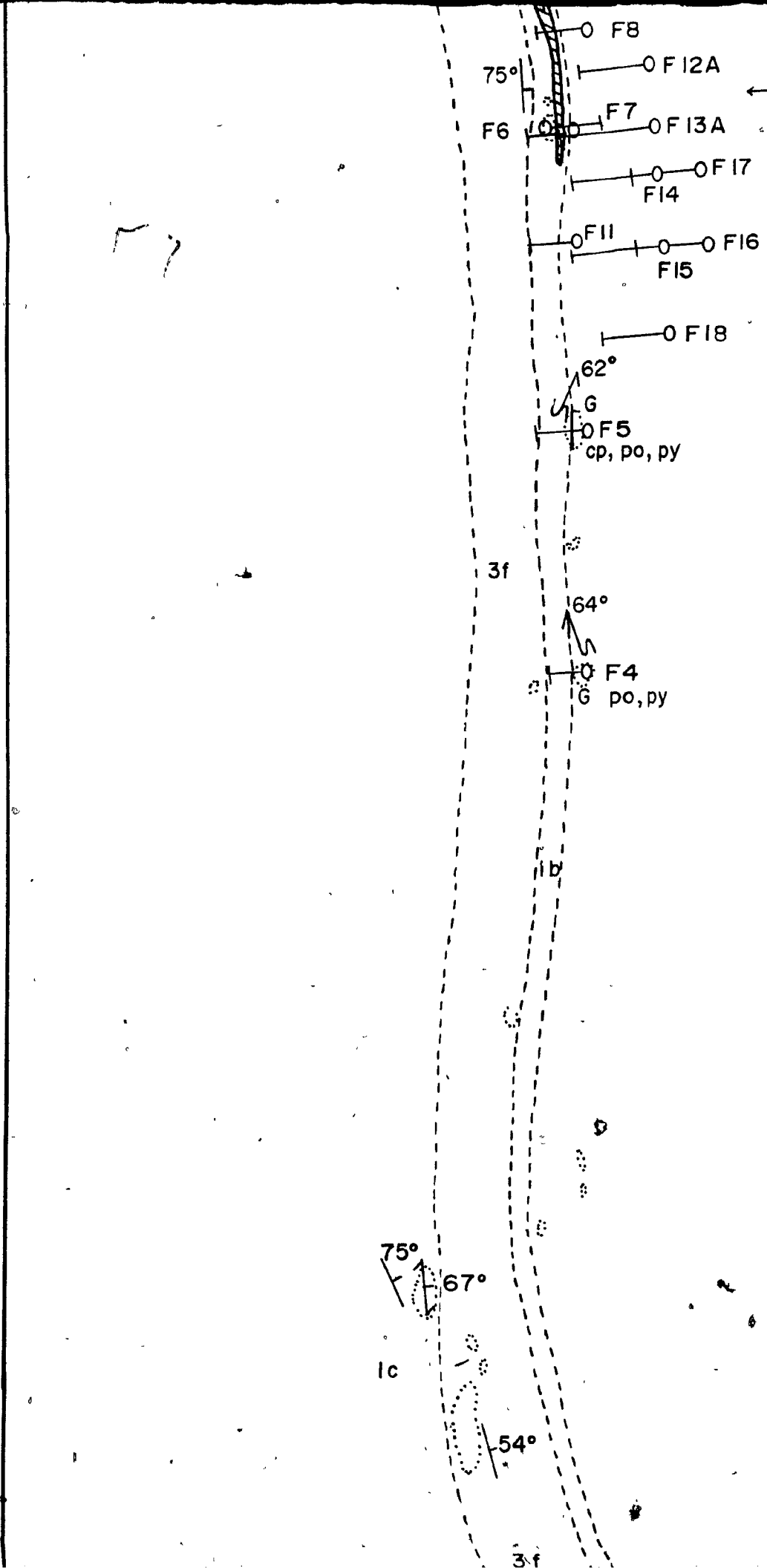
FREDERICKSO
F8
75°
F12A
po, py, sp, cp, ga
F6
F7
F13A
F17
F14
F11
F16
F15
F18
62°
G
F5
cp, po, py
3f
64°
F4
G
po, py
1b
75°
67°
1c
54°
3f

ON LAKE NORTH

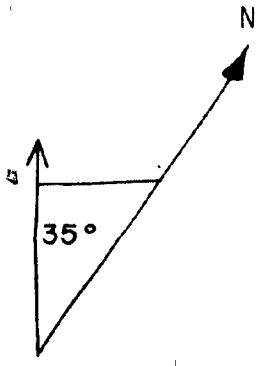

ation of outcrops and diamond drill holes

m Griffis (1945) and Hogg (1957)

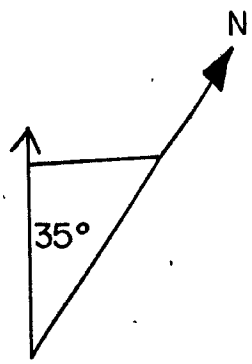

sp, cp, ga

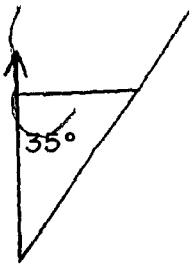

location of outcrops and diamond drill holes from Griffis (1945) and Hogg (1957)

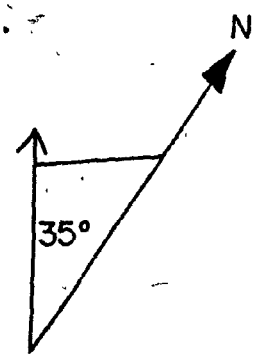

200 m

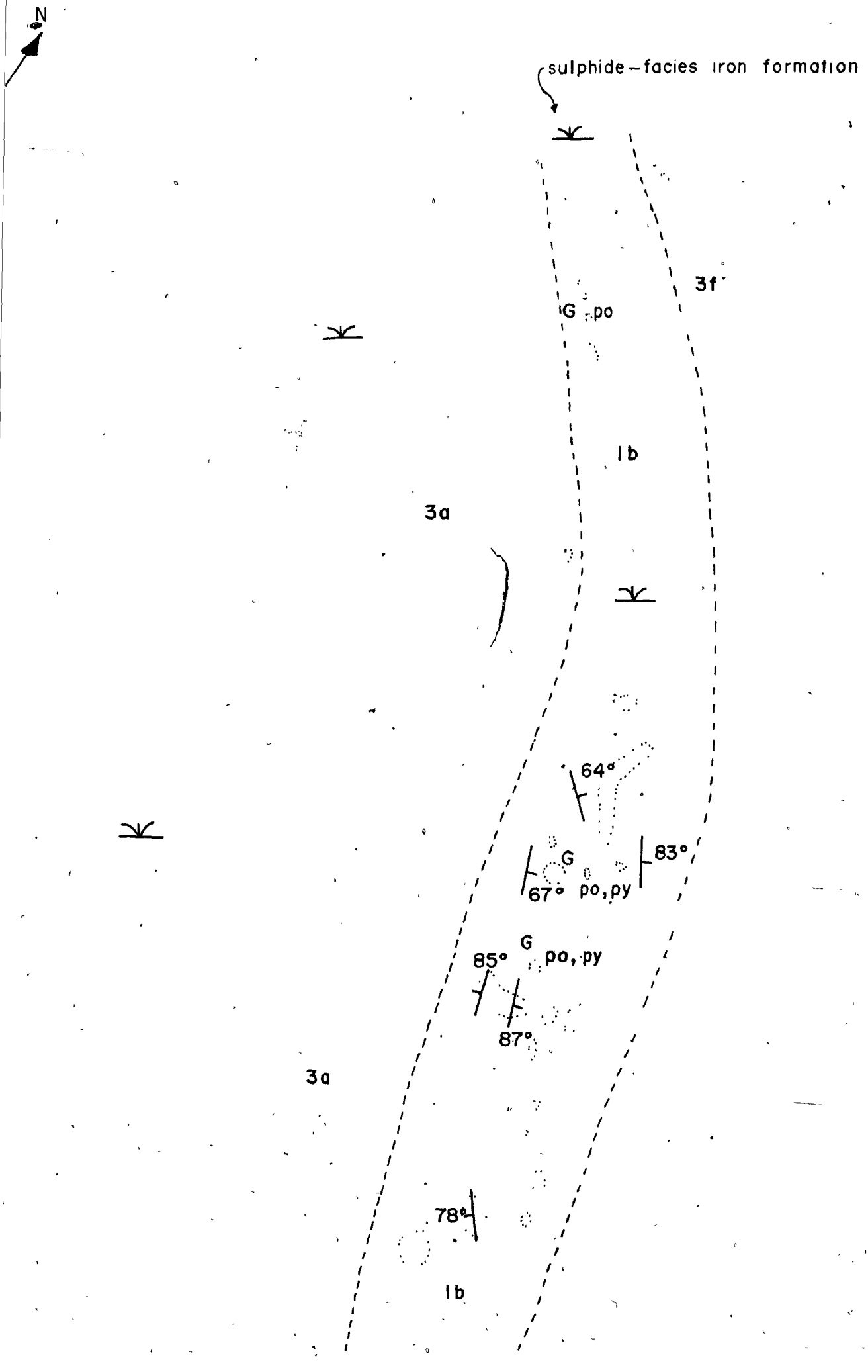
N
sulphide-facies iron formation
3f
G po
1b
3a
64°
G
83°
67°
po, py
G
85°
po, py
87°
3a
78°
1b

2 **Murdoch Formation**

chlorite schist

1 **Menihek Formation**

a shale
b argillite (po - py indicates sulphide
c siltstone - sandstone
d basalt
e tuff


swamp


outcrop

X small outcrop


frost-wedged rock fragment


bedding


foliation


lineation

S minor fold

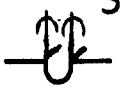
antiformal syncline


regional fault


local fault

geological contact

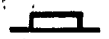
joint

e facies)

—o diamond drill hole

—≺ trench

▨ mineralized zone

—P tops

py pyrite

po pyrrhotite

cp chalcopyrite

ga galena

sp sphalerite

pn pentlandite

G gossan

JIMMICK LAKE SHOWING - DDH

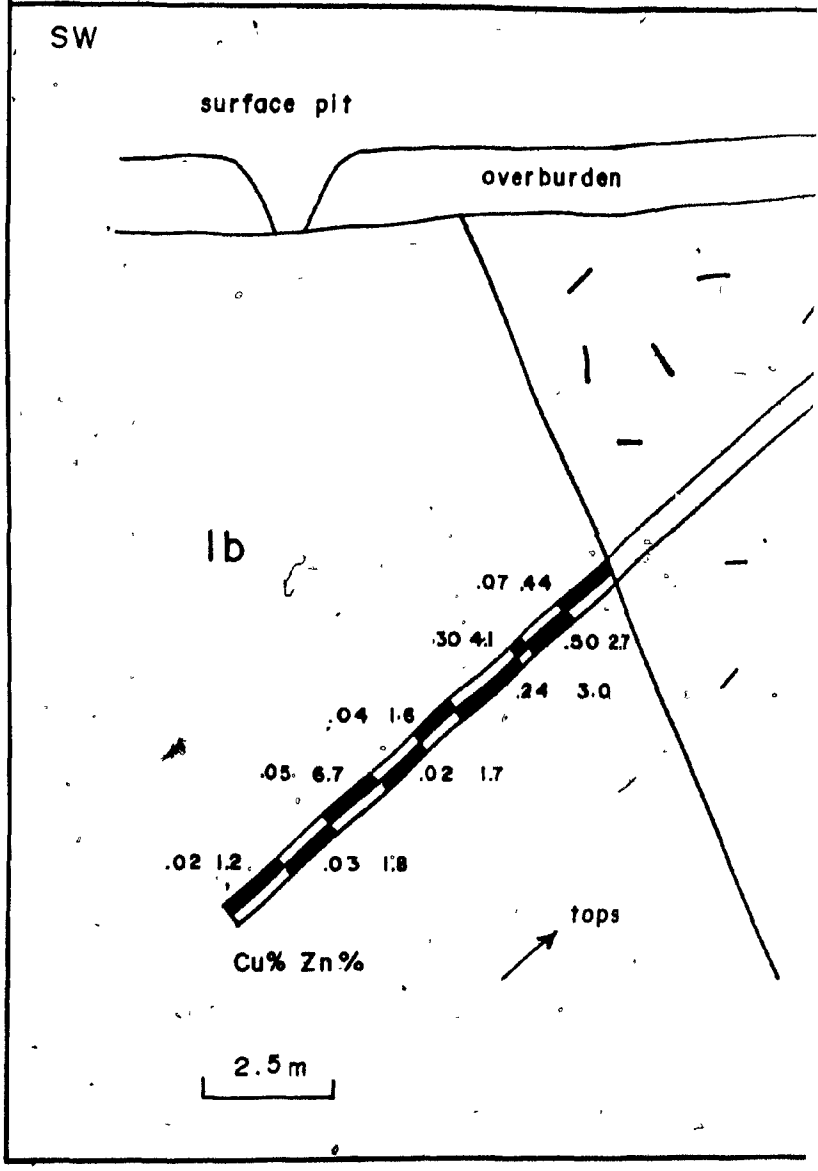

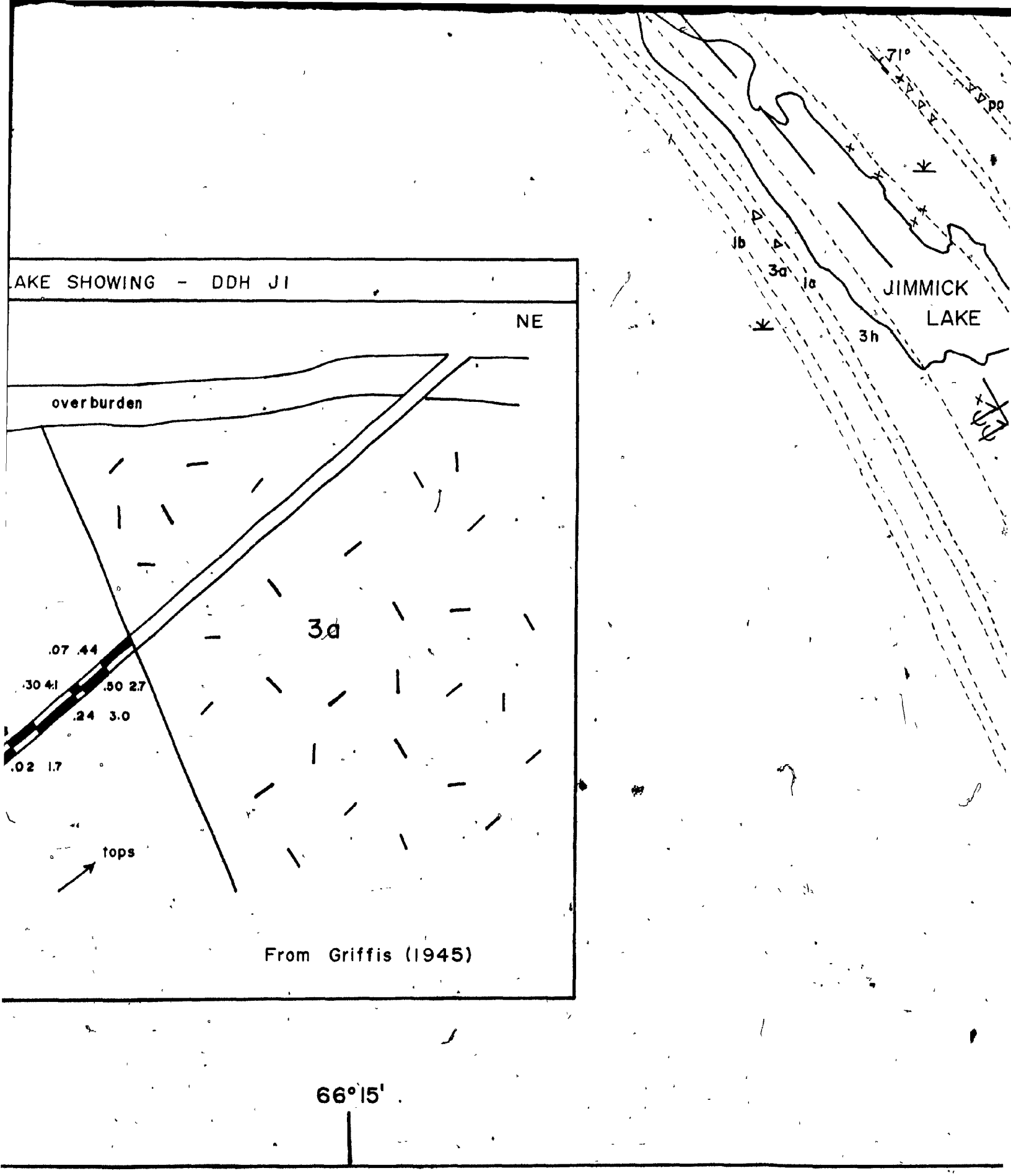

AKE SHOWING - DDH J1

From Griffis (1945)

66°15'

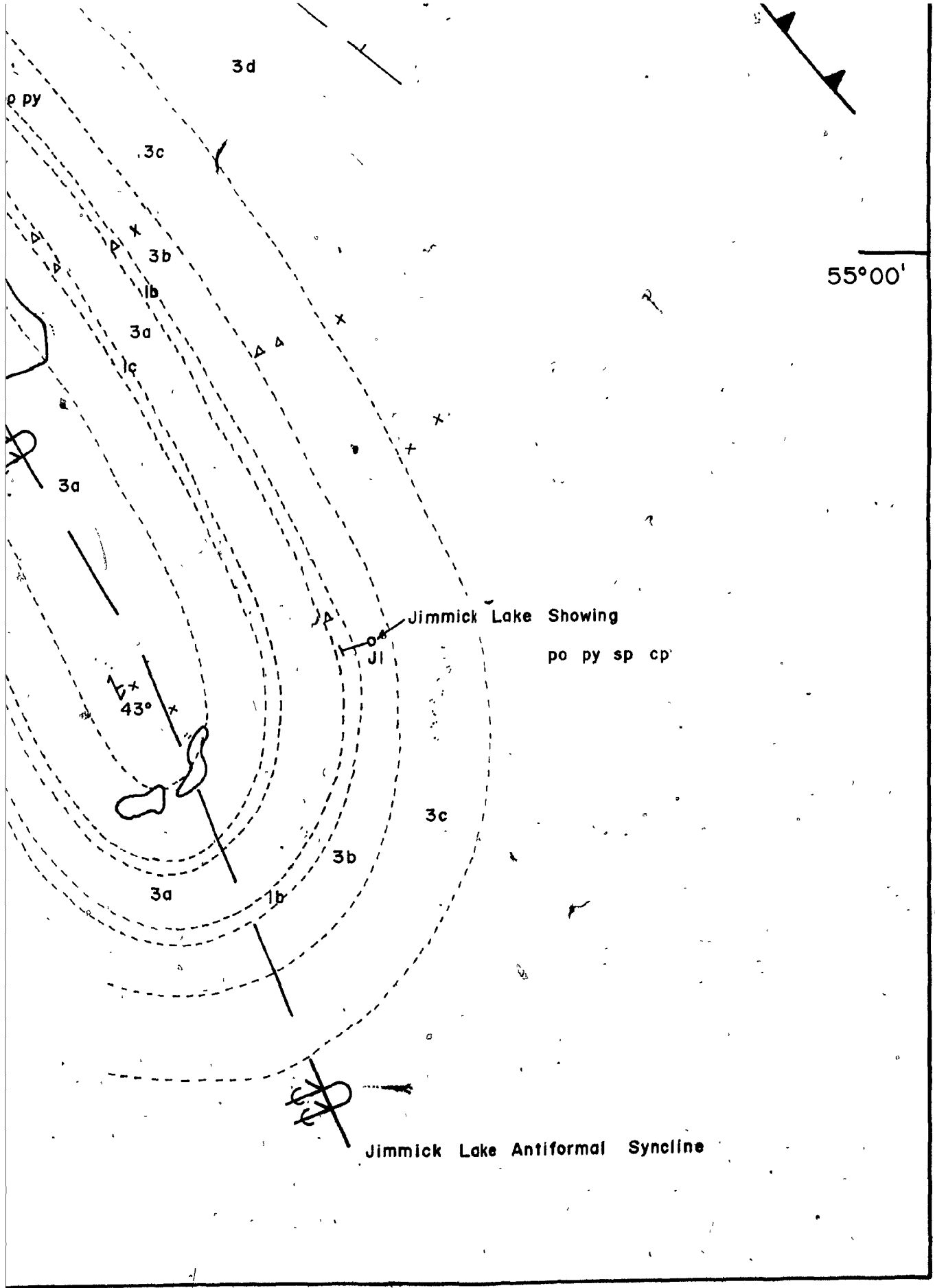
3d
po py
3c
3b
1b
3a
1c
3a
55°00'
Jimmick Lake Showing
po py sp cp
JI
43°
3c
3b
3a
1b
Jimmick Lake Antiformal Syncline

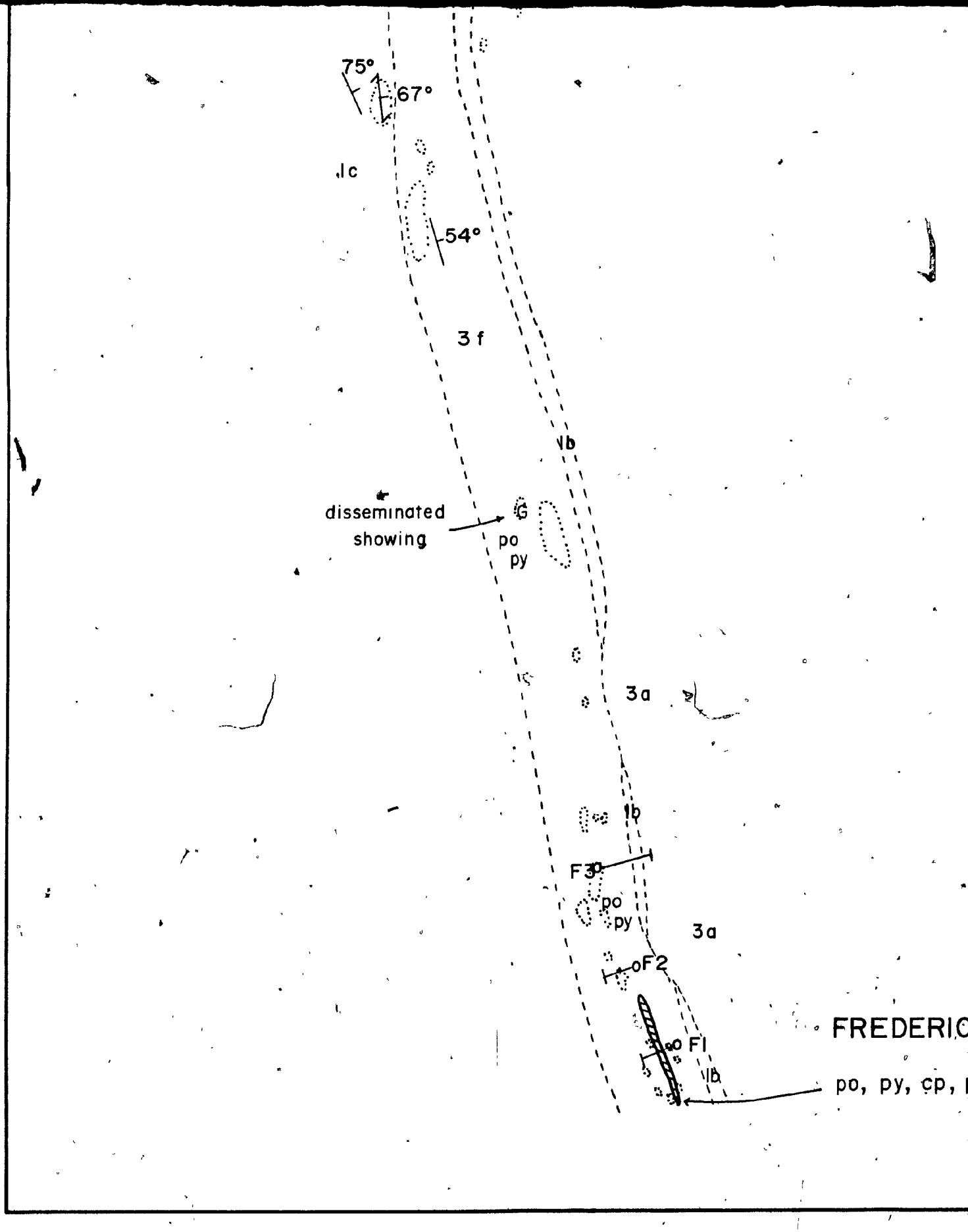
75°
67°
Ic
54°
3f
Ib
disseminated
showing
G
po
py
3a
Ib
F3
po
py
3a
oF2
oF1
Ib
FREDERIC
po, py, cp,

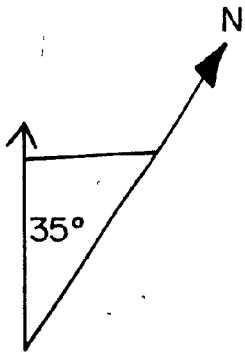

200 m

CKSON LAKE SOUTH

pn

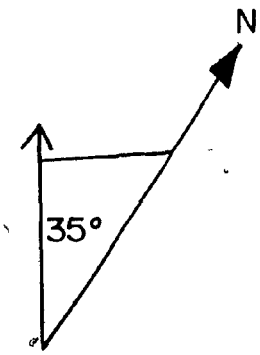

200 m

FREDERICKSON LAKE SOUTH

po, py, cp, pn

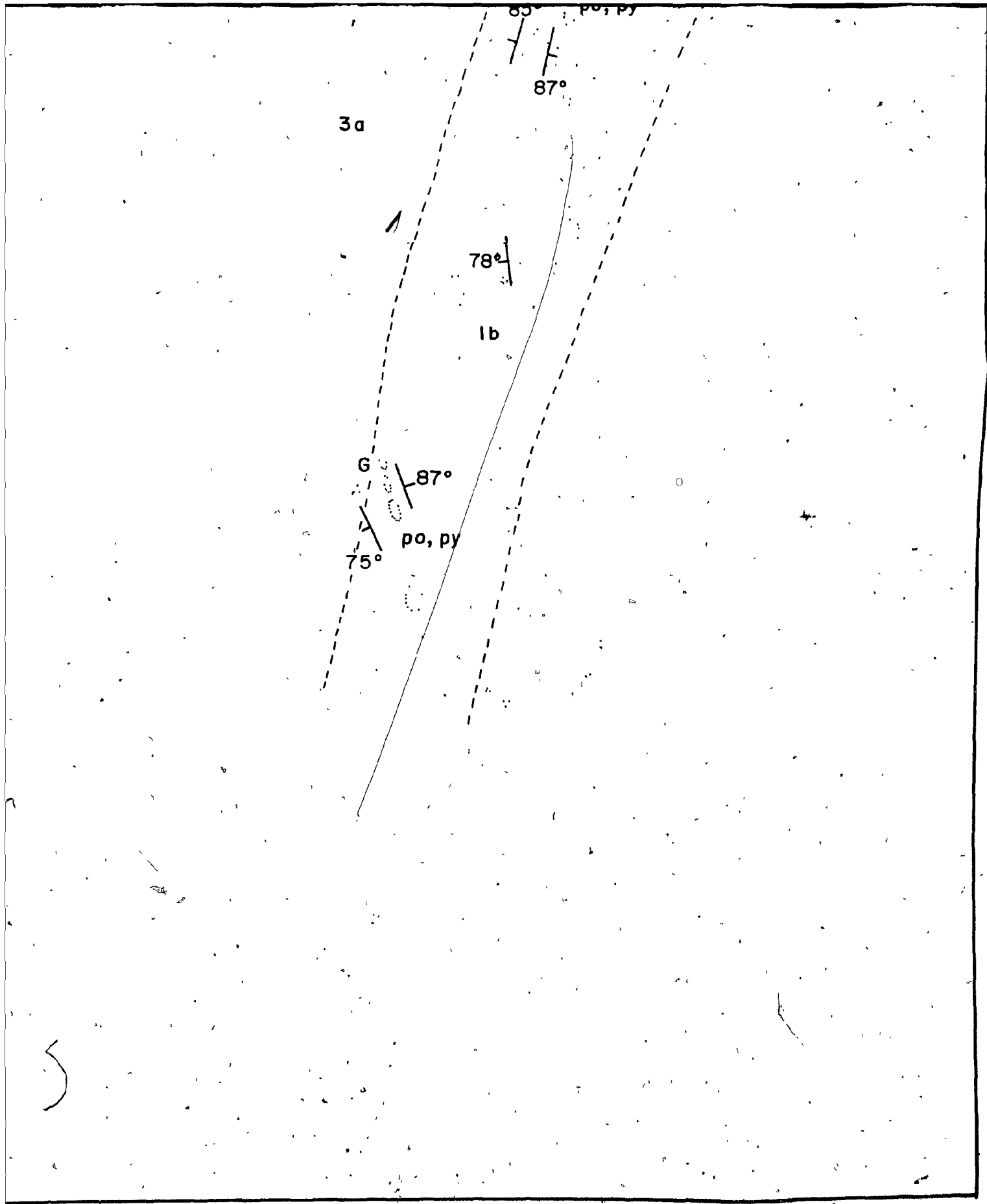
85°
po, py
87°
3a
78°
1b
G
87°
po, py
75°